Orogenic evolution of the northern Calabria–southern Apennines system in the framework of the Alpine chains in the central–western Mediterranean area

Article *in* Geological Society of America Bulletin · September 2024

DOI: 10.1130/B37474.1

2 authors:

Sabatino Ciarcia
University of Sannio

Stefano Vitale
University of Naples Federico II

THE GEOLOGICAL SOCIETY OF AMERICA®

Orogenic evolution of the northern Calabria–southern Apennines system in the framework of the Alpine chains in the central-western Mediterranean area

Sabatino Ciarcia[1] and Stefano Vitale[2,†]
[1]*Dipartimento di Scienze e Tecnologie, Università del Sannio, via de Sanctis, 82100 Benevento, Italy*
[2]*Dipartimento Scienze della Terra, dell'Ambiente e delle Risorse, Università di Napoli Federico II, Via Cupa Nuova Cintia 21, 80126 Napoli, Italy*

ABSTRACT

The northern Calabrian ranges and the southern Apennines are part of a single orogenic segment of the Alpine chain system framing the central-western Mediterranean Sea. Three main tectonic complexes characterize this orogenic chain: (1) remnants of the overriding plate, including Variscan Paleozoic basement (Calabria-Peloritani terrane), which tectonically cover (2) an Alpine metamorphic belt, corresponding to an exhumed subduction channel, formed by slices of the Calabria-Peloritani terrane, meta-ophiolites (metamorphic Ligurian Units), and some successions of the continental Adria plate (downgoing plate), which are in turn superposed onto (3) a fold-and-thrust belt composed of remnants of an oceanic accretionary prism (nonmetamorphic Ligurian Units) on the top and an underlying imbricate orogenic pile consisting of shallow-water to pelagic continental Adria successions, also including buried shallow-water carbonates of the Apulian Platform. The exposed Apulian Platform domain (Puglia region) and the Adriatic Sea represent the current foreland. The orogenic chain results from the subduction of Ligurian Ocean lithosphere beneath the European plate/Calabria-Peloritani terrane starting during the Paleocene–Eocene. The restored mean tectonic vergences indicate that the thrust front migrated to the south in the Eocene–Langhian period, turning to the east during the Serravallian–Pleistocene interval. After the complete closure of the Ligurian Ocean in the Early Miocene, the subduction continued with the involvement of the continental part of the Adria plate, triggering crustal shortening until the middle Pleistocene. Complex geometries, reflecting the articulated paleogeographic domains formed by alternating shallow-water carbonate platforms and deep basins, controlled the shape of the thrust front–foredeep–forebulge system. Thin- and thick-skinned thrusting episodes have alternated during the orogenic shortening; however, since the early Pliocene, deep-seated, ramp-dominated thrust faults have driven the crustal shortening, resulting in widespread envelopment thrusting, and out-of-sequence structures in the allochthonous wedge. The alternating different tectonic styles also resulted from the involvement in the subduction system of the continental Adria lithosphere, which is thicker under the carbonate platforms and thinner under the interspersed pelagic basins and the western margin facing the Ligurian Ocean. The involvement of thicker lithosphere during the subduction process caused two main backstops that triggered thick-skinned tectonics. The synorogenic sedimentation was ruled by the migration of the forebulge-foreland basin system, with flexure of the continental part of the Adria plate since the Oligocene and erosion of a large part of the Apennine and Apulian carbonates that fed the foredeep basins with calciclastic supply. Siliciclastic input, which originated from both the overriding plate and orogenic wedge, joined with orogenic volcaniclastics, marks the sedimentation in the foreland basin system, including the mature stage of the foredeep troughs and the wedge-top basins located on the top of the chain, with the latter also recording calciclastic sedimentation that originated from the erosion of the piled-up Adria carbonate successions.

1. INTRODUCTION

The construction of mountains is a complex interplay of different geologic processes. The most important are (1) crustal shortening, ruled by thrust faults and folds and secondarily by extensional and strike-slip faulting, and (2) synorogenic sedimentation within the foreland basin system (e.g., Bally et al., 1966; Dickinson, 1974; Davis et al., 1983; Ingersoll, 1988; Willett et al., 1993; Beaumont et al., 1996; Willett, 1999; Tavarnelli and Prosser, 2003; Garzanti et al., 2007; DeCelles, 2012; Ingersoll, 2012; Faccenna et al., 2013; Sobolev and Brown, 2019; Bucci et al., 2019, 2020; Faccenna et al., 2021; Barchi and Tavarnelli, 2022). The northern Calabria–southern Apennines system (Figs. 1A and 1B) is a noteworthy example of such an orogenic belt where construction was accompanied by synorogenic sedimentation in the foreland basin system, including (from the foreland to hinterland) the backbulge, forebulge, foredeep, and wedge-top basins (Selli, 1962; Ogniben, 1969; D'Argenio et al., 1973; Amodio-Morelli et al., 1976; DeCelles and Giles, 1996; Patacca and Scandone, 2007; DeCelles, 2012; Carminati and Doglioni, 2012; Vitale and Ciarcia, 2013). The characterization and dating of all these deposits have allowed geologists to constrain the timing of the tectonostratigraphic evolution of this orogen (e.g., Patacca and Scandone, 2007; Carminati and Doglioni, 2012; Vitale and Ciarcia, 2013). The northern Calabria–southern Apennines system (Fig. 1A) forms a segment of the Alpine belt in the central-western Mediterranean Sea (Fig. 1B). The first general tectonostratigraphic model of the orogenic wedge architecture at shallow crustal levels was proposed in the 1960s–1970s (Selli, 1962; Ogniben,

Sabatino Ciarcia https://orcid.org/0000-0003-3741-6029
Stefano Vitale https://orcid.org/0000-0003-1952-0463
†stefano.vitale@unina.it

GSA Bulletin; https://doi.org/10.1130/B37474.1.

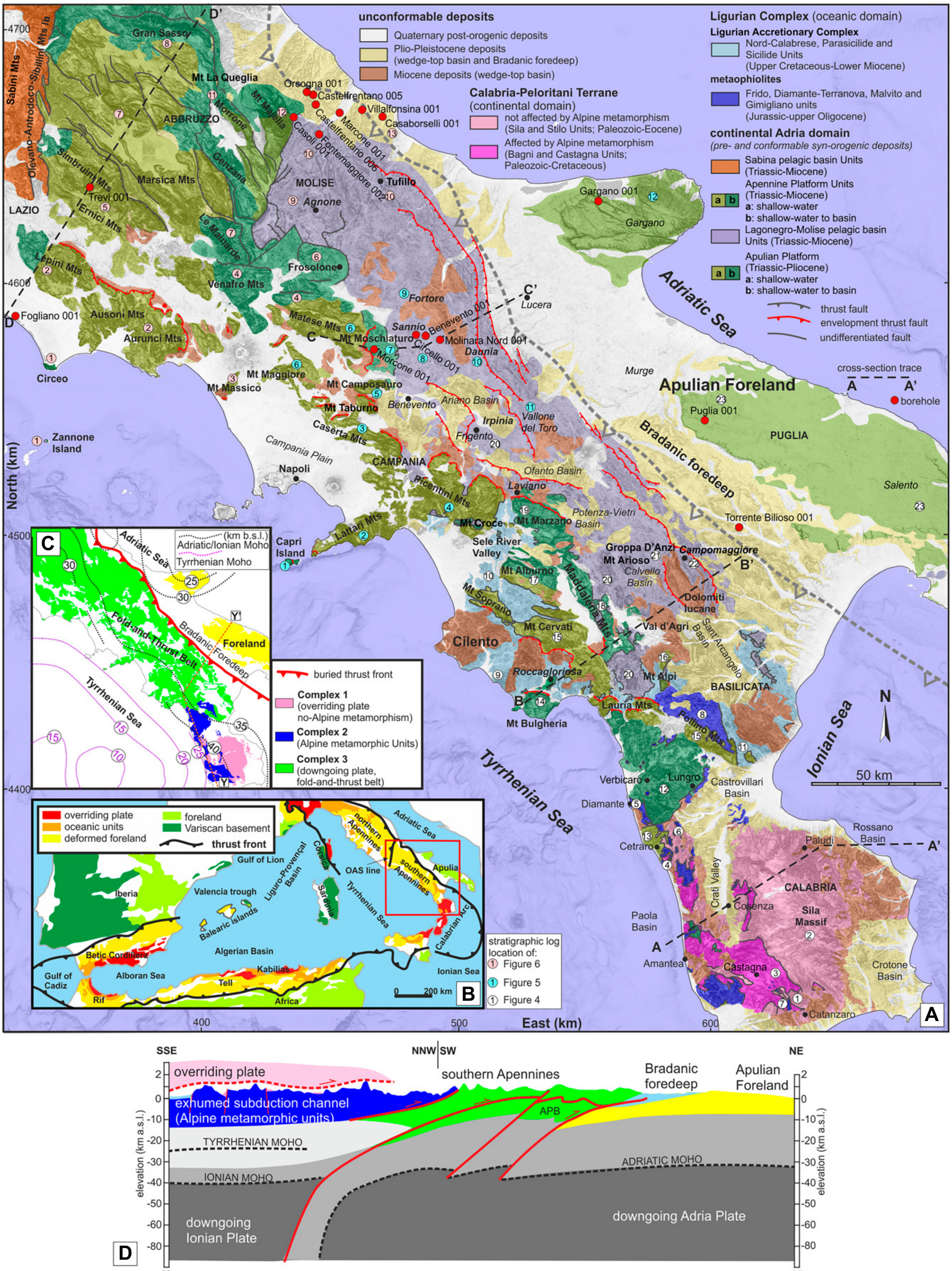
unconformable deposits
Quaternary post-orogenic deposits
Plio-Pleistocene deposits (wedge-top basin and Bradanic foredeep)
Miocene deposits (wedge-top basin)
Calabria-Peloritani Terrane (continental domain)
not affected by Alpine metamorphism (Sila and Stilo Units; Paleozoic-Eocene)
Affected by Alpine metamorphism (Bagni and Castagna Units; Paleozoic-Cretaceous)
Ligurian Complex (oceanic domain)
Ligurian Accretionary Complex
Nord-Calabrese, Parasicilide and Sicilide Units (Upper Cretaceous-Lower Miocene)
metaophiolites
Frido, Diamante-Terranova, Malvito and Gimigliano units (Jurassic-upper Oligocene)
continental Adria domain
(pre- and conformable syn-orogenic deposits)
Sabina pelagic basin Units (Triassic-Miocene)
Apennine Platform Units (Triassic-Miocene)
a: shallow-water
b: shallow-water to basin
Lagonegro-Molise pelagic basin Units (Triassic-Miocene)
Apulian Platform (Triassic-Pliocene)
a: shallow-water
b: shallow-water to basin
thrust fault
envelopment thrust fault
undifferentiated fault
cross-section trace
borehole
Adriatic Sea
Apulian Foreland
Bradanic foredeep
Tyrrhenian Sea
Ionian Sea
50 km
North (km)
East (km)
buried thrust front
Complex 1 (overriding plate no-Alpine metamorphism)
Complex 2 (Alpine metamorphic Units)
Complex 3 (downgoing plate, fold-and-thrust belt)
(km b.s.l.)
Adriatic/Ionian Moho
Tyrrhenian Moho
Fold-and-Thrust Belt
Foreland
Bradanic Foredeep
overriding plate
oceanic units
deformed foreland
foreland
Variscan basement
thrust front
stratigraphic log location of:
Figure 6
Figure 5
Figure 4
SSE
NNW
SW
NE
southern Apennines
Bradanic foredeep
Apulian Foreland
exhumed subduction channel (Alpine metamorphic units)
APB
TYRRHENIAN MOHO
IONIAN MOHO
ADRIATIC MOHO
downgoing Ionian Plate
downgoing Adria Plate
elevation (km a.s.l.)
A
B
C
D

Figure 1. (A) Geologic map of the northern Calabria–southern Apennines (NCSA) system (modified after Vitale and Ciarcia, 2022). UTM coordinate system, WGS84 global datum. (B) Tectonic sketch of western-central Mediterranean Alpine belts (modified after Vitale et al., 2015). OAS—Olevano-Antrodoco-Sibillini line. (C) Map of the orogenic complexes. (D) Schematic lithospheric cross section through northern Calabria, southern Apennines and Apulian Foreland (the trace Y–Y′ is shown in Fig. 1C). APB— buried Apulian Platform; a.s.l.—above sea level; b.s.l.—below sea level.

1969; D'Argenio et al., 1973; Amodio-Morelli et al., 1976); this model interpreted the tectonic structure as having formed by the superposition of different allochthonous thrust sheets, including metamorphic and sedimentary successions. Generally speaking, the chain is defined along a transect running from northern Calabria to the southern Apennines (Figs. 1C and 1D), and it is composed of a tectonic pile formed by Paleozoic basement and Mesozoic sediments (overriding plate) and covering metamorphic units (derived from both oceanic and continental domains), which, in turn, are superposed onto a nonmetamorphic fold-and-thrust belt made of continental successions from the downgoing Adria plate. However, a great leap forward in knowledge of the structure at depth was achieved through hydrocarbon exploration with several hundreds of boreholes that reached a maximum depth of 7 km (Visibility of Petroleum Exploration Data in Italy [ViDEPI Project], 2009–2015) and the Crosta Profonda (CROP) Project, with tens of seismic lines that investigated down to 15 km (http://www.crop.cnr.it), including the CROP04 profile through the southern Apennines (e.g., Cippitelli, 2007; Patacca and Scandone, 2007). Although different and sometimes contrasting interpretations of the tectonic architecture have been proposed, seismic and borehole data mark the existence of a buried imbricated parautochthonous belt made of Apulian Platform carbonates below the allochthonous Apennine wedge. More recent studies (Casero et al., 1988; Doglioni et al., 1996; Menardi Noguera and Rea, 2000; Shiner et al., 2004; Mazzoli et al., 2006, 2008; Scrocca, 2010; Cippitelli, 2007; Carminati and Doglioni, 2012; Vitale and Ciarcia, 2013) highlight the general structure of the southern Apennines as defined by prevailing low-angle thrusts separating the major thrust sheets, which are, in turn, crosscut by high-angle thrusts nucleated in the Apulian Platform carbonates. These different thrust faults resulted from alternating thin- and thick-skinned tectonics, with a prevalence of the latter during the Pliocene, which triggered deep breaching thrusting (e.g., Butler, 1987; Morley, 1988) or envelopment thrusting (Bally et al., 1966) and significant surficial out-of-sequence thrusting that involved the wedge-top basin deposits (Vitale et al., 2017, 2020a, 2020b).

The northern Calabria–southern Apennines system (Fig. 1A) resulted from the subduction of Neo-Tethys (Ligurian) oceanic lithosphere under the Europe/Calabria-Peloritani terrane starting during Paleocene–Eocene time (Schenk, 1980; Rossetti et al., 2001, 2004; Lustrino et al., 2009; Vignaroli et al., 2012; Vitale et al., 2019a) and subsequently from the deformation of the continental Adria slab in the Oligocene–middle Pleistocene time range. It is considered to be a retreating thrust belt where the subduction rate exceeds the convergence rate (Royden, 1993), triggering the formation of back-arc basins of the Ligurian-Provençal and Tyrrhenian Seas and stretching of the overriding plate, including the Sardinia-Corsica and Calabria-Peloritani terrane blocks (Faccenna et al., 1996; Gueguen et al., 1998; Martin, 2006; Carminati and Doglioni, 2012).

During the Oligocene–middle Pleistocene, the thrust front–foredeep–forebulge system mainly migrated toward the E/SE (e.g., Vitale and Ciarcia, 2013; Sabbatino et al., 2020, 2021), and foredeep sedimentation was generally preceded by emersion and erosion of the shallow-water domains caused by flexure of the downgoing Adria plate (forebulge stage; Sabbatino et al., 2020). The youngest foredeep basin sediments (Table 1) constrain the lower timing limit of thrust-front migration. In contrast, the oldest overlying unconformable wedge-top basin deposits (Table 2), locally sealing contacts between different thrust sheets, fix the upper temporal limit of the thrusting pulse (e.g., Cosentino et al., 2003; Bonardi et al., 2009; Vitale and Ciarcia, 2013, 2018).

This study aimed to combine the vast amounts of available stratigraphic and tectonic data to provide a coherent stratigraphic framework of the successions cropping out in the northern Calabria–southern Apennines system and a model of the orogenic evolution from the Eocene to Pleistocene consistent with the stratigraphic evolution of the synorogenic deposits. Compared to previous works (e.g., Vitale and Ciarcia, 2013, and references therein), the main novelty is the detailed description of the foreland basin system deposits, paying particular attention to the forebulge-related deposits, which constrain the architecture of the foreland during orogenic evolution. Furthermore, the provided paleogeographic maps and reconstruction of the orogenic evolution highlight the role of out-of-sequence thrusting events associated with the deep-seated structures involving the buried Apulian Platform carbonates. We have reinterpreted the available literature to reach this purpose, joining stratigraphic and tectonic data, and we used metamorphic and thermochronologic data to better reconstruct the orogenic accretion, subduction, and exhumation history of the thrust sheets of the northern Calabria–southern Apennines system following the forebulge stage.

Furthermore, we furnish an up-to-date framework of tectonic vergence data available from the literature that were restored according to the orogenic rotations resulting from the recent paleomagnetism studies. These data were combined with the paleogeographic maps to better constrain the thrust-front migrations during the late Oligocene to Pleistocene.

2. GEOLOGIC SETTING

From a paleogeographic point of view, the northern Calabria–southern Apennines system (Fig. 1A) includes tectonic units derived from (1) the overriding plate, including Paleozoic crystalline basement (Calabria-Peloritani terrane; Bonardi et al., 2001), (2) the oceanic to ocean-continent transition basin, and (3) the continental Adria plate (e.g., Mazzoli et al., 2008).

To better illustrate the tectonic architecture of the northern Calabria–southern Apennines system, we present some geologic cross sections representative of northern Calabria (Fig. 2, A–A′), and the southern (Fig. 2, B–B′), central (Fig. 2, C–C′), and northern (Fig. 2, D–D′) sectors of the southern Apennines, extending from the carbonate relief of the Aurunci, Ausoni, Lepini, Simbruini, Marsica, Gran Sasso, Morrone, and Majella Mountains in the north down to the mountains located at the northern Calabria-Basilicata boundary to the south (Fig. 1A). The northern and southern Apennines are separated by the Olevano-Antrodoco-Sibillini line (Parotto and Praturlon, 1975), consisting of a thrust fault active in the late Messinian–early Pliocene interval (Calamita et al., 2012).

The orogenic structure includes the superposition of three orogenic complexes (Fig. 1C). Complex 1, located on the top of the chain, comprises remnants of the overriding plate (Calabria-Peloritani terrane), which cover an Alpine metamorphic belt (complex 2) corresponding to the exhumed subduction channel, formed by Calabria-Peloritani terrane units, metamorphic ophiolitic units, and some metamorphic Meso-zoic–Cenozoic thrust sheets of the continental

TABLE 1. DESCRIPTION OF THE CONFORMABLE SYNOROGENIC DEPOSITS AND THEIR ACRONYMS USED IN THE TEXT WITH AGES AND REFERENCES

Acronym	Formation name and reference(s)	Stratigraphic age and reference(s)
AAF	Anversa degli Abruzzi Fm (Patacca et al., 1992a)	Upper Messinian (“lago-mare”)–Lower Pliocene p.p. (Cipollari et al., 1999)
ALB	Arenarie di Albanella Fm (Donzelli and Crescenti, 1962; Selli, 1962)	Middle Burdigalian (Critelli et al., 1994)
ANR	Calcareniti di Andrano Fm (Martinis, 1967)	Lower Messinian (ISPRA, 2013)
APV3	Flysch della Vallimala Fm (Scandone and Sgrosso, 1974); La Foresta Mb (ISPRA, 2016c)	Serravallian p.p.–lower Tortonian? (ISPRA, 2016c)
ARM	Clays and marls (ViDEPI Project, 1962)	Upper Pliocene–Lower Pleistocene (ViDEPI Project, 1962)
ARZ	Arenarie di Zannone (Pantosti and Velonà, 1986; Pantosti et al., 1986)	Lower Miocene (Pantosti and Velonà, 1986; Pantosti et al., 1986)
ASP	Argille Subappennine and Montemarano sands fms (Servizio Geologico d’Italia, 1968b, 1971)	Lower Pleistocene (ISPRA, 2017a)
AVG	Mezzana di Forte Fm (Basso et al., 2002); Argille Varicolori with gypsum (Vitale and Ciarcia, 2018)	Upper Messinian–lowermost Zanclean (Vitale and Ciarcia, 2018)
AVS	Argille Varicolori Superiori Fm (Ogniben, 1969)	Aquitanian p.p.–lower Burdigalian (Ciarcia et al., 2009a)
BIF	Arenarie del Bifurto Fm (Selli, 1957)	Upper Burdigalian–Langhian (ISPRA, 2014b)
BSM	Calcarenite Coralligena di Serra del Mito Fm (ISPRA, 2013)	Langhian–Tortonian? (ISPRA, 2013)
CAR	Mt. Caramola Fm (Bonardi et al., 1993)	Upper Eocene–Oligocene (Vitale et al., 2013b)
CBZ	Calcari a Briozoi a Litotamni Fm (Accordi et al., 1967; Civitelli and Brandano, 2005)	Upper Burdigalian–upper Serravallian (Sabbatino et al., 2021; ISPRA, 2010c)
CDR	Calcareniti di Recommone Fm (Scandone and Sgrosso, 1965)	Burdigalian–Serravallian (ISPRA, 2014c)
CFR	Calcareniti a Macroforaminiferi Fm (ISPRA, 2010c)	Paleogene p.p.–Lower Miocene (ISPRA, 2010c)
CON	Contursi Fm (Ciarcia et al., 2009a)	Aquitanian–lower Burdigalian (Ciarcia et al., 2009a)
CTT	Calcari di Trombetta Fm (ISPRA, 2017b)	Upper Messinian (ISPRA, 2017b)
CUS	Cusano Fm (Selli, 1957)	Burdigalian–lower Serravallian (ISPRA, 2015)
FAE	Faeto Fm (Crostella and Vezzani, 1964)	Upper Burdigalian–Tortonian (ISPRA, 2011b)
FCE	Cerchiara Fm (Selli, 1957)	Middle Aquitanian–lower Burdigalian (ISPRA, 2016b, 2010a, 2014b)
FFA	Frasci Fm (ISPRA, 2016c)	Upper Cretaceous–Aquitanian p.p. (ISPRA, 2016c)
FFP	Fontana Porcellara Fm (ISPRA, 2016c)	Aquitanian p.p. (ISPRA, 2016c)
FFS	Frosinone Fm (Accordi, 1964)	Upper Tortonian (Accordi, 1964; Cosentino et al., 2003)
FLB3	Alberosa Fm, Serra Costantino Mb (ISPRA, 2010e)	Oligocene–Lower Miocene (ISPRA, 2010e)
FMJ	Flysch della Majella (Patacca et al., 1992a)	Middle–upper Zanclean (Cosentino et al., 2003)
FMS	Monte Sant’Arcangelo Fm (Selli, 1962)	Oligocene–Aquitanian p.p. (Ciarcia et al., 2009a; Vitale et al., 2019a)
FYB	Flysch di S. Biase Fm (ISPRA, 2011c)	Upper Tortonian–lower Messinian (ISPRA, 2011c)
FYN	Numidian Flysch Fm (Ogniben, 1960)	Uppermost Burdigalian–Langhian (Patacca et al., 1992b)
GES	Gessoso-Solfifera Fm (Selli, 1960)	Messinian (ISPRA, 2010 g)
GIP	Argilliti e Calcari di San Giovanni a Piro Fm (ISPRA, 2016b)	Aquitanian–Burdigalian p.p. (ISPRA, 2016b)
GIP1	Argilliti e Calcari di San Giovanni a Piro Fm, Aria della Serra Mb (ISPRA, 2016b)	Lower (Middle p.p.?) Miocene (ISPRA, 2016b)
GOD	Macchiagodena Fm (Pescatore, 1965)	Oligocene–Burdigalian p.p. (ISPRA, 2015)
GRA	Calcareniti di Gravina Fm (Servizio Geologico d’Italia, 1968b)	Piacentian?–Gelasian (ISPRA, 2017b)
GUA	Guadagnolo Mb (ISPRA, 2021)	Lower Miocene p.p. (ISPRA, 2021)
LAF	Laga Fm (Scarsella, 1953)	Messinian (ISPRA, 2010d)
LAP	Lama dei Peligni Flysch (Patacca and Scandone, 2021)	Lower Pliocene p.p. (Patacca and Scandone, 2021; ViDEPI Project, 1956b, 1958, 1981)
LAV	Laviano Fm (Selli, 1957)	Serravallian p.p.–lower Tortonian (ISPRA, 2016c)
LBG	Limestone with bryozoa and glauconite fm (ViDEPI Project, 1958)	Oligocene–Middle Miocene (ViDEPI Project, 1958)
LIT	Lithothamnion limestone fm (Patacca and Scandone, 2021)	Tortonian p.p.–Messinian p.p. (Patacca and Scandone, 2021)
LNG	Longano Fm (Selli, 1957)	Lower Serravallian p.p.–middle Tortonian (ISPRA, 2015)
LUT	Calcareniti di Cava Iannazzo Fm (ISPRA, 2014b)	Upper Tortonian–lower Messinian (ISPRA, 2014b)
MLB	Marly limestone with reworked bryozoan unit (ViDEPI Project, 1983)	Messinian (ViDEPI Project, 1983)
MRD	Marne Rosse e Verdi di Colle Dolce Fm (ISPRA, 2011c)	Upper Burdigalian–Langhian? (ISPRA, 2011c)
MSO	Flysch del Molise Fm (ISPRA, 2011c)	Upper Tortonian–lower Messinian (ISPRA, 2011c, 2015)
OBF	Occhio del Bue Succession (Cosentino et al., 2002)	Upper Serravallian (Cosentino et al., 2002)
ORB	Orbulina Limestone Fm (Patacca and Scandone, 2007)	Langhian p.p.–Tortonian p.p. (Patacca and Scandone, 2021)
PAA	Serra Palazzo Fm (Selli, 1962)	Upper Burdigalian–Serravallian p.p. (ISPRA, 2017a)
PBB	Calcareniti e Calciruditi di Pietrabbondante Fm (ISPRA, 2011c)	Lower Miocene? (ISPRA, 2011c)
PLE	Pietra Leccese Fm (D’Erasmo, 1956)	Middle–Upper? Miocene (Servizio Geologico d’Italia, 1969; ISPRA, 2013; Mazzei et al., 2009)
PRJ	Flysch di Pietraroja (Selli, 1957)	Middle–upper Tortonian (Bonardi et al., 2009)
RIV	Mt. Crivari Fm (ISPRA, 2015)	Langhian?–lower Serravallian p.p. (ISPRA, 2015)
SAR	Saraceno Fm (Selli, 1962)	Upper Eocene–lowermost Aquitanian (Vitale and Ciarcia, 2018; ISPRA, 2016b)
SCA*	Scaglia-type Fm (ISPRA, 2007b, 2007c, 2007d)	Upper Albian p.p.–Lower Miocene p.p. (ISPRA, 2007b, 2007c, 2007d)
SCAd	Scaglia Detritica Fm (ISPRA, 2011a, 2010d, 2016a)	Cenomanian p.p.–Oligocene (ISPRA, 2011a, 2010d, 2016a)
SER	Serroni Fm (Basso et al., 2002)	Serravallian–lower Messinian (Vitale and Ciarcia, 2018)
SFL	Scisti del Fiume Lao (Burton, 1971)	Upper Aquitanian–upper Burdigalian (Iannace et al., 2007)
SFT	Unità Spongolitica Fm (ISPRA, 2010d)	Lower Miocene (ISPRA, 2010d)
SGG	San Giorgio Fm (Selli, 1962)	Upper Serravallian–middle Tortonian (Pescatore et al., 2008; Vitale and Ciarcia, 2018)
SOV	Sovereto Fm (ISPRA, 2016b)	Lower Aquitanian–lowermost Burdigalian (Vitale and Ciarcia, 2018; ISPRA, 2016b)
TFA	Torrente Flaga Fm (ISPRA, 2017a)	Serravallian p.p.–Tortonian (ISPRA, 2017a)
TFI	Torre Fico succession (Pantosti et al., 1986)	Middle–Upper Miocene (Pantosti et al., 1986; Pantosti and Velonà, 1986)
TFL	Tufillo Fm (Patacca et al., 1992a)	Upper Langhian–upper Tortonian (ISPRA, 2011c)
TIT	Conglomerati e Arenarie di Cima S. Croce Fm (ISPRA, 2014b)	Lower Messinian (ISPRA, 2014b)
TMI	Arenarie di Termini Fm (ISPRA, 2014c)	Serravallian? (ISPRA, 2014c)
TPC	Toppo Capuana Fm (Crostella and Vezzani, 1964)	Upper Tortonian–lower Messinian (ISPRA, 2011b)
TPL	Tripoli Fm (ISPRA, 2017b)	Lower Messinian (ISPRA, 2017b)
TRB	Trubi Fm (ISPRA, 2007e)	Lower Pliocene (ISPRA, 2007e)
TUT	Tufiti di Tusa Fm (Ogniben, 1960)	Middle Burdigalian (Lentini, 1979; Zuppetta et al., 1984)
UAM	Marne ad Orbulina Mb (ISPRA, 2006)	Middle Miocene p.p.–Upper Serravallian–Messinian (ISPRA, 2006)
UGC	Uggiano La Chiesa Fm (ISPRA, 2013)	Upper Piacentian?–Gelasian (ISPRA, 2013)

Note: The list is in alphabetical order. Fm—Formation; Mb—Member; p.p.—pro parte.
*The Scaglia-type deposits include different diachronous sediments with an age ranging between late Albian p.p. and early Miocene p.p.

Adria plate (downgoing plate). Finally, this orogenic prism tectonically covers a thrust-and-fold belt (complex 3) defined by a series of stacked thrust sheets, including successions of different paleoenvironments, from deep basin to shallow-water platform (e.g., Mostardini and Merlini, 1986; Casero et al., 1988; Doglioni et al., 1996; Ciarapica and Passeri, 1998; Menardi Noguera and Rea, 2000; Faccenna et al., 2001a, 2001b;

TABLE 2. DESCRIPTION OF THE UNCONFORMABLE SYNOROGENIC DEPOSITS AND THEIR ACRONYMS USED IN THE TEXT WITH AGES AND REFERENCES

Acronym	Formation name and reference(s)	Stratigraphic age and reference(s)
PLU	Paludi Fm (Dubois, 1976)	Upper Oligocene–Aquitanian (Bonardi et al., 2005)
Cilento Group (CIG)		
POL	Pollica Fm (Ietto et al., 1965)	Burdigalian/Langhian boundary–Langhian (Amore et al., 1988)
MAU	San Mauro Fm (Ietto et al., 1965)	Serravallian–lower Tortonian (Amore et al., 1988; Russo et al., 1995)
ABD	Albidona Fm (Selli, 1962; Vezzani, 1970)	Langhian–lower Tortonian (ISPRA, 2014b, 2016b)
Castelvetere Group (CVTG)		
MSA	Mt. Sacro Fm (Selli, 1962)	Upper Tortonian(?)–Lower Pliocene(?) (ISPRA, 2016b)
RMA	Ruditi dei Monti Alburni Fm (Santo, 1996)	Middle–upper Tortonian (Bonardi et al., 2009)
ATP	Arenarie di Toppa del Prato Fm (Patacca et al., 1992a)	Middle–upper Tortonian (Bonardi et al., 2009)
SIE	Mt. Siero Fm (Castellano and Sgrosso, 1996)	Upper Tortonian (ISPRA, 2010a, 2014a)
PON	Vallone Ponticello Fm (Basso et al., 2002)	Middle/upper Tortonian (Ciarcia et al., 2009b)
BPC	Brecce di Punta del Capo Fm (De Blasio et al., 1981)	Upper Tortonian (ISPRA, 2011a)
CVT	Castelvetere Fm (Pescatore et al., 1970)	Upper Tortonian–lower Messinian (Critelli and Le Pera, 1995)
SBO	San Bartolomeo Fm (Crostella and Vezzani, 1964)	Middle/upper Tortonian–lower Messinian (ISPRA, 2010f)
GOR	Flysch di Gorgoglione Fm (Selli, 1962)	Upper Tortonian (Bonardi et al., 2009)
ORI	Oriolo Fm (Selli, 1962)	Upper Tortonian–lower Messinian (Critelli, 1999)
CAI	Arenarie di Caiazzo Fm (Ogniben, 1957)	Upper Tortonian–lower Messinian (ISPRA, 2010b)
PER	Perosa succession (Vezzani, 1966)	Middle/upper Tortonian (Vezzani, 1966)
GTC	Gavignano-Gorga Fm (Alberti et al., 1975)	Upper Tortonian (Cipollari and Cosentino, 1995; Cosentino et al., 2003)
TOR	Arenarie di Torrice Fm (La Monica, 1966)	Lower Messinian (Cipollari and Cosentino, 1995)
VRT	Falvaterra Chaotic Complex (Centamore et al., 2007)	Lower Messinian (ISPRA, 2011d)
ROS	Rossano and Crotone Basin deposits (Ogniben, 1962; Roda, 1964)	Serravallian–Tortonian (Barone et al., 2008; Vignaroli et al., 2012; Massari and Prosser, 2013)
AMA	Amantea Basin deposits (Perri, 1996; Mattei et al., 2002)	Serravallian–Tortonian (Perri, 1996; Mattei et al., 2002)
Altavilla Group (ALTG)		
COP	Mt. Coppe Fm (Patacca et al.,1992a), including Lago-Mare facies (Cipollari et al., 1999)	Uppermost Messinian–Zanclean p.p. (Patacca et al.,1992a; Cipollari et al., 1999)
VIC	Le Vicenne conglomerates fm (Colacicchi et al., 1967)	Uppermost Messinian–Zanclean p.p. (Cipollari et al., 1999)
ANZ	Anzano Fm (Crostella and Vezzani, 1964)	Uppermost Messinian–Zanclean p.p. (ISPRA, 2011b)
ALT	Altavilla Unit (Ippolito et al., 1973)	Uppermost Messinian–Zanclean p.p. (Vitale and Ciarcia, 2013)
BAR	Baronia Fm (Ciarcia and Vitale, 2013)	Upper Zanclean (Amore et al., 1998; Ciarcia et al., 2003; ISPRA, 2011b; Ascione et al., 2012)
MCR	Minturno (Servizio Geologico d'Italia, 1968a), Campobasso (Servizio Geologico d'Italia, 1970b) and Rigopiano Fms (Centamore et al., 1992)	Upper Zanclean (Centamore et al., 1992; Patacca et al., 1992a; ISPRA, 2015)
SFE	Sferracavallo Fm (Ciarcia et al., 2003)	Piacentian (Amore et al., 1998; Ciarcia et al., 2003; ISPRA, 2011b; Ascione et al., 2012)
CMU	Castilenti and Mutignano Fm (Ghisetti and Vezzani, 1988a)	Lower Piacentian (Vezzani and Ghisetti, 1998a)
ARC	Sant'Arcangelo Basin deposits (Pieri et al., 1994)	Upper Piacentian–uppermost Calabrian (Patacca and Scandone, 2001; Di Stefano et al., 2002; Sabato et al., 2005; ISPRA, 2005d; Ascione et al., 2012)

Note: The list is in age order. Fm—Formation; Mb—Member; p.p.—pro parte.

Catalano et al., 2004; Shiner et al., 2004; Guerrera et al., 2005; Patacca and Scandone, 2007; Mazzoli et al., 2008; Bonardi et al., 2009; Cosentino et al., 2010; Scrocca, 2010; Vezzani et al., 2010; Roure et al., 2012; Vitale and Ciarcia, 2013; Bucci et al., 2014; Vitale and Ciarcia, 2018; Guerrera et al., 2020; Vitale et al., 2020a, 2020b; Vitale and Ciarcia, 2022). The youngest thrust front is buried below the Bradanic foredeep basin deposits (e.g., Tropeano et al., 2002). The exposed carbonates of the Puglia region and the Adriatic Sea represent the current foreland (Fig. 1C). Figure 1C also shows the isobaths of the Adriatic/Ionian and Tyrrhenian Moho discontinuities. The schematic cross section in Figure 1D illustrates the current lithospheric architecture along a transect running from northern Calabria to the Puglia region (trace in Fig. 1C), along with the subduction of Ionian oceanic lithosphere.

Complex 1 (Fig. 1C) is formed by Variscan Paleozoic continental crust and related sedimentary Mesozoic cover (Sila and Stilo Units). Complex 2 (Fig. 1C) includes all successions affected by Alpine metamorphism, comprising (i) the Castagna and Bagni Units of the Calabria-Peloritani terrane (Amodio-Morelli et al., 1976; Bonardi et al., 2001); (ii) meta-ophiolites of the Diamante-Terranova, Malvito, Gimigliano, and Frido Units (Figs. 1A and 2; Amodio-Morelli et al., 1976; Bonardi et al., 2001; Rossetti et al., 2001, 2004; Liberi et al., 2006; Liberi and Piluso, 2009; Vitale et al., 2019a, and references therein); and (iii) the Lungro-Verbicaro and Cetraro Units of continental Adria (Iannace et al., 2007; Vitale et al., 2020c). Cross-section A–A′ (Fig. 2), showing a transect across northern Calabria, highlights a western sector formed by the superposition of different high-pressure–low-temperature (HP-LT) metamorphic units, including Calabria-Peloritani terrane units above the Ligurian meta-ophiolites, in turn overlying the Apennine Platform units. The Sila Unit tectonically covers all these thrust sheets. In the eastern sector, the latter unit is widespread and crosscut by NE-verging thrust faults that deform the wedge-top basin deposits of the Paludi Formation (Table 2), which are both unconformably topped by Rossano Basin deposits (Table 2).

Complex 3 (Fig. 1C) is composed of the sedimentary (i) Nord-Calabrese, Parasicilide, and Sicilide Units (Ligurian accretionary complex; Figs. 1A and 2; Selli, 1962; Ogniben, 1969; Bonardi et al., 1988a; Ciarcia et al., 2009a, 2012; Vitale et al., 2010, 2019a) and (ii) continental Adria units of the Mesozoic–Cenozoic Apennine and Apulian Platforms and the Lagonegro-Molise Basin (D'Argenio et al., 1973; Bonardi et al., 1988b; Patacca and Scandone, 1989; Bigi et al., 1992; Cosentino et al., 2003; Patacca and Scandone, 2007; Bonardi et al., 2009) detached from their pre-Triassic basement in the central and external sectors of the chain (Fig. 2, cross-section C–C′; e.g., Casero et al., 1988; Menardi Noguera and Rea, 2000; Shiner et al., 2004; Cippitelli, 2007).

The shallow crustal structure of the southern part of the southern Apennines (Fig. 2, cross-sections B–B′ and C–C′) is dominated by low-angle thrusts between (i) oceanic units (on the top; Ligurian complex; Fig. 1A), (ii) carbonate platform/slope successions of the Apennine Platform, and (iii) thrust sheets of the pelagic

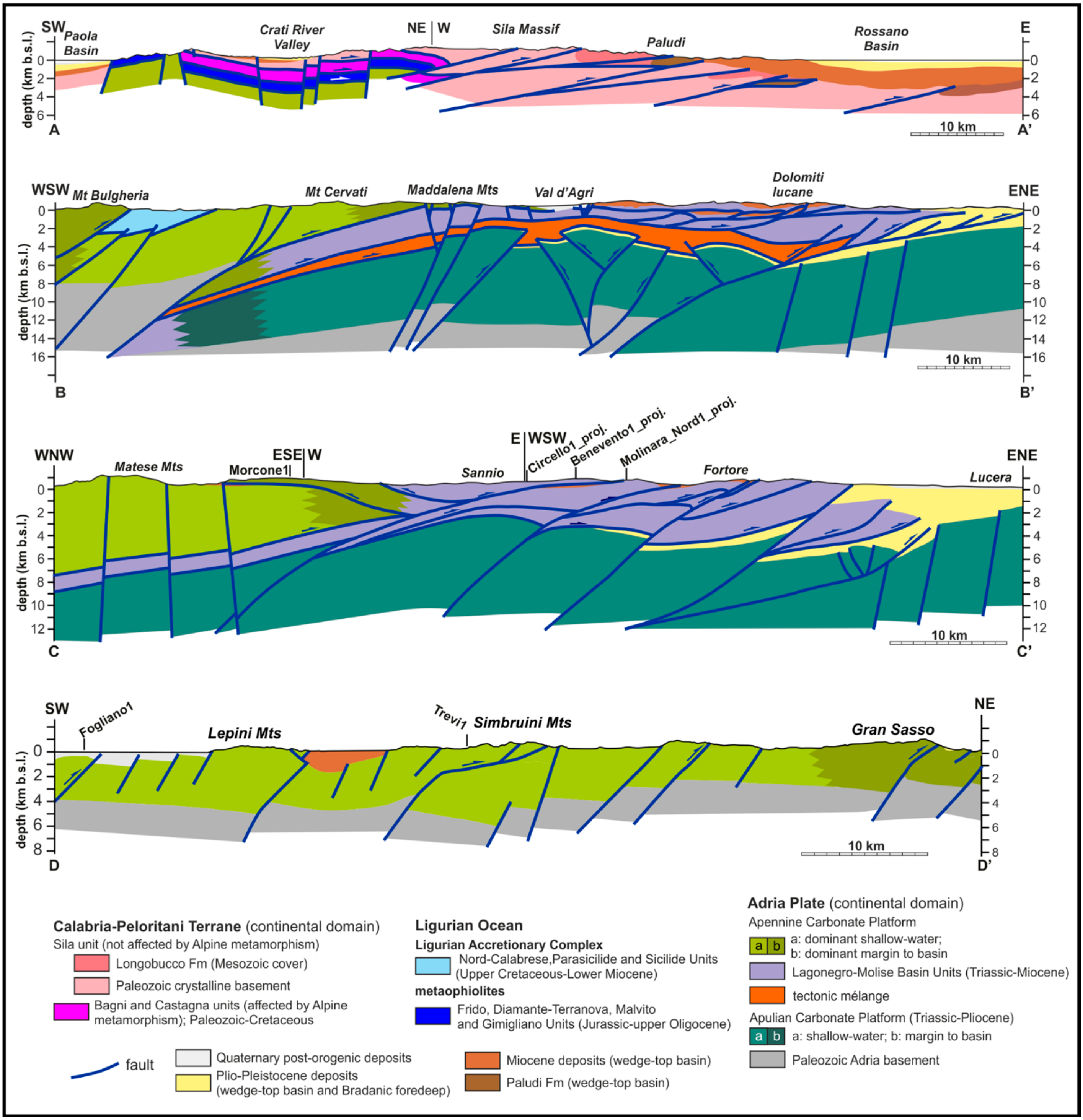

Figure 2. Geologic cross-sections A–A′ (modified after Vitale et al., 2019a), B–B′ (slightly modified after Mazzoli et al., 2013), C–C′ (slightly modified after Vitale and Ciarcia, 2018), and D–D′ (modified after Tozer et al., 2002); b.s.l.—below sea level.

Lagonegro-Molise Basin successions (Mostardini and Merlini, 1986). On the contrary, at depth, the crustal structure is characterized by high-angle faults affecting the buried Apulian Platform and the allochthonous wedge (Fig. 2, cross-sections B–B′ and C–C′). The northern sector of the southern Apennines (Fig. 2, cross-section D–D′) is less shortened compared to the southern sector and consists of a tectonic pile characterized by high-angle thrusts rooted in the Paleozoic basement still attached to the Mesozoic–Cenozoic cover (e.g., Tozer et al., 2002).

According to several paleogeographic reconstructions (e.g., Rossetti et al., 2004; Schettino and Turco, 2011; Vezzani et al., 2010; Patacca and Scandone, 2007, 2011), the pre-orogenic paleogeography of the western-central Mediterranean area (latest Cretaceous–Paleocene;

Fig. 3A; modified after Vitale and Ciarcia, 2013) shows the Ligurian Ocean separating the continental sector of the European plate, which includes the Calabria-Peloritani terrane and the Sardinia-Corsica block, from the Africa-Adria plate. In this period, the Alps were forming from the subduction of the oceanic part of the European plate (Piemont Ocean) beneath the continental part of the Adria plate (Handy et al., 2010; Schmid et al., 1996). In contrast, the southern part of the continental Adria plate and the northern sector of the Africa plate were undergoing crustal stretching, interpreted as the result of a rifting stage (Vitale and Ciarcia, 2022, and references therein) or a far-field stress state associated with the orogenic processes that involved the northern edge of the Adria plate (Agosta et al., 2021). In this reconstruction (Fig. 3A), the Ligurian and Ionian Oceans were separated by a strip joining the continental parts of the Adria and Africa plates. In Cretaceous time, this continental bridge between the two plates allowed dinosaurs to migrate between the two sectors (Zarcone et al., 2010). However, in the latest Cretaceous, this emerged/shallow-water area partially drowned, resulting in the complete separation of the Apennine (Adria domain) and Panormide (Africa domain) Platforms (Vitale et al., 2013a; Vitale and Ciarcia, 2022), despite the fact that the two parts (Apennine and Panormide Platforms) still belonged to a single plate (e.g., Channell, 1996).

The close-up map of the Apennine Platform/Lagonegro-Molise Basin/Apulian Platform area (Fig. 3B; Vitale and Ciarcia, 2022) shows the articulated pre-orogenic paleogeography of the southern continental sector of the Adria plate. To reconstruct this paleogeography, we started from the available maps (Vezzani et al., 2010; Patacca and Scandone, 2007, 2011; Vitale and Ciarcia, 2013, 2022). In particular, we considered the paleoenvironments reconstructed for the major successions, including the uppermost Cretaceous–Paleocene shallow-water and margin to slope-basin deposits of the Apennine and Apulian Platforms, and the pelagic basin successions of the Lagonegro-Molise Basin domain. In this reconstruction, the Apennine-Apulian Platform system was isolated, surrounded by pelagic basins, including the Lagonegro-Molise Basin to the south, the Ligurian Ocean to the west, the Umbria-Marche Basin to the north, and, finally, the Adriatic Basin to the east (Fig. 3B). It is worth noting that the Apulian Platform hosts a NW-SE–elongated basin where pelagic sediments were deposited, as shown in borehole reconstructions (Patacca and Scandone, 2014).

In the next section, we describe the stratigraphy of the pre-orogenic successions of the three main complexes (Calabria-Peloritani terrane, oceanic units, and continental Adria units). Figures 4, 5, and 6 show stratigraphic logs of the major tectonic units and representative stratigraphic successions, grouped in agreement with their paleogeographic locations

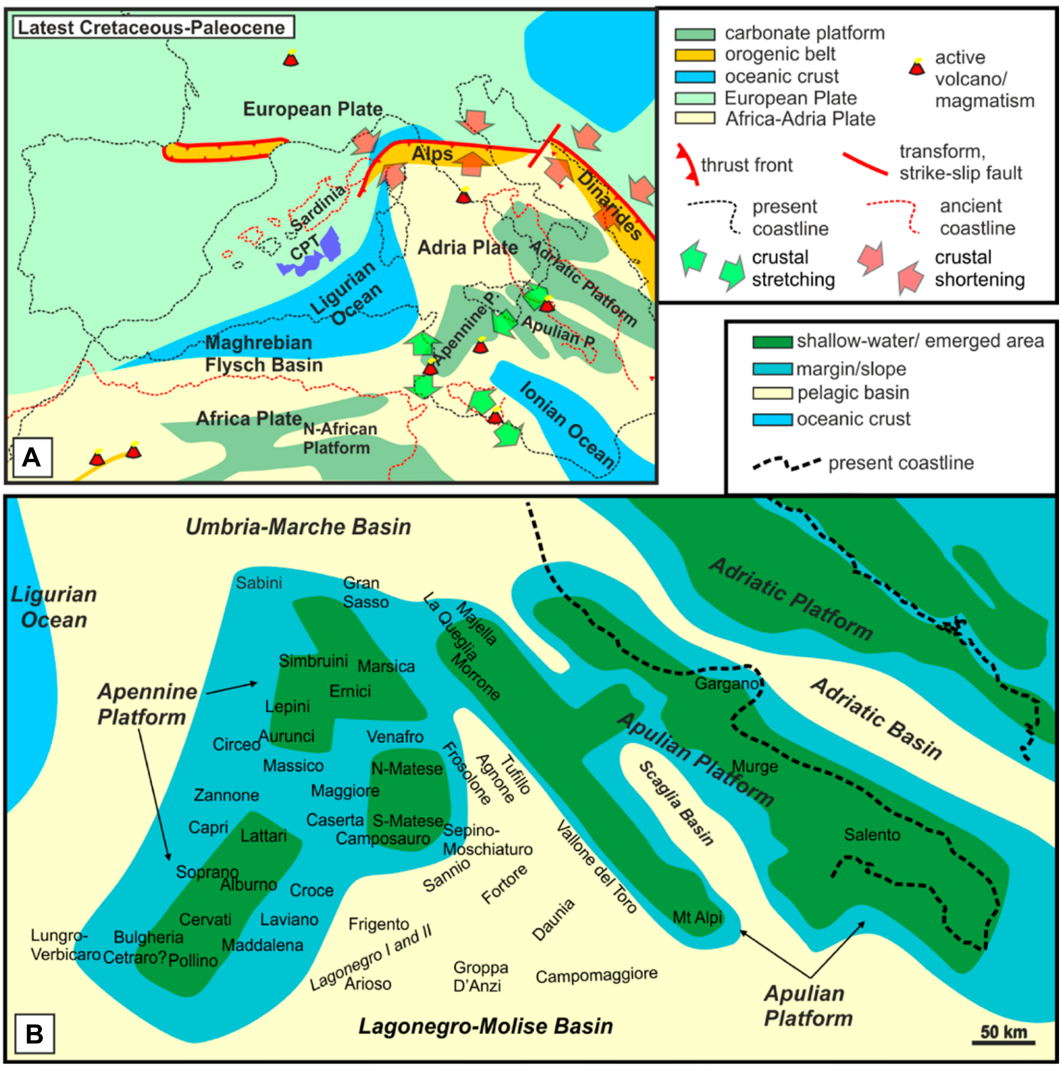

Figure 3. Latest Cretaceous–Paleocene paleogeographic maps: (A) western-central Mediterranean area (modified after Vitale and Ciarcia, 2013) and (B) close-up of the Apennine Platform/Lagonegro-Molise Basin/Apulian Platform area (modified after Vitale and Ciarcia, 2022). CPT—Calabria-Peloritani terrane; P.—Platform.

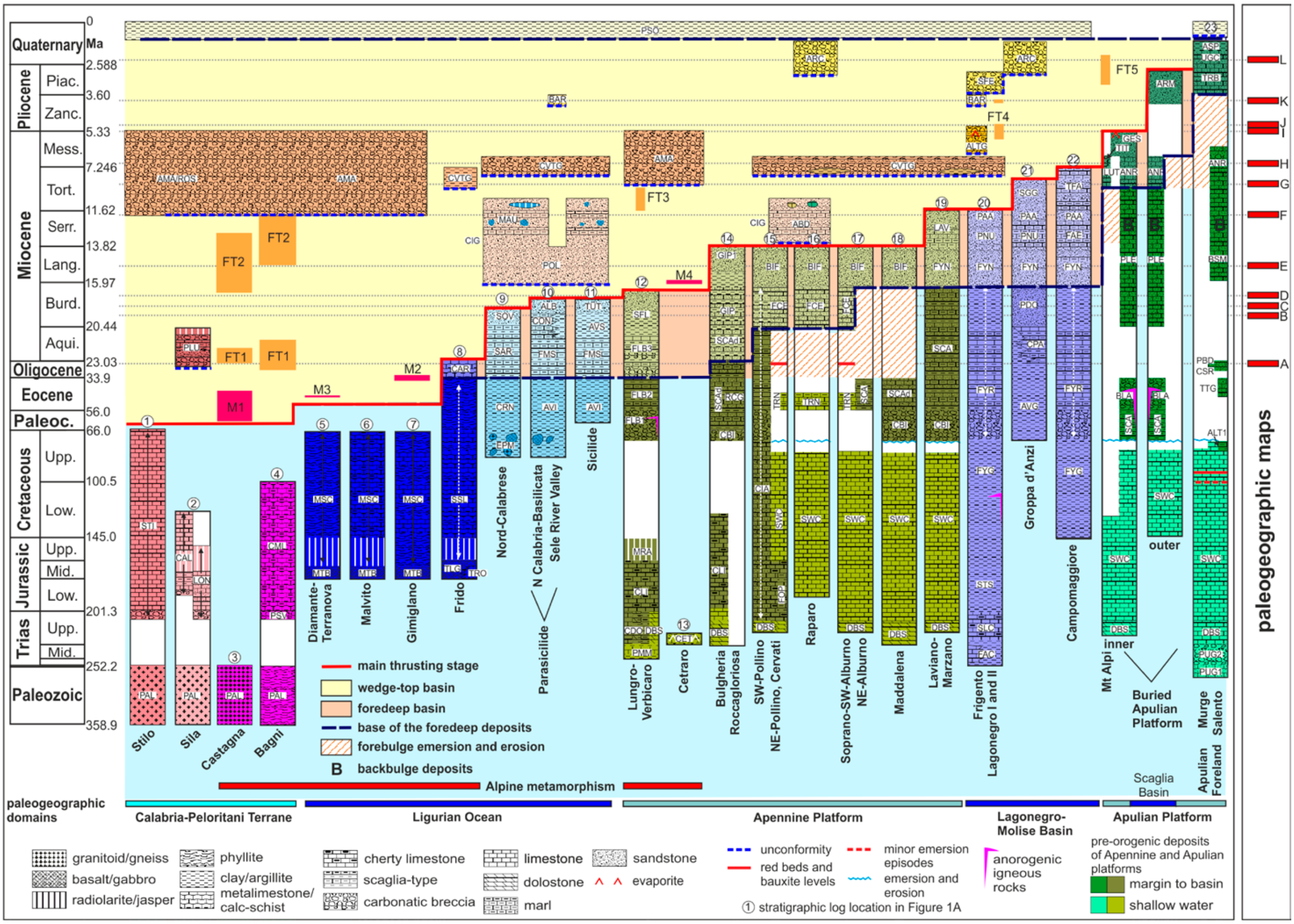

Figure 4. Schematic stratigraphic logs of the northern Calabria-southern Apennines (southern sector). Southern sector, Calabria-Peloritani terrane: CAL—Caloveto and Longobucco groups; CML—cherty meta-limestone; PAL—Paleozoic basement; PSV—Pseudo-Verrucano Formation (Fm). Ligurian Ocean: ALB—Albanella Fm; AVI—Argille Varicolori Inferiori Fm; AVS—Argille Varicolori Superiori Fm; CAR—Mount Caramola Fm; CON—Contursi Fm; CRN—Crete Nere Fm; EPM—Episcopia mélange; FMS—Mount Sant'Arcangelo Fm; MSC—undifferentiated metasedimentary cover; MTB—undifferentiated metabasalts; NRV—Noce River Valley mélange; POS—Postiglione Fm; SAR—Saraceno Fm; SOV—Sovereto Fm; SSL—S. Severino Lucano Fm; TLG—Tempa La Guardia Fm; TRO—Tempa Rotalupo Fm; TUT—Tufiti di Tusa–Arenarie di Corleto Fms. Apennine Platform: BIF—Bifurto Fm; CBI—Calcari Cristallini Fm; CDO—cherty dolomites; CIA—slope limestones of Pollino-Ciagola Unit; CLI—cherty limestone; DBS—Dolomia Superiore Fm; FCE—Cerchiara Fm; FLB1—Alberosa Fm (Brecce Poligeniche member [mb]); FLB2—Alberosa Fm (Calcari a Nummiliti mb); FLB3—Alberosa Fm (Serra Costantino mb); FOP—Dolomie e Calcari di Monte Foraporta Fm; FYN—Numidian Flysch Fm; GIP—Argilliti e Calcari di S. Giovanni a Piro Fm; LAV—Laviano marls, calcarenites, and sandstones; MRA—meta-radiolarites; PMM—phyllites, meta-limestones, and meta-renites; RCG—Calcari e Argilliti di Roccagloriosa Fm; SCA—Scaglia-type deposits; SCAd—Scaglia Detritica–type deposits; FL—Scisti del F. Lao Fm; CET—Cetraro Unit; SWC—Jurassic–Cretaceous shallow-water carbonates; TRN—Trentinara Fm. Lagonegro-Molise Basin: AVG—Argille Variegate Fm; CPA—Corleto Perticara Fm; FAC—Monte Facito Fm; FAE—Faeto Fm; FYG—Flysch Galestrino Fm; FYN—Numidian Flysch Fm; FYR—Flysch Rosso Fm; PAA—Serra Palazzo Fm; PDO—Paola Doce Fm; PNU—post-Numidian succession; SGG—San Giorgio Fm; SLC—Calcari con Selce Fm; STS—Scisti Silicei Fm; TFA—Torrente Flaga Fm. Apulian Platform: ALT1—Calcare del Ciolo mb (Calcare di Altamura Fm); ANR—Calcareniti di Andrano Fm; ARM—clay and marl of buried outer Apulian Platform; ASP—Argille Subappennine and Montemarano sands Fms; BLA—Brecce di Lavello Fm; BSM—Calcarenite Coralligena di Serra del Mito Fm; CSR—Calcare di Castro Fm; DBS—Dolomia Superiore Fm; GES—Gessoso-Solfifera Fm; LAP—Lama dei Peligni Flysch; LUT—Calcareniti di Cava Iannazzo; PBD—Calcareniti di Porto Badisco Fm; PLE—Pietra Leccese Fm; PUG1—sandstones; PUG2—breccias; SCA—Scaglia-type deposits; SWC—Jurassic–Cretaceous shallow-water carbonates (Calcari di Bari and Calcari di Altamura Fms); TIT—Conglomerati e Arenarie di Cima S. Croce; TTG—Calcare di Torre Tiggiano; TRB—Trubi Fm; UGC—Uggiano La Chiesa Fm. Wedge-top deposits: ABD—Albidona Fm (CIG); ALTG—Altavilla Group; AMA—Amantea; ARC—S. Arcangelo Basin deposits; BAR—Baronia Fm; CVTG—Castelvetere Group; MAU—S. Mauro Fm (CIG); PLU—Paludi Fm; PER—Perosa Fm; POL—Pollica Fm (CIG); ROS—Rossano basin deposits; SFE—Sferracavallo Fm. Postorogenic successions: PSO—Upper Pleistocene to present deposits. Metamorphic ages: M1—

Castagna Unit (Schenk, 1980); M2—Gimigliano Unit (Rossetti et al., 2001, 2004); M3—Diamante-Terranova Unit (Shimabukuro et al., 2012); M4—Cetraro Unit (Iannace et al., 2007). Thermochronologic ages: Castagna and Bagni Units—FT1 zircon fission tracks (Thomson, 1998), FT2 apatite fission tracks (Thomson, 1998); Lungro-Verbicaro Unit—FT3 apatite fission tracks (Iannace et al., 2007); Lagonegro I and II Units—FT4 apatite fission tacks (Mazzoli et al., 2008); M. Alpi—FT5 apatite fission tracks (Mazzoli et al., 2006). Other abbreviations: Paleoc.—Paleocene; Aqui.—Aquitanian; Burd.—Burdigalian; Lang.—Langhian; Serr.—Serravallian; Tort.—Tortonian; Mess.—Messinian; Zanc.—Zanclean; Piac.—Piacenzian; Low.—Lower; Mid.—Middle; Upp.—Upper.

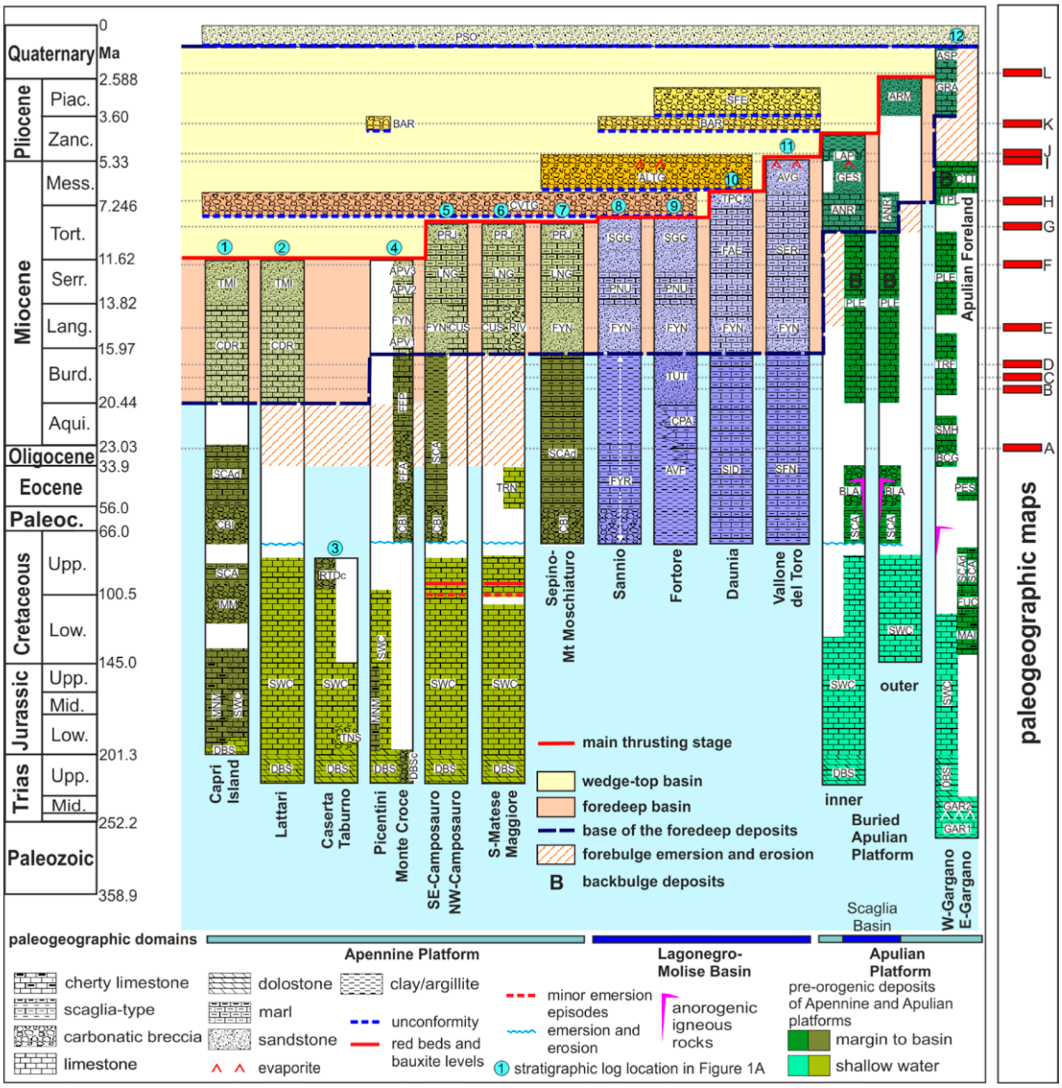

Figure 5. Schematic stratigraphic logs of the northern Calabria-southern Apennines (central sector). Central sector, Apennine Platform: APV1—Serra della Manca Member (Mb) (Flysch della Vallimala Formation [Fm]); APV2—Serralonga Mb (Flysch della Vallimala Fm); APV3—La Foresta Mb (Flysch della Vallimala Fm); BDSc—reworked Dolomia Superiore Fm; CBI—Calcari Cristallini Fm; CDR—Calcareniti di Recommone Fm; CUS—Cusano Fm; DBS—Dolomia Superiore Fm; FFA—Frasci Fm; FFP—Fontana Porcellara; FPJ—Pietraroja Fm; FYN—Numidian Flysch Fm; IMM—Calciruditi e Calcareniti del Limmo Fm; LNG—Longano Fm; MNM—Calcari e Dolomie con selce dei Monti Mai Fm; REC—Calcareniti di Recommone Fm; RIV—Mount Crivari Fm; RTDc—reworked Calcari a Radiolidliti Fm; SCA—Scaglia-type deposits; SCAd—Scaglia Detritica–type deposits; SWC—Jurassic–Cretaceous shallow-water carbonates; TMI—Arenarie di Termini Fm; TNS—Conglomerati Calcarei di Tuoro Maleconsiglio; TRN—Trentinara Fm. Lagonegro-Molise Basin: AVF—Argille Varicolori del Fortore Fm; AVG—Argille Varicolori with gypsum; CPA—Corleto Perticara Fm; FAE—Faeto Fm; FYN—Numidian Flysch Fm; FYR—Flysch Rosso Fm; PNU—post-Numidian succession; SER—Serroni Fm; SFN—Serra Funaro Fm; SGG—San Giorgio Fm; SID—Mount Sidone Fm; TPC—Toppo Capuana Fm; TUT—Tufiti di Tusa Fm. Apulian Platform: ANR—Calcareniti di Andrano Fm; ARM—clay and marl of buried outer Apulian carbonate platform; ASP—Argille Subappennine and Montemarano sands formations; BCG—Breccia di Cagnano Fm; CTT—Calcari di Trombetta, Brecce e Conglomerati di Stazione S. Giacomo and Calcari di Fiumicello Fms; DBS—Dolomia Superiore Fm; FUC—Marne a Fucoidi Fm; GAR1—shales, dolostones, and limestones; GAR2—sandstones, dolostones, and limestones; GRA—Calcareniti di Gravina Fm; GES—Gessoso-Solfifera Fm; LAP—Lama dei Peligni Flysch; LAV—Brecce di Lavello Fm; MAI—Maiolica Fm; PES—Peschici Fm; PLE—Pietra Leccese Fm; SCA—Scaglia-type deposits; CAd—Scaglia Detritica–type deposits; SMH—Calcari di Grotta San Michele Fm; SWC—Jurassic–Cretaceous shallow-water carbonates (Calcari di Bari and Calcari di Altamura Fms); TPL—Tripoli Fm; TRF—Torre Rossa Fm. Wedge-top deposits: CVTG—Castelvetere Group; ALTG—Altavilla Group; BAR—Baronia Fm; SFE—Sferracavallo Fm. Postorogenic successions: PSO—Upper Pleistocene to present deposits. Other abbreviations: Paleoc.—Paleocene; Aqui.—Aquitanian; Burd.—Burdigalian; Lang.—Langhian; Serr.—Serravallian; Tort.—Tortonian; Mess.—Messinian; Zanc.—Zanclean; Piac.—Piacenzian; Low.—Lower; Mid.—Middle; Upp.—Upper.

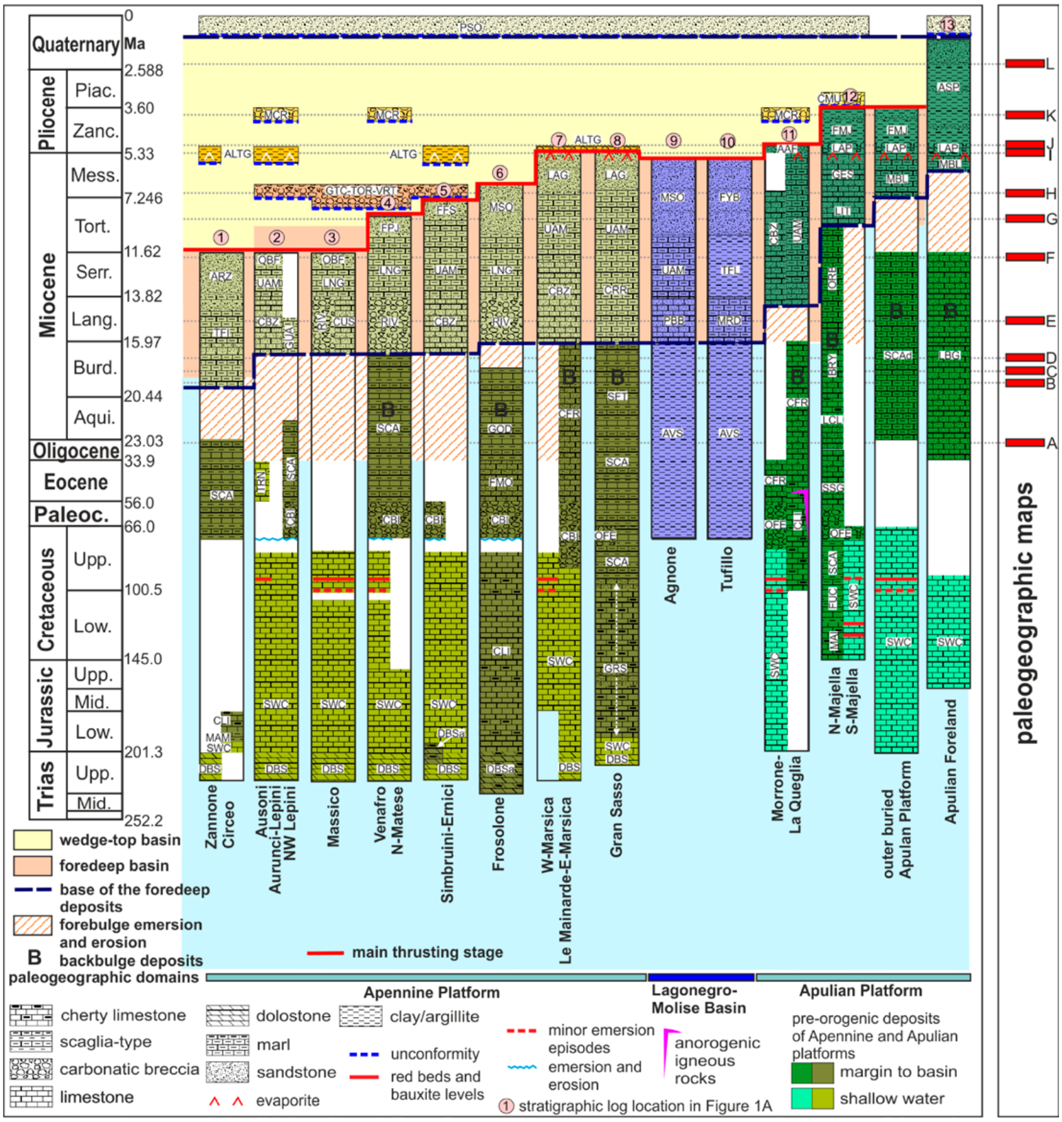

Figure 6. Schematic stratigraphic logs of the northern Calabria-southern Apennines (northern sector). Northern sector, Apennine Platform: AAF—Anversa degli Abruzzi Formation (Fm); ARZ—Arenarie di Zannone; CBI—Calcari Cristallini Fm; CBZ—Calcari a Briozoi a Litotamni Fm; CFR—Calcareniti a Macroforaminiferi Fm; CLI—cherty limestones; CRR—Marne con Cerrogna Fm; CUS—Cusano Fm; DBS—Dolomia Superiore Fm; DBSa—cherty dolomites; FFS—Frosinone Fm; FMO—Monaci Fm; FPJ—Pietraroja Fm; FYB—Flysch di S. Biase Fm; GOD—Macchiagodena Fm; GRS—Corniola, Verde Ammonitico e Calcari e Marne a Posidonia, Calcari Bioclastici Inferiori, Calcari Diasprigni, Maiolica Detritica, Calcari Bioclastici Superiori and Calcareniti e Calciruditi a Fucoidi Fms; GUA—Guadagnolo Member (Mb); LAF—Laga Fm; LNG—Longano Fm; MAM—marls with ammonites; MSO—Flysch del Molise Fm; OBF—Occhio del Bue succession; OFE—Orfento Fm; RIV—Mount Crivari Fm; SCA—Scaglia-type deposits; SFT—Unità Spongolitica Fm; TFI—Torre Fico succession; SWC—Jurassic–Cretaceous shallow-water carbonates; TFL—Tufillo Fm; UAM—Marne a Orbuline, and Argille a Orbulina Fms. Lagonegro-Molise Basin: AVS—Argille Varicolori Superiori Fm; MRD—Marne Rosse e Verdi di Colle Dolce Fm; MSO—Flysch del Molise Fm; PBB—Calcareniti e Calciruditi di Pietrabbondante Fm; UAM—Argille a Orbulina Fm. Apulia Platform: ASP—Argille Subappennine and Montemarano sands formations; BRY—bryozoan limestone fm; FMJ—Flysch della Majella Fm; FUC—Marne a Fucoidi Fm; GES—Gessoso-Solfifera Fm; LAP—Lama dei Peligni Flysch; LBG—limestone with bryozoa and glauconite; LCL—*Lepidociclina* and *Cerratina* cherty limestones fms; LIT—lithothamnion limestone fm; MAI—Maiolica Fm; MBL—marly limestone with reworked bryozoan unit; OFE—Orfento Fm; ORB—*Orbulina* limestone fm; SCA—Scaglia-type deposits; SSG—Santo Spirito Group; SWC—Jurassic–Cretaceous shallow-water carbonates (Calcari di Bari and Calcari di Altamura Fms). Wedge-top deposits: ALTG—Altavilla Group; CMU—Castilenti and Mutignano Fms; GTC—Gavignano-Gorga, and Torrice Fms; MCR—Minturno conglomerates, Campobasso conglomerates, and Rigopiano Fm. Postorogenic successions: PSO—Upper Pleistocene to present deposits. Other abbreviations: Paleoc.—Paleocene; Aqui.—Aquitanian; Burd.—Burdigalian; Lang.—Langhian; Serr.—Serravallian; Tort.—Tortonian; Mess.—Messinian; Zanc.—Zanclean; Piac.—Piacenzian; Low.—Lower; Mid.—Middle; Upp.—Upper.

(Calabria-Peloritani terrane, Ligurian Ocean, Apennine Platform, Lagonegro-Molise Basin, and Apulian Platform) and separated into (1) pre-orogenic, (2) conformable synorogenic (foredeep and backbulge basin deposits), (3) unconformable synorogenic (wedge-top basin deposits), and (4) postorogenic rocks. From left to right, the order of the stratigraphic logs follows the ages of the foredeep deposits or the youngest ages of the pre-orogenic rocks. The synorogenic succession will be described in the subsequent section within the orogenic evolution of the northern Calabria–southern Apennines system.

3. STRATIGRAPHY OF THE PRE-OROGENIC SUCCESSIONS

In the following descriptions, we consider the pre-orogenic successions, defined as all the deposits that formed before the forebulge and foredeep stages (Figs. 4, 5, and 6). The

Calabria-Peloritani terrane and meta-ophiolites of the Diamante-Terranova, Malvito, and Gimigliano successions are all characterized by pre-orogenic rocks with ages older than the Paleocene–Eocene, i.e., the time proposed for the onset of oceanic subduction (Schenk, 1980; Rossetti et al., 2001; Lustrino et al., 2009; Vignaroli et al., 2012; Vitale et al., 2019a). On the contrary, the Frido, Ligurian accretionary complex, and continental Adria successions were all formed by pre- and synorogenic successions, with ages varying according to their paleogeographic positions. The first orogenic event recorded in the continental part of the Adria plate was the Oligocene forebulge stage that produced uplift and erosion of the Apennine Platform and sedimentation in the surrounding basins. Subsequently, the forebulge ridge migrated toward E/NE (Sabbatino et al., 2020). In our reconstruction, the pre-orogenic successions are all deposits older than (1) Eocene for the Gimigliano, Malvito, and Diamante-Terranova Units, (2) Oligocene for the Frido, Nord-Calabrese, Sicilide, and Parasicilide Units, and the western side of the Apennine Platform (Lungro-Verbicaro Unit), (3) Aquitanian–Langhian for central and eastern sectors of the Apennine Platform and the Lagonegro-Molise Basin, (4) Serravallian–Tortonian for the buried Apulian Platform, and, finally, (5) Messinian–Zanclean for the exposed Apulian Platform.

The continental sector of the Adria plate experienced different pre-orogenic tectonic episodes of rifting. This area recorded a Late Triassic–Early Jurassic extensional event that profoundly changed the shallow-water domain that characterized the Late Triassic paleogeography (Bosellini and Hsü, 1973). This rifting stage produced an articulated paleogeography characterized by two main carbonate platforms (Apennine and Apulian) defined by shallow-water areas passing to surrounding pelagic basins through margin and slope environments. The Apennine Platform passed southward to the Panormide Platform (Sicily), which was connected to the Constantine Platform (Tunisia) (e.g., Randazzo et al., 2021). The Lagonegro-Molise Basin was a pelagic realm between the Apennine and Apulian Platforms (Mostardini and Merlini, 1986). This part of Adria underwent a new extensional stage in the Late Cretaceous–Eocene (Vitale and Ciarcia, 2022) that further dismembered the original shallow-water domains, creating new slope-to-basin areas, including the Scaglia Basin within the Apulian Platform (Fig. 3B; Mostardini and Merlini, 1986; Patacca and Scandone, 2014). This event also caused the separation of the Apennine Platform from the Panormide Platform (Vitale et al., 2013a). We refer to the latest Cretaceous–Paleocene paleogeography shown in Figure 3 as the starting point for the Eocene–Holocene stratigraphic and tectonic reconstructions.

3.1. Calabria-Peloritani Terrane (Northern Calabria)

The successions referred to the Calabria-Peloritani terrane exposed in northern Calabria (Bonardi et al., 2001) are formed by the Stilo, Sila, Castagna, and Bagni Units (Fig. 4). The Stilo Unit (Bonardi et al., 2001) consists of Silurian–Lower Carboniferous phyllites, meta-arenites, quartzites, meta-limestones, porphyroids, metabasites, muscovite-biotite hornfels, mica schists, paragneisses, amphibolites, Ca-silicate granofels, and Carboniferous–Permian metaluminous granites/granodiorites and peraluminous leucogranites (Paleozoic basement). Variscan metamorphism grading from lower greenschist facies to upper amphibolite facies and late Variscan, up-to-amphibolite hornfels–facies metamorphism, characterize the Paleozoic basement. The Mesozoic–Cenozoic sedimentary cover of the Stilo Unit (Bonardi et al., 2001; Perri et al., 2011) consists of continental Verrucano-like deposits, Upper Triassic in age, passing upward to Upper Triassic–Jurassic dolomites, calcareous breccias, and neritic limestones, followed by Cretaceous limestones and breccias with rudists, and Chattian–Aquitanian lepidocycline and lithothamnion-rich calcarenites.

The Sila Unit (Bonardi et al., 2001; Langone et al., 2010, and references therein) is composed of Paleozoic basement and Mesozoic cover. The former includes (1) Upper Cambrian to Lower Carboniferous low-grade metamorphic rocks (Bocchigliero Complex), (2) Paleozoic low- to medium-grade metamorphic rocks (Mandatoriccio Complex), (3) Paleozoic medium- to high-grade metamorphic rocks (Monte Gariglione–Polia–Copanello Complex), and, finally, (4) Upper Carboniferous–Lower Permian plutonic rocks. The Mesozoic cover is formed by the Longobucco and Caloveto Groups. The Longobucco Group (Young et al., 1986; Passeri et al., 2014; Innamorati and Santantonio, 2018; Santantonio and Fabbi, 2020) consists of Rhaetian–Sinemurian p.p. continental red beds passing to mixed carbonate-siliciclastic shelf sediments, followed by Sinemurian p.p. to Kimmeridgian? deeper shelf-basin environment marls bearing ammonites and belemnites, siliciclastic turbidites, pelagic *Posidonia* limestones with cherty limestone-bearing calciclastic turbidites, and pelagic polychrome radiolarian cherts.

The Caloveto Group (Santantonio and Teale, 1987; Innamorati and Santantonio, 2018; Santantonio and Fabbi, 2020) is composed of Pliensbachian p.p.–Lower Toarcian conglomerates, followed by shallow-water limestones with coral buildups. The succession continues with Toarcian–Hauterivian unconformable *Posidonia* marls, radiolarian cherts, *Saccocoma* and *Aptychus* limestones, and *Maiolica*-like limestones.

The Castagna Unit (Bonardi et al., 2001; Tursi et al., 2020) is formed by a Paleozoic basement of paragneisses, mica schists, augen gneisses, metagranitoids, amphibolites, marbles, and Ca-silicate granofels, characterized by pre-Variscan and late Variscan intermediate to felsic intrusive rocks. The orthogneisses have magmatic protoliths dated at ca. 545 Ma (Fornelli et al., 2020).

Finally, the Bagni Unit (Bonardi et al., 2001) shows a Paleozoic basement of phyllites, metaconglomerates, meta-arenites, quartzites, porphyroids, and metabasites, covered by Late Triassic Verrucano-type continental clastics (PSV), followed by Jurassic–Lower Cretaceous pelagic limestones, radiolarites, and massive dolomites (CMI).

3.2. Ligurian Ocean

In northern Calabria, oceanic successions are exposed under the Calabria-Peloritani terrane units, whereas in the southern Apennines, they are located on the top of the orogenic wedge. The Ligurian successions (Fig. 4) include the meta-ophiolites of the Diamante-Terranova, Malvito, Gimigliano, and Frido Units (Liberi et al., 2006; Liberi and Piluso, 2009; Vitale et al., 2019a) and the sedimentary successions of the Nord-Calabrese, Parasicilide, and Sicilide Units (Ligurian accretionary complex; Selli, 1962; Bonardi et al., 1988a; Di Staso and Giardino, 2002; Guerrera et al., 2005; Bonardi et al., 2009; Ciarcia et al., 2009a, 2012; Vitale et al., 2013a; Critelli, 2018; Vitale et al., 2019a, and reference therein). The Diamante-Terranova, Malvito, and Gimigliano Units are all characterized by Alpine HP-LT metamorphism. They are exposed in northern Calabria (Fig. 1A) and include Middle Jurassic metabasalts (MTB) at the base, covered by Dogger (Middle Jurassic) meta-radiolarites and Cretaceous cherty meta-limestones and metapelites (MSC). Unlike the other meta-ophiolites, the Alpine HP-LT, ocean-continent transition Frido Unit includes continental crustal masses (granitoids and gneisses; TRO) alternating with oceanic crust (TLG) at the base. The pre-orogenic succession evolves to Dogger (Middle Jurassic) meta-radiolarites and Cretaceous–Oligocene phyllites, calc-schists, and quartzites (SSL). The Ligurian accretionary complex successions are detached from their basement and are probably made of ocean-continent transition crust (Vitale et al., 2013a). They mainly crop out in the Cilento area, Sele River Valley, and Basilicata region (Fig. 1A). The pre-orogenic Nord-

Calabrese succession is formed by Upper Cretaceous–Eocene black shales (CRN) embedding the Episcopia tectonic mélange (EPM); on the other hand, the Parasicilide and Sicilide deposits consist of Upper Cretaceous–Eocene deep-water varicolored argillites (AVI) at places including basaltic clastics.

3.3. Continental Adria Plate

3.3.1. Apennine Platform

The pre-orogenic successions referred to this paleogeographic domain include deposits sedimented along the western margin, platform sensu stricto, and eastern margin (e.g., D'Argenio et al., 1973; Pescatore and Sgrosso, 1973; Parotto and Praturlon, 1975, 1981; Bonardi et al., 2009; Cosentino et al., 2003; Patacca and Scandone, 2007; Vitale and Ciarcia, 2013, 2018; Cardello et al., 2021). From south to north, the western margin is represented by the Alpine metamorphic units of Lungro-Verbicaro and Cetraro (Fig. 4) and the sedimentary successions of the SW Pollino Mountains, Mount Bulgheria, Roccagloriosa, Capri Island, Zannone Island, Mount Circeo, and some sectors of the Lepini and Simbruini Mountains (Bonardi et al., 2009; Iannace et al., 2007; Pantosti and Velonà, 1986; Pantosti et al., 1986; Patacca and Scandone, 2007; Scandone et al., 1964; Vitale and Ciarcia, 2013, 2018, 2022; ISPRA, 1997, 2005a). The platform sensu stricto includes the successions of NE Pollino, Cervati, Raparo, SW Alburno, Caserta, Taburno, Picentini, NW Camposauro, Matese, Maggiore, Pietravairano, Volsci Range (Aurunci, Ausoni, and Lepini), Massico, Simbruini, Ernici, and W Marsica Mountains (Bonardi et al., 2009; Cosentino et al., 2002, 2003, 2010; Damiani et al., 1992; Iannace et al., 2007; Patacca and Scandone, 2007; Vitale and Mazzoli, 2009; Vitale and Ciarcia, 2013, 2018; Cardello et al., 2021). The eastern margin encompasses the successions of Maddalena, NE Alburni, Marzano, Laviano, Croce, SE Camposauro, Sepino-Moschiaturo, Venafro, N Matese, Frosolone, Gran Sasso, and E Marsica Mountains (Bernoulli, 2001; Bonardi et al., 2009; Corrado et al., 1998; Cosentino et al., 2003, 2010; Patacca and Scandone, 2007; Patacca et al., 1992a; Vitale and Ciarcia, 2013, 2018, 2022).

3.3.1.1. Apennine Platform western margin. The Lungro-Verbicaro succession (Iannace et al., 2007) consists of Anisian–Carnian phyllites, meta-limestones, meta-arenites, and dolomites (PMM), Norian dolomites (DBS) and cherty dolomites (CDO), Jurassic cherty limestones (CLI), Dogger (Middle Jurassic) meta-radiolarites (MRA), Maastrichtian–Paleocene calcareous breccias and calcarenites (FLB1) with anorogenic basaltic intrusions (limburgites; Quitzow, 1935), and Eocene–Aquitanian Scaglia-type deposits (FLB2).

Carnian phyllites, meta-limestones, dolomites, and evaporites (CET; Iannace et al., 2007) characterize the Cetraro Unit (Dietrich, 1976). The SW Pollino Mountains (Fig. 4) consist of Norian shallow-water dolomites (DBS) upward passing to a Jurassic–Burdigalian margin succession formed by reworked limestones (CIA). The Mount Bulgheria succession (Fig. 4; ISPRA, 2016a, 2016b) is composed of shallow-water Norian dolomites (DBS) evolving upward to Jurassic–Lower Cretaceous cherty limestones (CLI), passing to Maastrichtian calcarenites and conglomerates with fragments of rudists (CBI) and Paleocene–Eocene Scaglia Detritica deposits (SCAd). The Roccagloriosa deposits (ISPRA, 2016a, 2016b) are similar to the aforementioned Maastrichtian–Eocene succession (RCG). The Capri Island succession (Fig. 5; ISPRA, 2011a) includes lowermost Jurassic shallow-water dolomites (DBS), evolving to Jurassic–Lower Cretaceous shallow-water (SWC) and margin-slope (MNM) limestones, Cretaceous calcareous breccias (IMM) and Scaglia-type deposits (SCA), calcareous breccia (CBI), and Eocene Scaglia Detritica deposits (SCAd).

At Zannone Island (Fig. 6; Pantosti et al., 1986), Norian dolomite (DBS) is covered by Maastrichtian–Eocene Scaglia-type limestones and marls with planktonic foraminifers (SCA; Segre, 1953). On the other hand, the Circeo succession (Pantosti and Velonà, 1986) comprises Lower Jurassic shallow-water limestones (SWC) passing to deep-basin marls with ammonites (MAM) and cherty limestones (CLI), capped by Maastrichtian–Eocene Scaglia-type deposits (SCA; Fogliano 001 well; ViDEPI Project, 1956a; Lombardi, 1968). NW Lepini and, locally, the Simbruini–Ernici Mountains (ISPRA, 1975) include Upper Triassic–Cretaceous shallow-water carbonates (DBS and SWC), calcareous breccia (CBI), and, in the NW Lepini Mountains (ISPRA, 2021), Eocene–Aquitanian p.p. Scaglia-type deposits (SCA).

3.3.1.2. Apennine Platform central sector. The platform sensu stricto facies (Figs. 4, 5, and 6) include Norian to Upper Cretaceous dominantly shallow-water carbonates (DBS and SWC), exposed from the Pollino Mountains to the Volsci-Simbruini and L'Aquila Mountains (D'Argenio et al., 1973; Damiani et al., 1992; Cipollari and Cosentino, 1995; Bonardi et al., 2009; Cosentino et al., 2002, 2003, 2010; Vitale and Ciarcia, 2013, and references therein). In the Simbruini Mountains (Filettino area), Rhaetian–Toarcian slope to basin cherty dolostones occur (Damiani et al., 1992).

In addition, some Triassic–Jurassic ephemeral intraplatform basin deposits are exposed in the Picentini Mountains (MNM; Iannace et al., 2005) and the Cervati Mountains (FOP; De Alfieri et al., 1986) made of cherty dolostones and limestones, conglomerates, and marls. The northern sector of the Apennine Platform (Camposauro, Maggiore, Matese, Ausoni, and W Marsica Mountains) presents Albian and Cenomanian bauxite levels (Boni et al., 2012); on the other hand, in the central sector (Soprano Mountains), only residual clays and terrestrial plant-rich fossil occur (Bartiromo et al., 2019). Generally, the shallow-water successions show a wide hiatus in the Late Cretaceous–Paleogene; however, in the southern sector (Cervati, SW Alburni, and Soprano Mountains) and locally in the northern part (Maggiore and Ausoni Mountains), Eocene shallow-water limestones, conglomerates, and green marls are locally present (TRN; Selli, 1957; Vecchio et al., 2006).

3.3.1.3. Apennine Platform eastern margin. The eastern margin of the Apennine Platform includes the successions of Maddalena, NE Alburni, Marzano, Laviano, Croce, SE Camposauro, Sepino-Moschiaturo, N Matese, Venafro, Mainarde, Frosolone, E Marsica, and Gran Sasso Mountains (Fig. 1A).

The Maddalena Mountains (Fig. 4; ISPRA, 2010a, 2014a; Vitale and Ciarcia, 2022), Mount Marzano, and Laviano successions (ISPRA, 2016c; Vitale et al., 2018) show shallow-water Norian–Upper Cretaceous successions (DBS and SWC) passing upward to Maastrichtian–Paleocene slope calcareous breccia (CBI) and Eocene nummulitids and alveolinids in calcarenites (SCA and SCAd). The Mount Croce deposits (Fig. 4), exposed in the Campagna tectonic window (Vitale et al., 2020b, and references therein), are characterized by Upper Triassic dolomite conglomerates (DBSc) covered by calcareous breccia (CBI) and Eocene–Aquitanian breccias (FFA), passing upward to Aquitanian–Burdigalian Scaglia-type rocks (FFP). The SE Mount Camposauro succession (Fig. 5; ISPRA, 2010b; Vitale and Ciarcia, 2022) and the Sepino-Moschiaturo (Fig. 5; Sgrosso, 1998; Vitale and Ciarcia, 2018, 2022), N Matese, Venafro, and Mainarde Mountains (Fig. 6; Cosentino et al., 2010; Vitale and Ciarcia, 2022) include shallow-water Norian–Upper Cretaceous carbonates (DBS and SWC) covered by calcareous breccia (CBI) and Eocene Scaglia-type deposits (SCA). The Frosolone succession (Fig. 6; ISPRA, 2015) is made of Upper Triassic cherty dolomites (DBSa; Frosolone 001 well; ViDEPI Project, 1961a) passing to Jurassic–Cretaceous cherty limestones (CLI), covered by calcareous breccia (CBI), Eocene nummulitids, and alveolinid calcarenites (FMO).

Upper Triassic–Cretaceous shallow-water carbonates (DBS and SWC), evolving to slope

Upper Cretaceous–Paleocene calcareous breccia (CBI) and finally Eocene calcarenites (CFR) form the Mainarde Mountains and E Mount Marsica (ISPRA, 2010c). The Gran Sasso Mount succession (ISPRA, 2010d) comprises Upper Triassic-Lower Jurassic shallow-water carbonates (DBS and SWC) at the base, passing upward to Lower Jurassic–Upper Cretaceous slope-to-basin bio- and litho-clastic limestones, marls, and jaspers (GRS). At Mount Prena–Vradda (Gran Sasso Mountain), Norian–Rhaetian bituminous dolostones occur, formed in euxinic intraplatform troughs (Cosentino et al., 2010). The succession continues with Upper Cretaceous–Aquitanian p.p. Scaglia-type deposits (SCA) locally, laterally passing to Campanian p.p.–Maastrichtian p.p. calcarenites (OFE; ISPRA, 2010d).

3.3.2. Lagonegro-Molise Basin

The deep-sea sedimentary successions, mainly exposed along the axial and external zones of the chain from southern Abruzzo to northern Calabria, belong to the vast pelagic realm of the Lagonegro-Molise Basin (Mostardini and Merlini, 1986). These successions form the following tectonic units, from south to north: Lagonegro I, Lagonegro II, Groppa d'Anzi, Campomaggiore, Sannio, Fortore, Daunia, Vallone del Toro, Tufillo, and Agnone (Basso et al., 2002; Bonardi et al., 2009; D'Argenio et al., 1973; Dazzaro et al., 1988; Pescatore et al., 1988, 2000; Patacca and Scandone, 2007; Patacca et al., 1992a; Vitale and Ciarcia, 2013, 2022; Milli et al., 2021).

The Lagonegro I and II Units (sensu Scandone, 1967, 1972; Fig. 4), otherwise named the Mount Arioso Unit (ISPRA, 2012; Di Nocera et al., 2011) in the Basilicata region or Frigento Unit (Basso et al., 2002; ISPRA, 2011b) in the Irpinia sector, consist, at the base, of Ladinian–Carnian slope-to-basin calcilutites and fine-grained sandstones with intercalations of recifal bodies (FAC), passing upward to Carnian–Norian cherty limestones (SLC) and Rhaetian–Jurassic radiolarites and reddish or greenish silicified argillites (STS), and, finally, to Lower Cretaceous dark silicified argillites with calcilutites and marls (FYG). Then, the succession evolves to slope-to-basin Upper Cretaceous–Burdigalian calciclastic coarse-to-fine sediments, marls, and varicolored clays (FYR). The Groppa d'Anzi Unit (Fig. 4; Pescatore et al., 1988) is formed by Upper Cretaceous(?)–Aquitanian varicolored clays and marls with calcilutites and calcarenites (AVG; ISPRA, 2007a), laterally passing, in the upper part, to Middle Eocene–Aquitanian marly limestones (CPA; Selli, 1962; Pescatore et al., 2000) and Lower Miocene volcaniclastic-bearing sandstones (PDO). The Lower Cretaceous–Miocene Campomaggiore Unit (Pescatore et al., 1988) is exposed in the southern external zones of the chain. It comprises the Vaglio and San Chirico Units (ISPRA, 2017a), which are made of FYG and FYR.

The Sannio Unit (Fig. 5; Pescatore et al., 2000), otherwise named Coltre Sannitica (Selli, 1962), is composed of Upper Cretaceous–Upper Burdigalian reworked carbonate sediments (FYR), including, from bottom to top, jaspers, calcareous breccias, and calcarenites with macroforaminifera, marls, and varicolored clays (Basso et al., 2002; Vitale and Ciarcia, 2022). The lower part of the pre-orogenic succession of the Fortore Unit (Pescatore et al., 2000) is the same as that of the Groppa d'Anzi Unit. However, starting in the Burdigalian, the succession evolved into volcaniclastic deposits (TUT; Ogniben, 1960; Pescatore et al., 1999, 2000). A pre-orogenic, dominantly calciclastic succession characterizes the Daunia Unit (Dazzaro et al., 1988), showing at the base Upper Oligocene–Middle Burdigalian clays, varicolored marls, and whitish calcilutites and calcarenites (SID; Dazzaro et al., 1988; Santo and Senatore, 1988). The Vallone del Toro Unit (Basso et al., 2002; ISPRA, 2011b) is formed by Upper Oligocene–Middle Burdigalian calcarenites, reddish and greenish argillites, and calcareous breccias (SFN; Crostella and Vezzani, 1964). The pre-orogenic rocks of the Agnone and Tufillo Units (Selli, 1962; Patacca et al., 1992a; ISPRA, 2011c) consist of Upper Cretaceous–Upper Burdigalian varicolored clays (AVS).

3.3.3. Apulian Platform

The Apulian Platform domain encompasses, in the central and southern sectors, a buried imbricate succession intensively drilled for hydrocarbon exploration (e.g., Sciamanna et al., 2004; Shiner et al., 2004; Butler et al., 2004; ViDEPI Project, 2009–2015). However, only a small part is exposed (Mount Alpi; Mazzoli et al., 2006). The southern sector (Fig. 5) is characterized by Upper Permian sandstone (PUG1, Puglia 001 well; ViDEPI Project, 1986; Butler et al., 2004; Fig. 1A), Lower Triassic polygenic breccias (PUG2), Upper Triassic shallow-water dolostones (DBS), and Jurassic–Cretaceous carbonates (SWC). The inner and outer buried Apulian Platform continues locally with Maastrichtian–Paleocene Scaglia-type deposits (SCA) and Eocene breccias (BLA; Patacca and Scandone, 2014) covered by Aquitanian–Langhian calcarenites (PLE). In the Murge and Salento areas (foreland; Ciaranfi et al., 1988; ISPRA, 2013), Maastrichtian carbonates pass locally and laterally to slope bioclastic calcarenites (ALT1). The succession continues with Middle–Upper Eocene calcilutites and calcarenites (TTG), Upper Oligocene limestones (CSR, PBD), and Langhian calcarenites (BSM).

The central sector (Fig. 6) is similar for the inner and outer buried successions, whereas, for the foreland, the Gargano promontory is characterized by Paleozoic shales, dolostones, and limestones (GAR1, Gargano 001 well; ViDEPI Project, 1982; Patacca and Scandone, 2007; Fig. 1A), followed by Lower Triassic sandstones, limestones, and dolostones (GAR2). The stratigraphic succession (Morsilli et al., 2017; ISPRA, 2017b) continues with two heteropic sequences. The western side is composed of Upper Triassic–Lower Cretaceous shallow-water carbonates (DBS and SWC) with evaporites at the base (Patacca and Scandone, 2007), covered by Oligocene breccias (BCG), Chattian–Aquitanian p.p. limestones (SMH), Burdigalian–Lower Langhian limestones (TRF), Upper Langhian–Upper Tortonian calcarenites (PLE), and Lower Messinian marls (TPL). The eastern side of Gargano consists of Lower Cretaceous deep-basin limestones (MAI), marls (FUC), Upper Cretaceous Scaglia-type deposits (SCAd and SCA), and Eocene calcarenites with nummulitids (PES).

In the northern sector, imbricate successions of the inner and outer Apulian Platform largely outcrop, including the Morrone, La Queglia, and Majella Mountains (Cosentino et al., 2003; Patacca and Scandone, 2007, 2021; Vezzani et al., 2010). The Morrone succession (ISPRA, 2005b) consists of Lower Jurassic–Upper Cretaceous shallow-water carbonates (SWC) evolving upward to calcareous breccia (OFE) and Oligocene–Lower Miocene ramp calcarenites with macroforaminifers (CFR).

The La Queglia succession (Fig. 6; Bigi and Di Bucci, 1987; Patacca et al., 1992a; Patacca and Scandone, 2007; ISPRA, 2005c) is composed of Upper Cretaceous–Eocene p.p. cherty limestones (CLI), hosting, in the upper part, an anorogenic lamprophyre, passing upward to Upper Oligocene?–Aquitanian distal ramp bioclastic limestones (CFR). The Mount Majella succession consists of two heteropic successions (Patacca and Scandone, 2007, 2021). In the southern sector, the Cretaceous pre-orogenic succession includes shallow-water limestones (SWC), hosting at least three levels of bauxites and marked by subaerial expositions. In contrast, on the northern side, the base is a pelagic succession, including pelagic limestones (MAI) at the base, passing upward to marls (FUC) and Scaglia-type deposits (SCA). Both successions are covered by Campanian–Maastrichtian calcarenites and calcirudites (OFE; Eberli et al., 2019). This deposit passes upward to Paleocene–Oligocene deep-water breccias (SSG), Upper

Oligocene *Lepidocyclina* limestones (LCL), and Burdigalian bryozoan limestones (BRY).

The eastern part is buried under the allochthonous wedge in the northern sector. It is composed of Lower Jurassic–Cretaceous shallow-water carbonates (SWC), locally with residual clays, passing upward to Lower Miocene marls and bioclastic limestones (SCAd) (Casoli 001 well, ViDEPI Project, 1955; Castelfrentano 005 well, ViDEPI Project, 1960a; Castelfrentano 006 well, ViDEPI Project, 1961b; Orsogna 001 well, ViDEPI Project, 1981; Marcone 001 well, ViDEPI Project, 1960b; Fig. 1A). The foreland succession is formed by Upper Jurassic–Lower Cretaceous shallow-water carbonates (SWC) passing upward to Oligocene–Lower Miocene bioclastic limestones (LBG) (Casaborselli 001 well, ViDEPI Project, 1956b; Villalfonsina 001 well, ViDEPI Project, 1958).

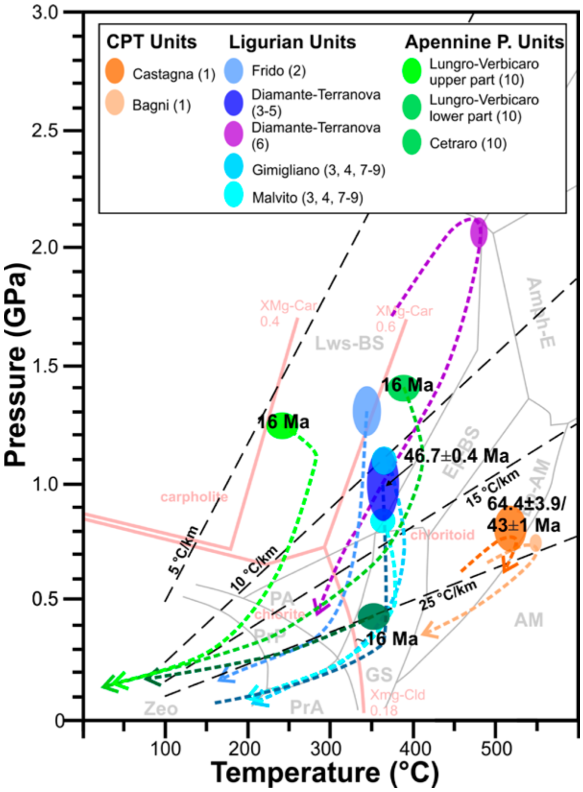

Figure 7. Pressure-temperature diagram of the Alpine metamorphic paths of the Calabria-Peloritani terrane (CPT), Ligurian, and Apennine units. References: 1—Brandt and Schenk (2020); 2—Vitale et al. (2013a, 2013b); 3—Liberi and Piluso (2009); 4—Liberi et al. (2006); 5—Fedele et al. (2018); 6—Tursi et al. (2020); 7–9—Rossetti et al. (2001, 2004); 10—Iannace et al. (2007). Pressure-temperature ranges for the metamorphic facies are modified after Rossetti et al. (2004) and Tsujimori and Ernst (2014). AM—amphibolite; Amph-E—amphibole-eclogite; Car—carpholite; Cld—chloritoid; Ep-AM—epidote-amphibolite; Ep-BS—epidote-blueschist; GS—greenschist; Lws-BS—lawsonite-blueschist; PA—pumpellyite-actinolite; PrA—prehnite-actinolite; PrP—prehnite-pumpellyite; XMg—mole fraction of magnesium; Zeo—zeolite.

4. METAMORPHISM AND TECTONIC EXHUMATION

Paleozoic rocks of the Sila and Stilo Units were affected by variable Variscan metamorphism, ranging from anchizone to greenschist, amphibolite, and granulite facies (Bonardi et al., 2001; Langone et al., 2010; Ortolano et al., 2020). The Castagna Unit (Bonardi et al., 2001; Tursi et al., 2020) is characterized by Variscan amphibolite facies with an Alpine metamorphic overprint defined by a lower amphibolite facies (480–560 °C and 0.7–0.9 GPa; Brandt and Schenk, 2020). The Paleozoic basement of the Bagni Unit (Bonardi et al., 2001) was affected by pre-Alpine greenschist metamorphism, overprinted by Alpine lower-amphibolite-facies conditions (545–565 °C and 0.71–0.77 GPa; Brandt and Schenk, 2020). The Castagna and Bagni Units show similar clockwise pressure-temperature paths for prograde Alpine metamorphism (Fig. 7). The age of the Alpine metamorphism of the Castagna Unit ranges between 64.4 ± 3.9 Ma (Ar-Ar biotite dating; Rossetti et al., 2001) and 43 ± 1 Ma (Rb-Sr biotite dating; Schenk, 1980).

Ligurian successions of the Frido, Diamante-Terranova, Gimigliano, and Malvito Units are overprinted by Alpine HP-LT metamorphism (Fig. 7). Phyllites of the Frido Unit host carpholite in quartz veins (Vitale et al., 2013b), aragonite in the calc-schists (Spadea, 1976), and blue-amphibole in metadolerites (Cristi Sansone et al., 2012) with peak conditions of 330–360 °C and 1.2–1.4 GPa (Vitale et al., 2013b). The Gimigliano Unit also hosts HP-LT carpholite/chloritoid assemblages in the metabasalt cover (Rossetti et al., 2004).

Blueschist metabasalts of the Diamante-Terranova Unit show an assemblage of blue Na-amphibole, lawsonite, chlorite, and pumpellyite (Liberi et al., 2006; Liberi and Piluso, 2009; Fedele et al., 2018) that furnishes a peak condition of 350–390 °C and 1.1–0.9 GPa (Fig. 7). However, Tursi et al. (2020) reported in the blueschists the occurrence of zoned clinopyroxene crystals, showing core-rim compositional variation from diopside to omphacite, which provide peak conditions of 2.0–2.1 GPa and 475–490 °C (Fig. 7) and decompression and cooling path characterized by ~380 °C and ~1.1 GPa and finally a mylonitic deformation under 290–315 °C and ~0.7 GPa conditions. The metamorphic peak age is 46.7 ± 0.4 Ma (Shimabukuro et al., 2012). Rossetti et al. (2001, 2004) reported late Eocene–Oligocene (ca. 38–33 Ma) Ar-Ar phengite age data for the HP-LT Gimigliano Unit. Due to the LT environment of peak Alpine metamorphism and microtextural evidence, these Ar ages should be regarded as a minimum estimate of the crystallization age of the high-pressure phengites during subduction metamorphism in the oceanic-derived units in Calabria.

Metabasalts, metapelites, and quartzites of the Gimigliano Unit show assemblages including crossite and phengite, suggesting a metamorphic peak of 350 °C and 1.0 GPa (Liberi et al., 2006), followed by nearly isothermal decompression to greenschist-facies conditions of 380 °C and 0.6 GPa, and then 300 °C and 0.3 GPa (Liberi et al., 2006). Finally, Malvito metabasalts with lawsonite and phengite indicate a metamorphic climax at 350 °C and 0.8–0.9 GPa (Fig. 7).

The only successions of the Apennine Platform affected by metamorphism are the Lungro-Verbicaro and Cetraro Units. HP-LT metamorphism defines the former unit, characterized by assemblages of Fe-Mg-carpholite and phengite in the Lower Miocene metapelites (SFL) and chloritoid and phengite in the Anisian–Ladinian phyllites (PMM; Iannace et al., 2007). The peak thermobaric conditions for the upper and lower parts of the succession are 320 °C and 1.3 GPa and 390 °C and 1.4 GPa, respectively. Subsequently, during the decompression path, an increase in temperature characterized both upper and lower parts, reaching 340 °C and 400 °C, respectively (Fig. 7). The retrograde decompression is recorded by the growth of chlorite and phengitic white mica as alteration products of both carpholite and chloritoid. Finally, the Cetraro Unit was affected by greenschist-facies metamorphism defined by pressure-temperature conditions of 380 °C and 0.4 GPa (Iannace et al., 2007).

Regarding the tectonic exhumation following the orogenic burial, temporal constraints come from the rock thermochronology studies. Data have been collected using zircon (Zr) and apatite (Ap) fission-track methods on Calabria-Peloritani terrane and continental Adria units. The Zr ages of exhumation for the Castagna and Bagni Units (Thomson, 1998) range between 29 Ma and 21 Ma (late Oligocene–early Aquitanian), whereas the Ap ages fall in the interval 15–11 Ma (late Burdigalian–early Serravallian). Apatite fission-track data indicate a Tortonian age for the Lungro-Verbicaro Unit (Iannace et al., 2007) and two main age clusters for the Lagonegro-Molise Basin Units (Aldega et al., 2003; Mazzoli et al., 2008), i.e., Messinian–Zanclean (5.5–5.0 Ma) and late Zanclean (3.9–3.8 Ma). Finally, for the Mount Alpi (Apulian Platform), ages between 3.2 Ma and 2.0 Ma were estimated (Mazzoli et al., 2006).

5. TECTONIC VERGENCE

Figure 8A shows the geologic map of the northern Calabria–southern Apennines, reporting the tectonic transport directions in present-day coordinates deduced from the literature (Cerisola and Montone, 1992; De Corso et al., 1998; Hippolyte et al., 1994; ISPRA, 2015; Naso and Tallini, 1993; Naso et al., 1995; Sani et al., 2004; Scrocca et al., 1995; Scrocca and Tozzi, 1999; Langone et al., 2006; Vezzani et al., 2010; Vitale et al., 2013a, 2013b, 2019a). The dataset consists of tectonic transport directions inferred from different kinematic indicators. In the case of dominant brittle deformation, they include fold asymmetry, S-C structures, Riedel shears, and shear veins associated with thrust faults. On the other hand, in the case of ductile strains such as those occurring in mylonites, we used stretching lineations, rotated porphyroclasts, S-C structures, and synthetic and antithetic

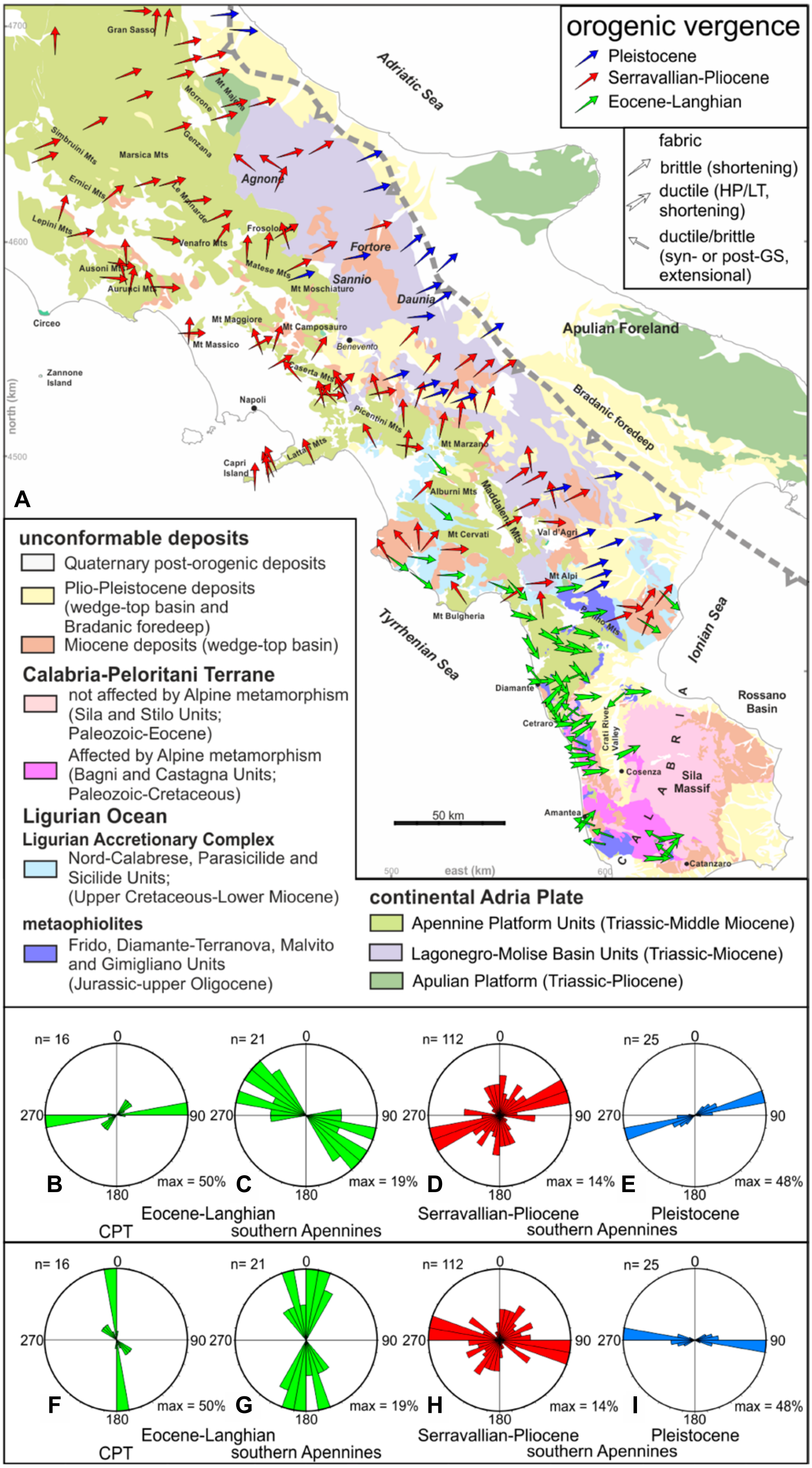

Figure 8. (A) Tectonic transport map, using data from Cerisola and Montone (1992); De Corso et al. (1998); Hippolyte et al. (1994); Istituto Superiore per la Protezione e la Ricerca Ambientale (ISPRA) (2015); Naso and Tallini (1993); Naso et al. (1995); Sani et al. (2004); Scrocca et al. (1995); Scrocca and Tozzi (1999); Langone et al. (2006); Vezzani et al. (2010); Vitale and Ciarcia (2013, 2019a, 2020a); and Ortolano et al. (2020). HP/LT—high-pressure/low-temperature metamorphism; GS—greenschist metamorphism; CPT—Calabria-Peloritani terrane. UTM coordinate system, WGS84 global datum. (B–I) Rose diagrams of tectonic transport directions.

S-C′ structures. According to the ages inferred by the respective authors, we grouped the tectonic vergences into three intervals: (1) Eocene–Langhian, (2) Serravallian–Pliocene, and (3) early–middle Pleistocene. The first interval was delineated because it refers to the tectonic units transported in the first stage of orogenic evolution. This interval includes the nonmetamorphic Ligurian units tectonically verging mainly to the E/SE and the metamorphic units of the Calabria-Peloritani terrane with tectonic transport vectors ranging between SE and NE (Faure, 1980; Carrara and Zuffa, 1976; Dietrich, 1988; Langone et al., 2006; Ortolano et al., 2020); Ligurian meta-ophiolites showing vergence to the E-SE (Vitale et al., 2013a, 2019a); and metamorphic Apennine Platform units with tectonic transport to the E-SE (Vitale et al., 2020c). For the metamorphic units, we also added the tectonic transport (hanging-wall movement) associated with extensional shear during tectonic exhumation under syn- or post-greenschist-facies metamorphism (Rossetti et al., 2001).

The Serravallian–Pliocene tectonic transport vectors refer to the movement of the thrust sheets in the southern Apennines (ranging between NW and E; Cerisola and Montone, 1992; De Corso et al., 1998; Giannandrea et al., 2014; ISPRA, 2015; Sani et al., 2004; Scrocca et al., 1995; Vezzani et al., 2010). The large variability of tectonic vergence in this period is related to the out-of-sequence thrusts, which frequently show two approximately orthogonal vergence directions (e.g., Vitale et al., 2020a), and to the arcuate nature of the thrust systems (Ghisetti and Vezzani, 1988b; Calamita et al., 2009).

The Pleistocene vergence regards only the thick-skinned thrusts involving Pleistocene deposits primarily in the external sectors of the southern Apennines with dominant E-NE vergence (e.g., Hippolyte et al., 1994).

Figures 8B–8E show rose diagrams of the directions of the tectonic vergence grouped for the three temporal intervals. For the Eocene–Langhian data, there is a prevalence of E-W (Calabria-Peloritani terrane; Fig. 8B) and NW-SE (southern Apennines; Fig. 8C) directions; for Serravallian–Pliocene time, there are two orthogonal directions, the first more developed as ENE-WSW and the second developed as NNW-SSE (Fig. 8D). Finally, the Pleistocene directions are constantly ENE-WSW (Fig. 8E). However, all these data are referenced to present-day coordinates. Taking into account the different rotations of the various sectors of the chain that occurred during orogenic evolution in the Eocene–Miocene interval, a counterclockwise rotation of 90° has to be considered for the Calabria-Peloritani terrane (Siravo et al., 2022), which leads to an original N-S direction (Fig. 8F), and a counterclockwise rotation of ∼60° should be considered for the Cilento/Basilicata region (Mattei et al., 2007, and references therein), with again an original N-S direction (Fig. 8G). For Serravallian–Pliocene time, a counterclockwise rotation of ∼30° occurred for the southern Apennines (Mattei et al., 2007, and references therein) with original E-W and secondary N-S directions (Fig. 8H). Finally, for Pleistocene time, counterclockwise rotations of 20° to 0° occurred for the southern Apennines (Mattei et al., 2007) with a restored E-W direction (Fig. 8I). It is worth noting that at the boundary between the Langhian and Serravallian, the direction of restored tectonic vergence changes ∼90°, from approximately N-S to approximately E-W.

6. FORELAND BASIN SYSTEM SYNOROGENIC SUCCESSIONS

In our reconstruction, we adopted the flexural model of bulge migration (Sabbatino et al., 2020) mainly due to the slab retreat process (rollback mechanism) of the downgoing Adria plate (e.g., Malinverno and Ryan, 1986; Royden et al., 1987; Patacca et al., 1990; Doglioni, 1993). This mechanism is invoked because the flexural bending cannot be explained by the load of the Apennine orogenic belt (e.g., Royden, 1988). Other processes, such as large-scale folding by buckling, have been considered for the Pliocene–Pleistocene evolution of the Adriatic domain (Bertotti et al., 2001) with the formation of synclines (Adriatic basins) and anticlines (Apulian forebulge) or basin inversion and vertical extrusion of the late Paleozoic–Mesozoic extensional basins such as hypothesized for the Umbria-Marche Apennines (Tavarnelli et al., 2019), immediately northward of the southern Apennines.

The continental part of the Adria plate underwent flexure beginning in the Oligocene (forebulge stage; Sabbatino et al., 2020). To better identify the synorogenic deposits of the different stages related to the thrust front–foredeep–forebulge system migration toward the E/NE until the middle Pleistocene, we show a schematic cross section of the foreland basin system (Fig. 9) with the forebulge, foredeep, and wedge-top basin deposits (modified after Sabbatino et al., 2020). Generally, the lithosphere flexure caused emersion and erosion of the shallow-water carbonates of the Apennine and Apulian Platforms, producing a calciclastic supply that fed the foredeep basin located to the W/NW and the backbulge basin to the E/NE. Usually, the foredeep basin was not filled to the forebulge crest (“underfilled” state; DeCelles and Giles, 1996, 2012). On the other hand, the foredeep was the location of the deposition of siliciclastic, calciclastic, and volcaniclastic sediments, which originated by the erosion of the overriding plate and the orogenic wedge itself.

The foreland basin system synorogenic deposits of the southern Apennines mainly consist of backbulge, foredeep, and wedge-top basin sediments from the foreland to the hinterland. The backbulge deposits (step 2 in Fig. 9) formed synchronously with the forebulge emersion and erosion of the shallow-water carbonates of the Apennine and Apulian Platforms and the formation of marls and calcarenites. The foredeep successions can be schematized as formed by shallow-water to slope calcarenites and calcirudites, recording the first stage of the downgoing plate drowning following the flexure (step 4). Shallow-water calcarenites were deposited above shallow-water Upper Cretaceous/Eocene limestones, always characterized by an erosive hiatus (Sabbatino et al., 2020). On the contrary, calcirudites were deposited in a slope environment, frequently covering a continuous slope-to-basin succession. These deposits evolved into planktonic marls (step 5), sandstones, and argillites (step 6). The flexure of the downgoing plate is also recorded by the formation of extensional fractures and faults, commonly synsedimentary with the orogenic deposits (Sabbatino et al., 2020). Where the Oligocene forebulge stage caused emersion and erosion of the Apennine Platform shallow-water carbonates, continental deposits formed in localized structural depressions (step 3) (Boni, 1974; Boni et al., 2012); they are made of lens-shaped reddish and purplish subaerial lateritic clays bearing fine- to coarse-grained crystalline rocks debris (Servizio Geologico d’Italia, 1970a; ISPRA, 2016b). The wedge-top sedimentation (step 7) is usually characterized by locally sharp, lateral, and vertical facies variations of sediments originating from the erosion of the thrust sheets forming the orogenic wedge. Frequently, these deposits encompass olistoliths and olistostromes. Several studies, including the official geological cartography, have analyzed and dated the different depocenters (backbulge, foredeep, and wedge-top) of the foreland basin system. However, the provided deposit ages are different and, in some cases, contrasting, and frequently, the ages have been inferred by the stratigraphic position.

In the following description, to avoid the ambiguities caused by the different ages of the foreland basin system synorogenic deposits, we quoted the most representative work that studied these deposits, and in general, we refer to the ages reported in the official geological cartography. Finally, in our reconstruction of the orogenic evolution, we constrained the temporal

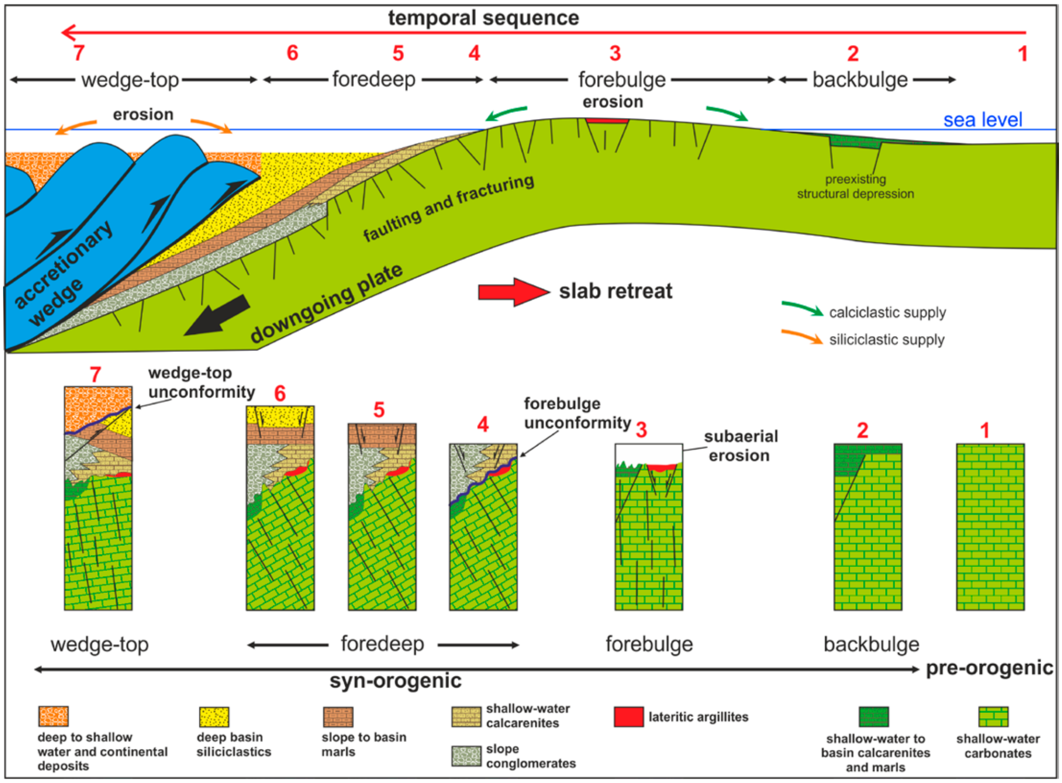

Figure 9. Schematic cross section of a foreland basin system, with the forebulge, foredeep, and wedge-top basin deposits (modified after Sabbatino et al., 2020).

activity of the thrust front (represented by a red line in the stratigraphic logs of Figs. 4, 5, and 6) to the period between the youngest age of the foredeep deposit and the oldest age of the first wedge-top basin deposit.

7. OROGENIC TECTONOSTRATIGRAPHIC EVOLUTION OF THE CENTRAL SECTOR OF THE ADRIA PLATE

In this section, we illustrate the orogenic evolution of the northern Calabria–southern Apennines system by describing paleogeographic maps of the central sector of the Adria plate and the synorogenic deposits from the late Oligocene until the present. The maps were drawn taking into account the available detailed paleogeographic reconstructions of this part of the Adria domain (e.g., Critelli, 1999; Patacca and Scandone, 2007, 2011; Vitale and Ciarcia, 2013; Critelli, 2018). Furthermore, we used the foredeep and wedge-top basin ages to fix the orogenic pulse's lower and upper temporal limits, allowing us to reconstruct the temporal thrust-front migration.

As concerns the orogenic evolution of the northern Calabria–southern Apennines system, two different models have been proposed in the literature (Alvarez, 1976; Michard et al., 2002; Rossetti et al., 2004; Guerrera et al., 2005; Handy et al., 2010; Schettino and Turco, 2011). The first model (Fig. 10A) envisages the presence of two branches of the Ligurian Ocean embedding surrounding the Calabria-Peloritani terrane, considered as a microcontinent (terrane). In the Late Cretaceous–Paleocene, the E Ligurian lithosphere subducted under the Calabria-Peloritani terrane; subsequently, in the Eocene, the Calabria-Peloritani terrane and Sardinia collided, and in the Oligocene, the subduction of the W Ligurian lithosphere under the Calabria-Peloritani terrane started. Finally, the back-arc basin opening separated the Calabria-Peloritani terrane from Sardinia in the Miocene. This model implies that the construction of the Apennines was younger than that of the Alps ("young Apennines"; Alvarez, 1991). The second model (Fig. 10B; Boullin, 1984; Knott, 1987; Rossetti et al., 2004; Schettino and Turco, 2011) considers a single ocean (Ligurian Ocean) between the European plate (Sardinia + Calabria-Peloritani terrane) and the Africa-Adria plate with the lithospheric subduction occurring under the European plate since the Late Cretaceous/Paleocene. In this model, the Apennines formed synchronously with the Alps ("ancient Apennines"; Alvarez, 1991). Our paleogeographic reconstructions (Fig. 11) start from the late Oligocene when the two models envisage the same evolution. (See Tables 1 and 2 for descriptions and acronyms of all synorogenic deposits mentioned in the following sections.)

7.1. Late Oligocene–Middle Burdigalian (Figs. 11A–11C): Ligurian Ocean Closure

The late Oligocene paleogeography (Fig. 11A) shows the subduction of the eastern sector of Ligurian Ocean lithosphere under the Calabria-Peloritani terrane. The undeformed oceanic domain included the Frido, Nord-Calabrese, Parasicilide, and Sicilide successions, passing eastward to the continental sector of the Adria plate. The foredeep sedimentation in the Ligurian realm and western margin of the Apennine Platform was dominated by calciclastic supply originating from erosion of part of the Apennine Platform that had emerged (forebulge stage). The calciclastic deposits include different formations within the Ligurian successions (CAR, SAR, and FMS) and the western margin of the Apennine Platform (FLB3 and SCAd). In the Oligocene, lateritic argillites (red beds) formed (Fig. 11A), locally located in structural depressions in the emerged areas. Such continental deposits are exposed in the southern sector of the southern Apennines (Servizio Geologico d'Italia, 1970a, 1970b; ISPRA, 2016b).

Calciclastic backbulge deposits occurred eastward of the emerged areas, including different formations (CFR, GOD, and SCA). Simulta-

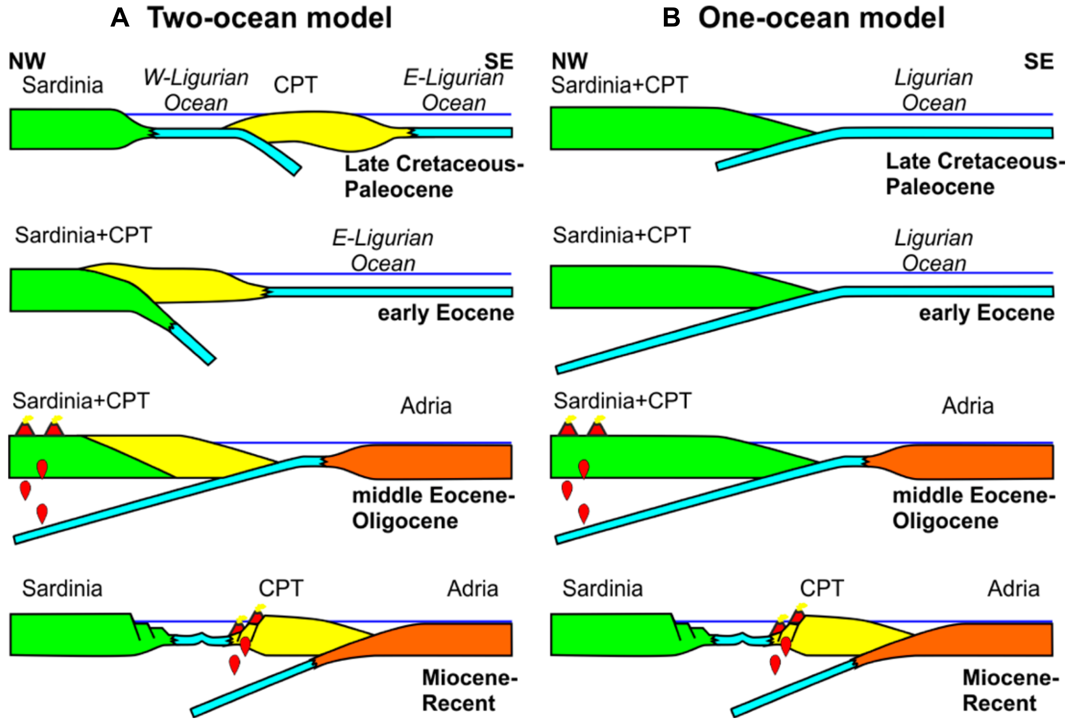

Figure 10. Scheme showing the two models for the orogenic evolution of the northern Calabria–southern Apennines system (modified after Alvarez and Shimabukuro, 2009). CPT—Calabria-Peloritani terrane.

neously, in the Camposauro and Sepino-Moschiaturo margins, the Scaglia-type (SCA and SCAd) sediments were deposited. Furthermore, in the Lagonegro-Molise Basin, not affected by emersion related to the forebulge stage, the sedimentation (FYR) was marked by several calciclastic inputs (CPA in Groppa d'Anzi and Fortore Units).

Following the complete subduction of the Frido realm (early Burdigalian; Fig. 11B), the foredeep of the Nord-Calabrese succession was characterized by the deposition of sandstones (SOV). Contemporaneously, the former forebulge uplift moved eastward with erosion and marly and clayey supply, feeding the western side. These deposits include different formations (AVS, CON, GIP, and SFL). Toward the emerged areas, the deposits were more calciclastic (CDR and FCE). The backbulge successions comprise different formations (CFR, GOD, and SFT). From the late Oligocene to Aquitanian, the Calabria-Peloritani terrane was the location of the first wedge-top basin deposit (Paludi Formation; PLU).

In the middle Burdigalian (Fig. 11C), the thrust front migrated to the east with the offscraping of the Nord-Calabrese sector and forming an accretionary wedge (Ligurian accretionary complex). At the same time, the Parasicilide and Sicilide sectors passed to the deposition of foredeep sandstones (ALB and TUT). The synorogenic successions in Zannone Island and Circeo start with Lower Miocene sandstones with calcarenites and marls with miogypsinids (TFI). In this interval, the tectonic vergences are meanly directed to S, both for the Ligurian and Apennine Platform Units.

7.2. Late Burdigalian–Late Serravallian (Figs. 11D–11F): Orogenic Prism Incorporates the Southern Sector of the Apennine Platform

In the late Burdigalian (Fig. 11D), the remaining successions of the Ligurian Ocean were included in the accretionary wedge, and the thrust front reached the western side of the Apennine Platform. In this stage, the Lungro-Verbicaro Unit was subducted. Meanwhile, the forebulge axis triggered the erosion and formation of clayey deposits in the Bulgheria-Roccagloriosa foredeep basin (GIP), and calciclastic ramp sediments were deposited in the Pollino-Cervati sector (FCE). Meanwhile, calciclastic backbulge sedimentation continued on the eastern side.

In latest Burdigalian–Langhian time (Fig. 11E), the foredeep sedimentation within the southern sector of the Apennine Platform was characterized by arenaceous deposition (GIP1 and BIF). These deposits include the Numidian sandstones (FYN), which consist of rounded and well-sorted quartz grains. These sediments are widespread in the whole western-central sector of the Mediterranean Sea, interpreted as a regional event that transferred desert sands into the deep basins surrounding northern Africa (Ogniben, 1960; Patacca et al., 1992b; Thomas et al., 2010; Vitale et al., 2013a; Fornelli et al., 2015). These sandstones were also deposited in other basin environments, including most of the Lagonegro-Molise Basin. Synchronously, the remaining part of the Apennine Platform was the location of calciclastic sedimentation from the erosion of the western side of the Apulian Platform, where the forebulge axis migrated. The emersion of the Apennine Platform is also marked by the occurrence of a hardground (Patacca et al., 1992a). The area, ranging between the forebulge and the thrust front, formed a W-dipping foreland carbonate ramp some hundreds of kilometers wide (Carminati et al., 2007), including calcarenites (CDR), calcarenites with lithothamnion and bryozoans (CUS, CBZ, and RIV), calcarenites and calcirudites (PBB), and marls (GUA and MRD). Coeval in the Apulian Platform, eastward of the forebulge area, the calciclastic sedimentation deposited marls and calcarenites (PLE and BSM), limestones with bryozoans and glauconite (LBG), and Scaglia Detritica deposits (SCAd). Above the orogenic wedge, starting from the latest Burdigalian, the wedge-top basin deposits of the Cilento Group (CIG; Amore et al., 1988; Bonardi et al., 1988a; Mehmood et al., 2023) were formed. The latter consist of thin-bedded arenaceous-pelitic turbidites, passing upward to medium-bedded arenaceous-pelitic-marly turbidites and rare layers of conglomerates (POL and ABD).

In the late Serravallian (Fig. 11F), dominantly siliciclastic foredeep sedimentation characterized the Lagonegro I and II (PAA), Sannio and

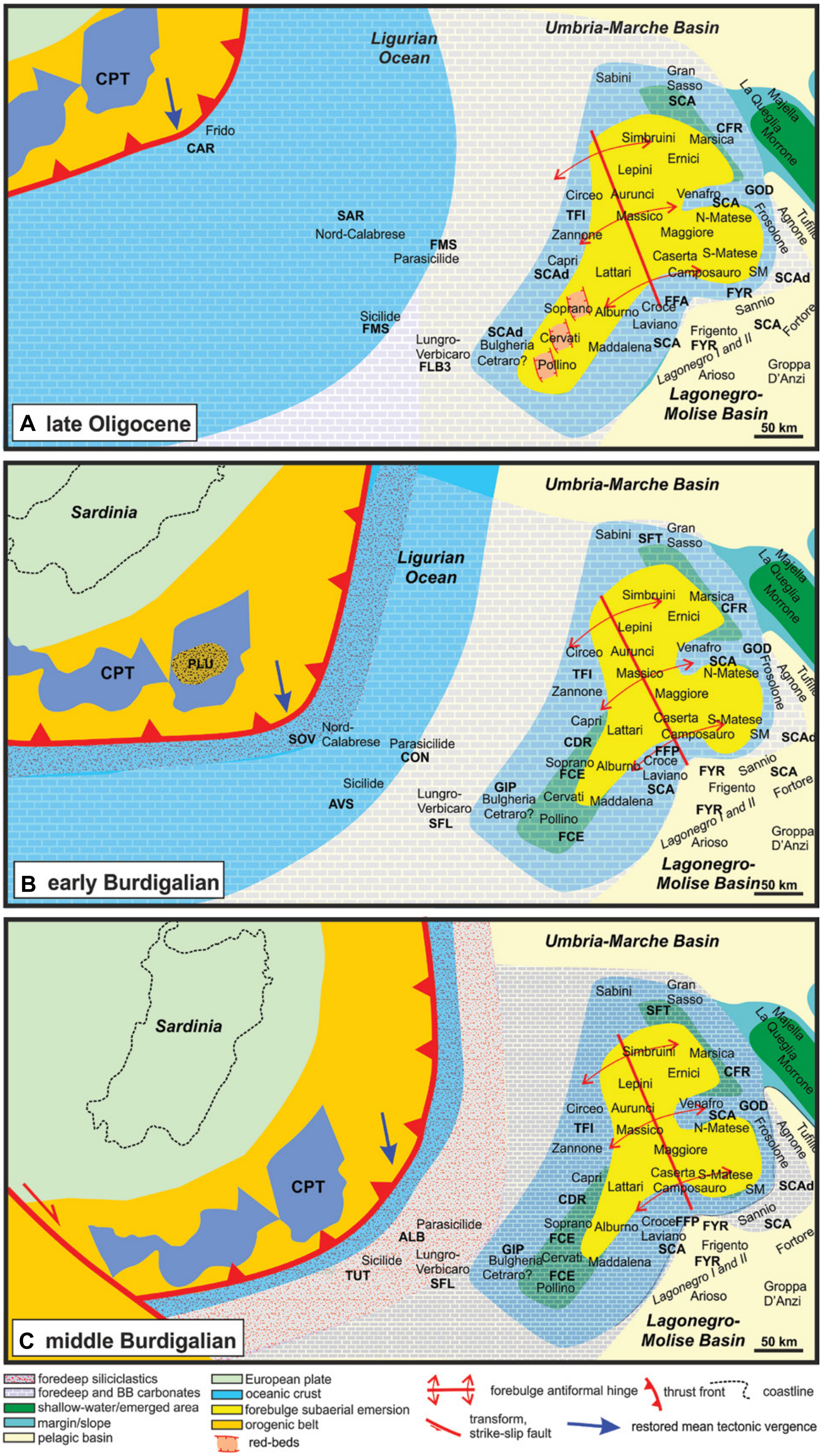

Figure 11. Paleogeographic maps of the central sector of the Adria plate in the intervals: (A–C) late Oligocene–middle Burdigalian; (D–F) late Burdigalian–late Serravallian; (G–I) middle Tortonian–late Messinian; (J–L) early Zanclean–early Pleistocene. For the labels, refer to the text and Figures 4, 5, and 6 captions. BB—backbulge; WBT—wedge-top-basin; CPT—Calabria-Peloritani terrane.

Fortore (SGG), Mount Marzano-Laviano (LAV), Mount Croce (APV3), Lattari (TMI), Zannone-Circeo (ARZ), and Aurunci-Lepini (OBF) successions, whereas calcareous and marly deposits occurred in the remnants of the Apennine Platform (CBZ, LNG, ORB, and UAM), and marly and clayey deposits occurred within the Lagonegro-Molise Basin (FAE, SER, TFL, and UAM). Sedimentation continued in the wedge-top basin of the Cilento Group (CIG) with the deposition of medium- to thick-bedded marls and conglomerates, which toward the top include clasts and olistoliths of metabasalts and pillow lavas (MAU and ABD).

Starting from this period, the Calabria-Peloritani terrane detached from Sardinia. The crustal thinning triggered the formation of extensional basins with siliciclastic sedimentation (Mattei et al., 2002), related to the rifting and opening of the Tyrrhenian back-arc basin, starting from the late Serravallian (AMA; Perrone et al., 1973; Di Nocera et al., 1974; Ortolani et al., 1979; Colella, 1995; Perri, 1996; Mattei et al., 2002; Vitale et al., 2019a, 2020c). Along the Ionian sector, coeval Rossano and Crotone successions (ROS) formed in wedge-top basins, sealing the thrust between the Sila Unit and the Paludi Formation (PLU).

As described before, in the late Oligocene to Langhian, the restored tectonic vergence mainly indicates a S direction; in contrast, starting in the Serravallian, the tectonic vergence for the Ligurian and Apennine Platform units is about orthogonal to the previous value, indicating a dominant approximately E direction for the thrusts faults.

7.3. Middle Tortonian–Late Messinian (Figs. 11G–11I): Orogenic Prism Incorporates the Northern Sector of the Apennine Platform and the Lagonegro-Molise Basin

Starting from the middle Tortonian (Fig. 11G), the arcuate thrust front migrated to the NE and SE in the northern and southern sectors of the Apennine Platform, respectively. The calciclastic and siliciclastic foredeep sedimentation affected the Simbruini, Ernici, N Matese, Venafro, Maggiore, Matese, and Camposauro successions (FFS and PRJ). In the Lagonegro-Molise Basin, the foredeep deposits include different formations (SGG and TFA). Meanwhile,

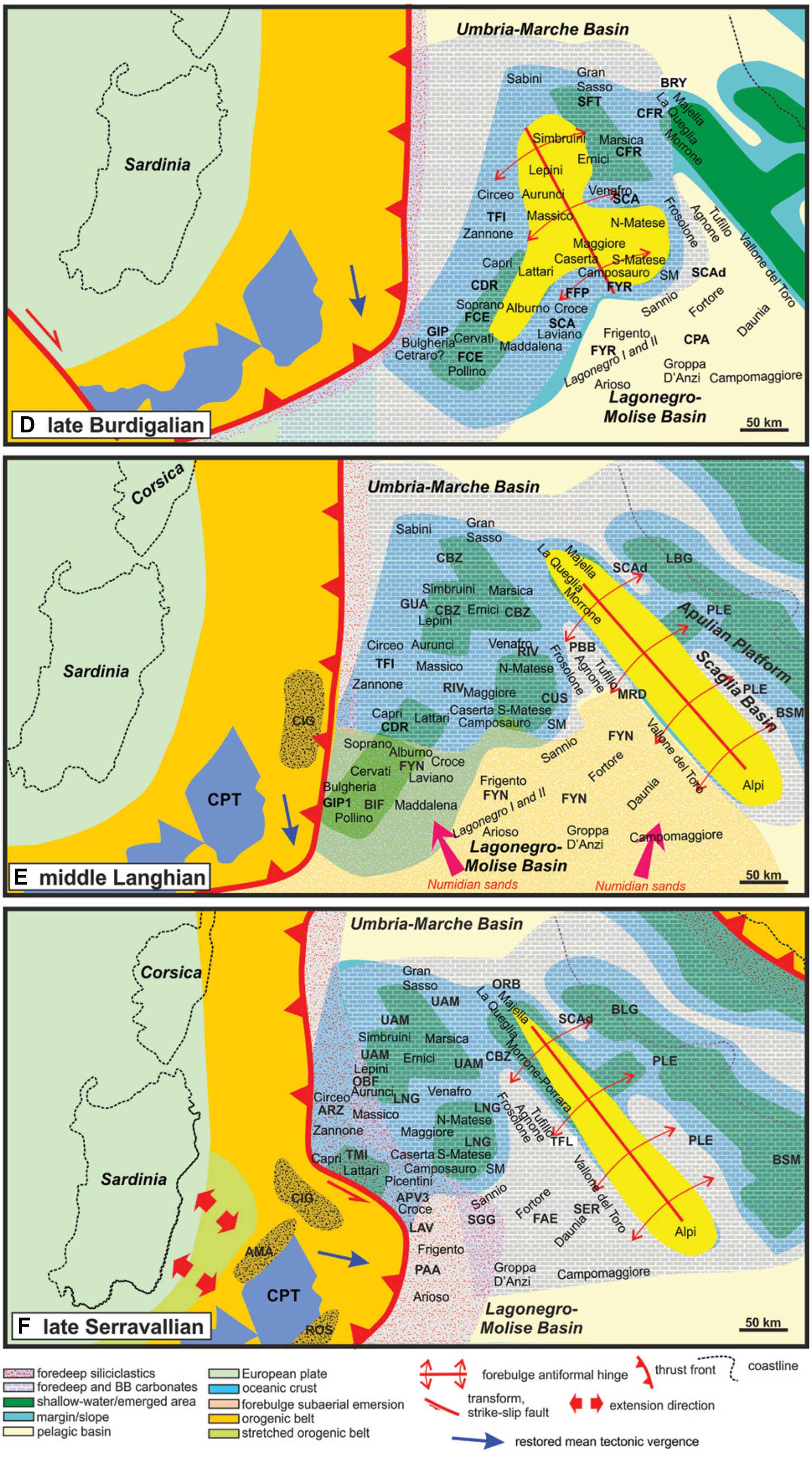

Figure 11. ***Continued***

the forebulge, localized on the eastern part of the Apulian Platform, fed the foredeep with the sedimentation of marls and calcarenites of CBZ, UAM, and lithothamnion limestones (LIT) and FAE, SER, and marly and siliciclastic deposits (FYB and MSO). Calcarenites were deposited in the Apulian Platform domain (ANR). The backbulge deposit on the eastern side of the forebulge is represented by limestones with bryozoans and glauconite (LBG). On the western side of the Calabria-Peloritani terrane, the siliciclastic sedimentation continued in the Amantea Basin (AMA), whereas on the eastern side, the Rossano Basin succession (ROS) was deposited.

In the early Messinian, the orogenic wedge incorporated more and more sectors of the northern Apennine Platform (Fig. 11H). In this stage, siliciclastic sedimentation occurred in the foredeep basins of Daunia (TPC), Frosolone (MSO), E Marsica and Gran Sasso Mount (LAF). Meanwhile, siliciclastic and calciclastic supply fed the Fortore (SER), Agnone and Tufillo (FYB), and La Queglia and Morrone (UAM) successions. In Mount Alpi, calciclastic sediments (LUT) were deposited in structural depressions (La Bruna et al., 2018), followed by alternating sandstones and calcareous conglomerates (TIT). Finally, the backbulge sediments included marls deposited in the Gargano succession (TPL).

Above the orogenic chain, several wedge-top basin deposits formed, including the late Tortonian–early Messinian Castelvetere Group (CVTG; Vitale and Ciarcia, 2018). This sedimentary complex is the largest clastic deposit in the southern Apennines, encompassing the following formations, commonly with heterotopic relationships: ATP, BPC, CAI, CVT, GOR, MSA, ORI, PON, PER, RMA, SBO, and SIE. These deposits, commonly, are formed by a base of calcareous conglomerates or calcarenites, locally embedded in an arenaceous matrix, passing upward to turbiditic sandstones with intercalations of clays, marls, and conglomerates frequently with crystalline clasts (Critelli and Le Pera, 1995; Pescatore et al., 2000; Ciarcia et al., 2009b; Vitale et al., 2017; Vitale and Ciarcia, 2018; Critelli, 2018). Olistostromes of the varicolored clays and Apennine Platform carbonate olistoliths occur in the upper parts of these successions. In Mount Massico, this deposit hosts olistoliths and clasts of marbles (Di Girolamo et al., 2000; Vitale et al., 2019b). In the northern sector of the orogenic chain, sandstones (GTC and TOR) and marls, clays, and silts with sandy, clayey, marly, and calcarenitic olistoliths (VRT) were deposited.

In the late Messinian (Fig. 11I), the orogenic wedge entirely covered the northern sector of the Apennine Platform and the eastern part of the Lagonegro-Molise Basin, with siliciclastic

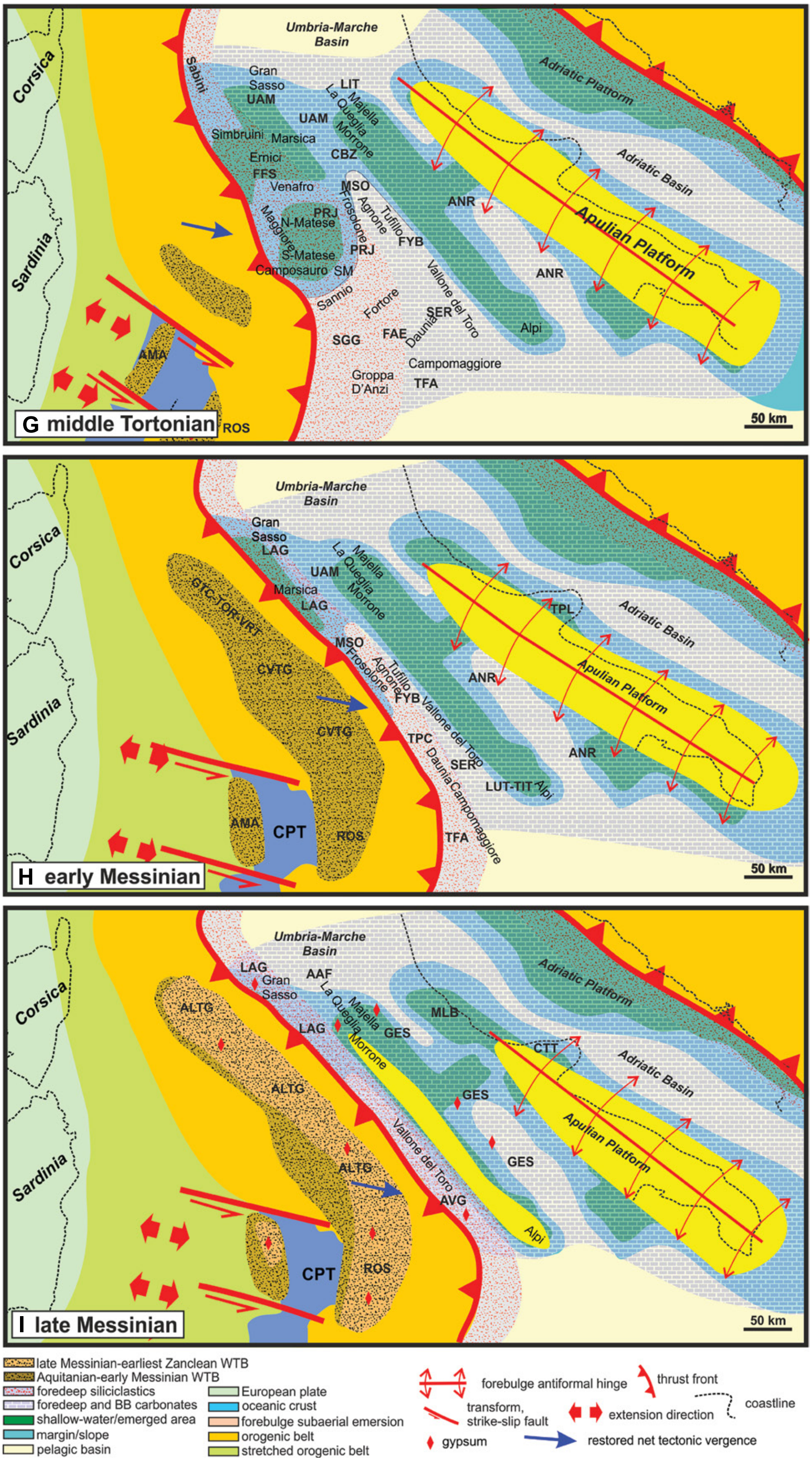

Figure 11. ***Continued***

deposition in the foredeep basins of Gran Sasso Mount and Marsica Mountains (LAF), and argillites with gypsum (AVG) comprising the Vallone del Toro Unit. In the latest Messinian, foredeep siliciclastic sedimentation also started in La Queglia and Morrone (AAF).

The forebulge was localized on the eastern part of the Apulian Platform that fed the western foredeep with the deposition of marly limestones and reworked bryozoans (MLB) and gypsum, evaporitic limestones, sulfur layers, and diatomites (GES). However, Morrone and Mount Alpi were also in subaerial conditions, recorded by an erosive stratigraphic gap. Hence, in this stage, related to the flexure of the downgoing lithosphere, two parallel emerged areas occurred separated by the Scaglia Basin, or, alternatively, the two structural highs formed two anticline structures separated by a syncline, in analogy with the buckling model proposed by Bertotti et al. (2001) for the Pliocene–Pleistocene evolution of this sector. Calcarenites (CTT) deposited in the Gargano area represent, in this period, the easternmost backbulge deposits.

Above the orogenic wedge, unconformable sedimentation occurred with the deposition of the Altavilla Group (ALTG) comprising different formations (ALT, ANZ, COP, and VIC). Gypsum deposits are widespread across the whole chain, within deposits of the Altavilla Group in the north and the Amantea (AMA) and Rossano and Crotone (ROS) deposits in the Calabria-Peloritani terrane. In the late Messinian, the tectonic vergence was mainly directed toward the E, indicating oblique orogenic transport with respect to the chain thrust front. Finally, it is worth noting that the crustal flexure shows an axis that was oblique to the orogenic fronts up to the early Messinian and subsequently parallel, probably following the docking with the thicker Apulian lithosphere.

7.4. Early Zanclean–Early Pleistocene (Figs. 11J–11L): Passage from Thin- to Thick-Skinned Tectonics and Shortening of the Western Sector of the Apulian Platform

In the early Zanclean (Fig. 11J), siliciclastic foredeep sedimentation locally continued in the La Queglia and Morrone successions (AAF), and calciclastic and siliciclastic sedimentation occurred in Mount Majella, the outer buried Apulian Platform, and the Apulian foreland with calcareous conglomerates, clays, and silty sandstones (LAP).

During the early–middle Zanclean (Fig. 11J), the orogenic style changed from thin-skinned tectonics to thick-skinned thrusting involving the buried Apulian Platform. These thrusts probably are the inversion of inherited normal faults hosted in the Paleozoic basement (Shiner et al., 2004), where upward prolongations cut the

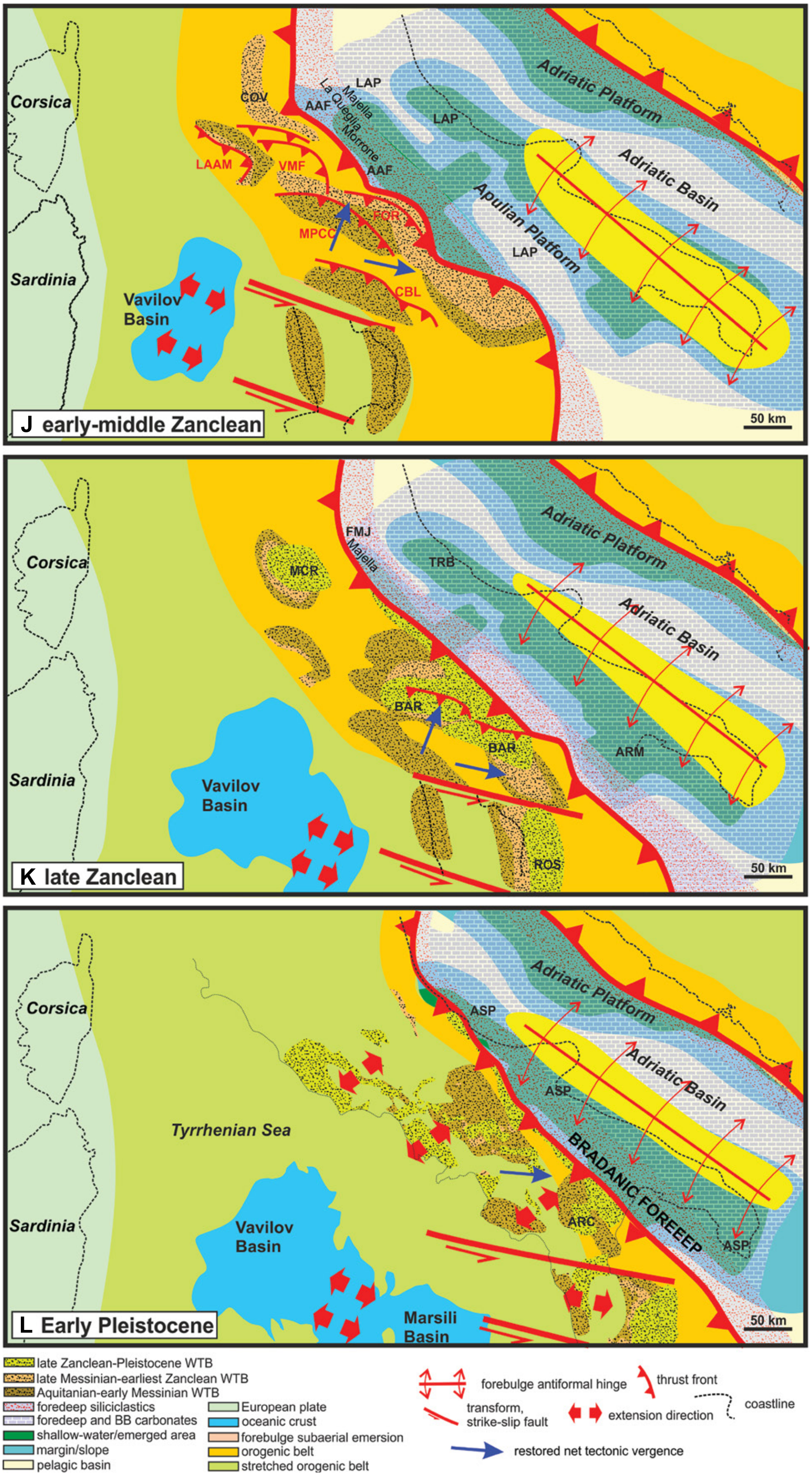

Figure 11. ***Continued***

allochthonous wedge, producing envelopment thrusting appearing as out-of-sequence structures at the outcrop scale (Vitale et al., 2019b, 2020a, 2020b). These thrust faults are scattered throughout the southern Apennines, deforming the late Miocene–earliest Pliocene wedge-top basin deposits. These out-of-sequence structures include the following thrust systems:

(1) Lepini-Aurunci-Ausoni-Massico Mountains (LAAM; Fig. 11J), where the Apennine Platform rocks superpose onto the wedge-top basin Castelvetere Group (CVTG; late Tortonian–early Messinian) and GTC, TOR, and VRT (early Messinian). In the western Aurunci Mountains, thrusts verge both to the N and E (Naso and Tallini, 1993).

(2) Venafro-Matese-Frosolone Mountains (VMF), defined by folds and thrusts (Scrocca and Tozzi, 1999) verging to the NW (Venafro Mountains), N (Matese anticline; Scrocca et al., 1995), and N/S (Montagnola di Frosolone; Naso et al., 1995).

(3) Marzano-Picentini-Caserta-Camposauro Mountains (MPCC). Here, the Mesozoic carbonates superpose onto the wedge-top basin deposits of the Castelvetere Group (CGTG) with vergences ranging between NW and E, and with a prevalence of the tectonic transport to the N (Vitale et al., 2017, 2020a). This system comprises the superposition of the Frigento Unit onto the Mount Croce Unit with the interposition of the Castelvetere Group deposit exposed in the tectonic window of Campagna (Vitale et al., 2020b).

(4) Fortore (FOR), where the Fortore Unit overthrust the wedge-top basin deposits of the Castelvetere Group with a vergence to the E (Pescatore et al., 2000; Vitale and Ciarcia, 2018; ISPRA, 2010 h).

(5) Cilento-Bulgheria-Lauria Mountains (CBL). Here, the thrust system includes thrusting verging to the N of the carbonate Bulgheria and Lauria Mountains onto the Ligurian accretionary complex and arcuate thrust faults bounding the Cilento area with vergences ranging between NW and E.

Contemporaneously with these thrusting episodes, the Calabria-Peloritani terrane migrated to the SE, and in the rear, basalts in the Vavilov Basin formed.

In the late Zanclean (Fig. 11 K), the thrust front mainly moved to the NE with the almost complete inclusion, within the allochthonous wedge, of the inner Apulian Platform, except the Majella area, where the siliciclastic foredeep occurred (FMJ), whereas calciclastic and siliciclastic sedimentation occurred in the outer buried Apulian Platform (TRB and ARM).

Starting from this period, different wedge-top depocenters formed, starting in the northern sector, including the Ariano (BAR and

SFE), Ofanto and Vietri-Potenza (BAR, SFE, and ARC), Calvello (BAR and ARC), and Sant'Arcangelo (ARC) Basins. In this large part of the chain, deposits record a migration of depocenters toward the SE (Ascione et al., 2012). These deposits were formed between 4 Ma (late Zanclean) and 0.7 Ma (Middle Pleistocene) triggered by slab breakoff of the downgoing Adria plate and progressive slab tearing toward the SE (Ascione et al., 2012). To the north, in the Abruzzi area, wedge-top basin sedimentation occurred with the emplacement of conglomerates (MCR). On the other hand, in northern Calabria, from the late Zanclean to Early Pleistocene, different deposits formed in extensional basins, including the Crati Valley and Castrovillari basins (Russo and Schiattarella, 1992; Schiattarella, 1998). In this temporal interval, restored tectonic vergence indicates a mainly approximately E direction and a secondary approximately N direction, both of which are associated with the emersion of the envelopment thrust faults.

Finally, in the Early Pleistocene (Fig. 11L), the pattern of the thrust front reached the present configuration, with the forebulge emersion located in the axial sector of the exposed Adria plate between the two opposite-verging southern Apennines and Dinarides chains. The foredeep sediments are represented by clays and sands (ASP).

From the later part of the Early Pleistocene, severe extension occurred along the Tyrrhenian margin of the chain (Hippolyte et al., 1994; D'Agostino et al., 1997; Macchiavelli et al., 2012), forming several grabens, including the Campanian Plain, amongst the larger structures (Fig. 1A; Cinque et al., 1993; Santangelo et al., 2017). The restored tectonic vergence shows a ubiquitous E direction.

8. OROGENIC EVOLUTION

The proposed orogenic reconstruction is in line with the model of "ancient Apennines" (Alvarez, 1991), and those of other circum-Mediterranean orogens, such as the Betic-Rif chain in the western sector, where a similar tectonic structure is reported (Chalouan and Michard, 1990; Michard et al., 2006; Vitale et al., 2015), and new data on the Alpine tectono-metamorphic evolution (Marrone et al., 2021) age of subduction zone metamorphism (38 Ma, late Eocene–Oligocene; Bessière et al., 2022) and Variscan inheritance (e.g., Rossetti et al., 2020), which have become recently available from continental-derived units that form the Alpine tectonic edifice.

Generally speaking, the orogenic evolution can be summarized as follows (Rossetti et al., 2001; Iannace et al., 2007; Liberi and Piluso, 2009; Vitale et al., 2019a; Fedele et al., 2018). In Paleocene–Eocene time, the subduction of the Ligurian lithosphere under the European plate, including the Calabria-Peloritani terrane and Sardinia-Corsica block, carried at depth some crustal slices of both the downgoing (Ligurian meta-ophiolites) and overriding (Castagna and Bagni Units) plates. The complete closure of the oceanic realm in the early Miocene concluded with the frontal accretion of the eastern sector of the ocean and the formation of the Ligurian accretionary complex. After that, the subduction zone involved the western margin of the Apennine Platform, with the subduction of some successions (Lungro-Verbicaro and Cetraro Units). From the middle Miocene to the middle Pleistocene, a thrust-and-fold belt formed, with the overthrust of different successions of the continental Adria plate and both thin- and thick-skinned tectonics. From the Oligocene to Tortonian, the subducted tectonic units of the Calabria-Peloritani terrane, Ligurian Ocean, and continental Adria plate were exhumed and accreted in the orogenic chain. Therefore, different geodynamic mechanisms have spanned the orogenic evolution, which acted synchronously or diachronously. We can describe the evolution of this collisional margin through the migration of the subduction channel boundaries (i.e., roof and basal décollements). Different geodynamic scenarios are associated with the movement of the main subduction channel décollement (Vannucchi et al., 2012). This surface can move up or down toward the foreland or hinterland. It follows that the subduction channel can be accreted or eroded, or these mechanisms can act in the frontal sector. To better describe this process, we illustrate the geodynamic evolution of the northern Calabria–southern Apennines (southern sector) in Figure 12. (See Table 2 for descriptions and acronyms of all synorogenic unconfromable deposits mentioned in the following text.)

Following the start of subduction of Ligurian Ocean lithosphere, the roof décollement migrated upward, inserting slices of the Calabria-Peloritani terrane in the subduction channel (upward basal erosion; Fig. 12A). Subsequently, the roof décollement migrated downward, adding oceanic slices to the subduction channel (downward accretion; Figs. 12B and 12C). These three steps occurred in the Paleocene–Eocene interval, chronologically constrained by the HP-LT metamorphic ages of Castagna (43 ± 1 Ma, Schenk, 1980; 64.4 ± 3.9 Ma, Rossetti et al., 2001) and ophiolite units (38–33 Ma, Rossetti et al., 2001, 2004; 46.7 ± 0.4 Ma, Shimabukuro et al., 2012). Synchronously, orogenic volcanism occurred in Sardinia, with the oldest event dated at 38.3 ± 0.3 Ma (Lustrino et al., 2009), consistent with the beginning of oceanic subduction within the interval 49–42 Ma (Ypresian–Lutetian; Lustrino et al., 2009).

In the Oligocene–Aquitanian (Fig. 12D), the easternmost ophiolite domain (Frido Unit) was subducted, reaching HP-LT metamorphic conditions; meanwhile, the downward accretion formed an orogenic stacked pile that triggered extension on the top of the overriding plate. This event was recorded by the age of zircon fission tracks in the subducted units (28–23 Ma; Thomson, 1998) and by formation of the wedge-top basin deposits of the Paludi Formation (PLU). In the early Burdigalian (Fig. 12E), the roof décollement moved toward the foreland with the frontal accretion of the Nord-Calabrese (NCA), Parasicilide (PAS), and Sicilide (SIC) Units (Ligurian accretionary complex). In the Burdigalian (Fig. 12F), the oceanic accretionary wedge (Ligurian accretionary complex) overthickened following the buttressing of the western margin of the Apennine Platform (Lungro-Verbicaro Unit, LVU) and collapsed (Fig. 12G), forming an extensional wedge-top basin where the Cilento Group (CIG) was deposited above the Burdigalian-Langhian boundary (Vitale et al., 2010; Corrado et al., 2019; Mehmood et al., 2023). In the Burdigalian–Langhian interval, the LVU was subducted (Fig. 12G). Apatite fission-track ages in Calabria-Peloritani terrane rocks (Thomson, 1998) indicate that tectonic exhumation of the subducted units continued in this period. In Langhian–Serravallian time (Fig. 12H), the Apennine Platform remnant was overthrust by the Ligurian accretionary complex concurrently, and the LVU was accreted in the subduction channel and started upward migration (tectonic exhumation) with the other metamorphic thrust sheets. The fast exhumation within the subduction channel was enhanced by the synchronous rifting of the Tyrrhenian Sea (e.g., Sartori et al., 2001), which caused the exhumation of the entire subduction channel mainly through extension in the upper crust. This process resulted in exposure of the metamorphic successions and clastic supply deposition within the surrounding structural lows, presently forming the Serravallian–Tortonian successions of the Amantea (AMA) and Rossano Basin deposits (ROS) in northern Calabria.

According to Faccenna et al. (2001a, 2001b), in the Serravallian, the subducted oceanic slab reached the upper-lower mantle boundary at 660 km depth, laying down the deepest slab segment along this buoyancy barrier. This event slowed down the roll-back migration rate and made the shallow downgoing slab segment vertical. The renewed slab retreat in Tortonian time (Fig. 12I) occurred with the subduction of thicker continental Adria lithosphere underlying the Apennine Platform, becoming the new

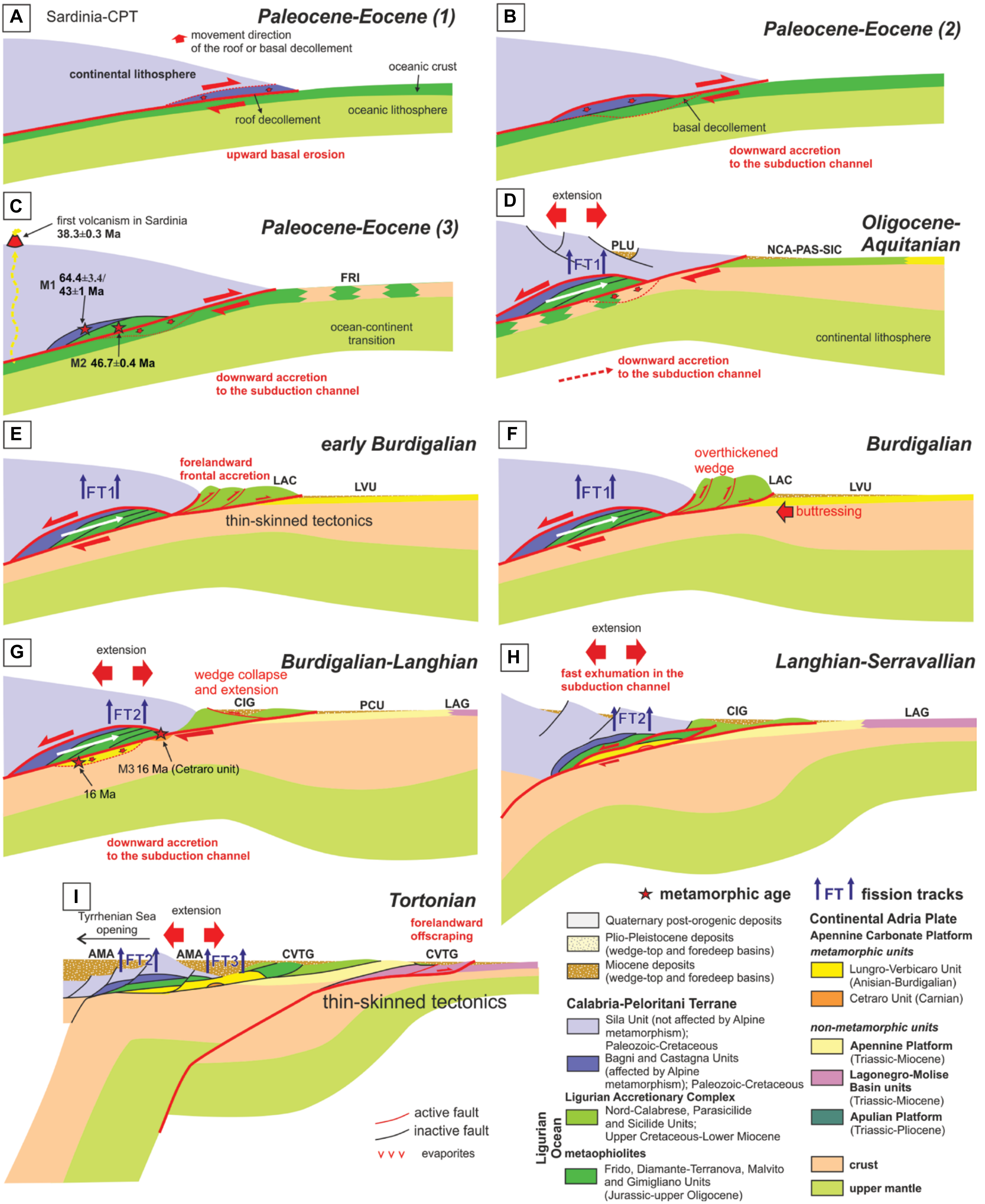
A
Sardinia-CPT
Paleocene-Eocene (1)
movement direction
of the roof or basal decollement
continental lithosphere
oceanic crust
oceanic lithosphere
roof decollement
upward basal erosion
B
Paleocene-Eocene (2)
basal decollement
downward accretion
to the subduction channel
C
first volcanism in Sardinia
38.3±0.3 Ma
Paleocene-Eocene (3)
M1 64.4±3.4/
43±1 Ma
FRI
ocean-continent
transition
M2 46.7±0.4 Ma
downward accretion
to the subduction channel
D
extension
PLU
FT1
NCA-PAS-SIC
Oligocene-
Aquitanian
continental lithosphere
downward accretion
to the subduction channel
E
early Burdigalian
FT1
forelandward
frontal accretion
LAC
LVU
thin-skinned tectonics
F
Burdigalian
overthickened
wedge
FT1
LAC
LVU
buttressing
G
extension
Burdigalian-Langhian
wedge collapse
and extension
FT2
CIG
PCU
LAG
M3 16 Ma (Cetraro unit)
16 Ma
downward accretion
to the subduction channel
H
extension
fast exhumation in the
subduction channel
Langhian-Serravallian
FT2
CIG
LAG
I
Tyrrhenian Sea
opening
extension
Tortonian
forelandward
offscraping
AMA
FT2
AMA
FT3
CVTG
CVTG
thin-skinned tectonics
active fault
inactive fault
evaporites
metamorphic age
FT fission tracks
Quaternary post-orogenic deposits
Plio-Pleistocene deposits
(wedge-top and foredeep basins)
Miocene deposits
(wedge-top and foredeep basins)
Calabria-Peloritani Terrane
Sila Unit (not affected by Alpine
metamorphism);
Paleozoic-Cretaceous
Bagni and Castagna Units
(affected by Alpine
metamorphism); Paleozoic-Cretaceous
Ligurian Accretionary Complex
Nord-Calabrese, Parasicilide
and Sicilide Units;
Upper Cretaceous-Lower Miocene
Ligurian Ocean
metaophiolites
Frido, Diamante-Terranova, Malvito
and Gimigliano Units
(Jurassic-upper Oligocene)
Continental Adria Plate
Apennine Carbonate Platform
metamorphic units
Lungro-Verbicaro Unit
(Anisian-Burdigalian)
Cetraro Unit (Carnian)
non-metamorphic units
Apennine Platform
(Triassic-Miocene)
Lagonegro-Molise
Basin units
(Triassic-Miocene)
Apulian Platform
(Triassic-Pliocene)
crust
upper mantle

Figure 12. Cartoon showing the tectonic evolution of the northern Calabria–southern Apennines system from the Paleocene to the present. Not to scale. AMA—Amantea; CIG—Cilento Group; CPT—Calabria-Peloritani terrane; CVTG—Castelvetere Group; FRI—Frido Unit; LAC—Ligurian accretionary complex; LAG—Lagonegro-Molise Units; LVU—Lungro-Verbicaro Unit; NCA—Nord-Calabrese Unit; PAS—Parasicilide Unit; PCU—Pollino-Ciagola Unit; SIC—Sicilide Unit.

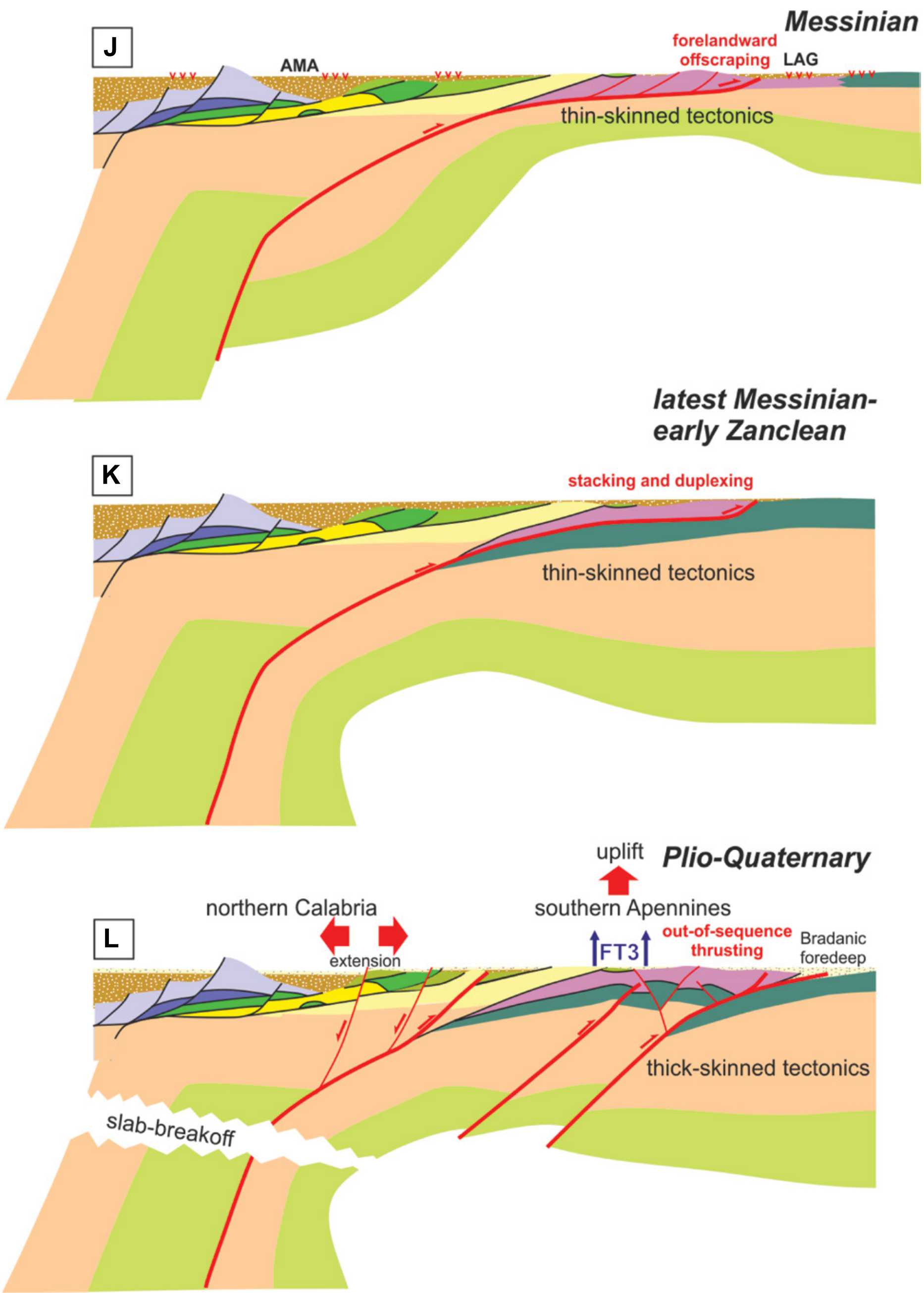

Figure 12. ***Continued***

backstop of the subduction system and triggering a forelandward jump of the main subduction detachment and thick-skinned thrusting. In this stage, the Apennine Platform units and the Paleozoic basement tectonically covered the Lagonegro-Molise Basin successions (LAG), which subsequently (Figs. 12J and 12 K) were accreted through forelandward offscraping and dominantly thin-skinned tectonics (Mattioni et al., 2006). In Serravallian–Tortonian time, the wedge-top basins located in various places of the orogenic wedge were fed by calciclastic, siliciclastic, and volcaniclastic sediments, including the Cilento (CIG) and Castelvetere (CVTG) Groups and Rossano Basin deposits (ROS). In the late Messinian, evaporite-bearing calciclastic sedimentation occurred in the Amantea (AMA) and Rossano (ROS) basins in northern Calabria, in some wedge-top basins in the southern Apennines (ALTG), and in the foredeep of the Vallone del Toro Unit.

In the Pliocene (Fig. 12L), the involvement of thicker continental Adria lithosphere, located under the Apulian Platform, created a new backstop for the subducting system, causing new thick-skinned thrusting (e.g., Mazzoli et al., 2013). This important orogenic event was probably associated with progressive slab breakoff and slab-tear propagation since ca. 4 Ma (Ascione et al., 2012), which ruled the formation and SE migration of the wedge-top basin depocenters and, in general, isostatic rebound and uplift. Synchronous with eastward thrust-front migration, extension at the rear occurred, affecting more and more areas of the orogenic wedge. Finally, in the southern Apennines, crustal shortening stopped in the middle Pleistocene, as recorded by the synfolding deposits sedimented in the wedge-top basin of Sant'Arcangelo (Sabato et al., 2005), and widespread extension in the chain occurring up to the present day (Macchiavelli et al., 2012).

9. OROGENIC EVOLUTION OF NORTHERN CALABRIA–SOUTHERN APENNINES SYSTEM WITHIN THE WESTERN-CENTRAL MEDITERRANEAN OROGENIC FRAMEWORK

Finally, to insert the northern Calabria–southern Apennines within the framework of the orogenic evolution of the western-central peri-Mediterranean Alpine chains, we illustrate some paleogeographic maps starting from the middle Eocene, when the western side of the Ligurian oceanic lithosphere was downgoing under the European plate (Fig. 13A). Due to the relatively low convergence rate between the African and European plates from the Late Cretaceous to Holocene (Dewey et al., 1989; Faccenna et al., 2001a, 2001b), the subduction of the oceanic lithosphere was probably driven by its negative buoyancy, resulting in roll-back migration of the foredeep–thrust front system (Malinverno and Ryan, 1986; Faccenna et al., 1996; van Hinsbergen et al., 2014).

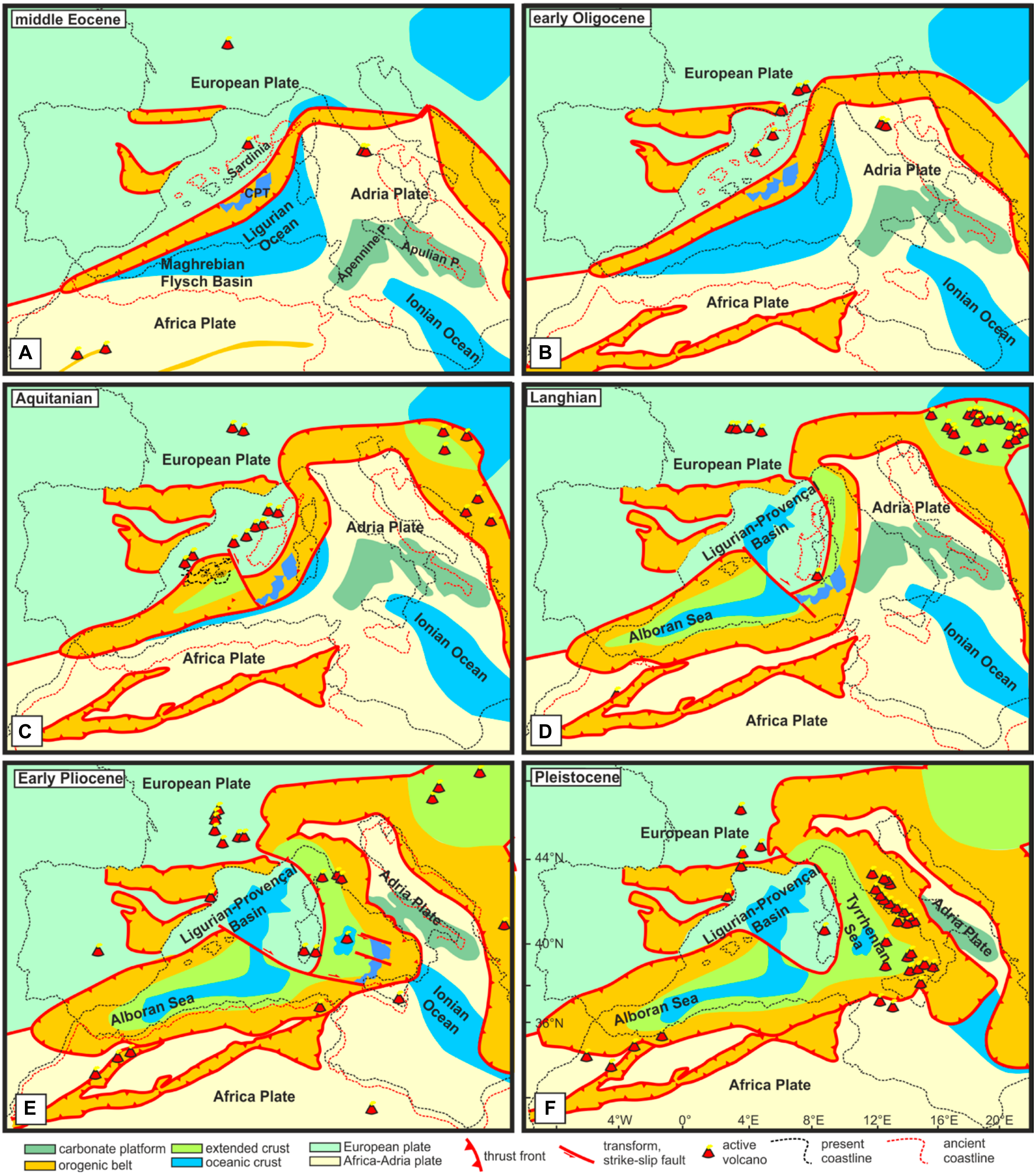

Figure 13. (A–F) Cartoons showing paleogeographic maps of the western-central Mediterranean area from the middle Eocene to Pleistocene (modified after Vitale and Ciarcia, 2013). CPT—Calabria-Peloritani terrane; P.—Platform.

In the early Oligocene (Fig. 13B), the subduction of oceanic lithosphere under the European plate produced the first manifestations of orogenic volcanism in Sardinia (Savelli, 2002; Carminati et al., 2012), with the maximum intensity in the Aquitanian (Fig. 13C). From this time, the Sardinia-Corsica block rotated counterclockwise, with the southern edge moving along a transform/strike-slip fault. In the Langhian (Fig. 13D), the Ligurian Ocean was completely closed, whereas the rotation of the Sardinia-Corsica block caused the opening of the Ligurian-Provençal basin. In the early Pliocene (Fig. 13E), the Apennine Platform was incorporated in the orogenic wedge, and the Calabria-Peloritani terrane, previously detached from the Sardinia-Corsica block, migrated southeastward with the opening of the back-arc basin of the southern Tyrrhenian Sea. At this time, oceanic lithosphere of the Ionian Sea was subducting under the Calabria-Peloritani terrane. Strike-slip faults allowed the Calabria-Peloritani terrane to move, including lithospheric structures separating northern and southern Calabria movements. The SE migration of the Calabria-Peloritani terrane caused the stretching of the lithosphere in the rear and the formation of the Vavilov Basin (Savelli, 2002). The Pleistocene paleogeography (Fig. 13F) depicts the last stage of orogenic evolution, characterized by (1) the Calabria-Peloritani terrane ending its orogenic migration with the Marsili Basin formation at the rear (Savelli, 2002) and creating a mountain bridge between the southern Apennines and the Sicilian Maghrebids, (2) the subduction of Ionian lithosphere under Calabria; and (3) the formation of the orogenic volcanic arc of the Aeolian Islands. In contrast, crustal shortening was no longer active in the southern Apennines. Currently, extension affects this sector, with active volcanism, especially along the eastern side of the Tyrrhenian Sea.

10. CONCLUSIONS

This paper provides a review and a reinterpretation of the knowledge of the northern Calabria–southern Apennines chain in terms of stratigraphy, metamorphism, tectonics, and paleogeography during its Tertiary–Quaternary orogenic evolution. Compared to the available literature, schematic stratigraphic logs and an exhaustive description of the main successions cropping out in this segment of the Alpine orogen are provided, with particular emphasis placed on the foreland basin system, which well constrains the timing of orogenic evolution. In the provided stratigraphic logs, the different orogenic stages are well identified, including the backbulge and forebulge stages, the foredeep basin, the main thrusting event, and the overlying wedge-top basin deposits.

We also provided a general framework for metamorphism, tectonic exhumation, and orogenic tectonic transport directions. We restored the latter data according to the available paleomagnetic studies on the orogenic rotations of the different sectors of the orogenic chain. The restored tectonic vergence directions were used to better constrain the orogenic thrust-front migration.

In our reconstruction, we attempted to link up the thrust-front geometry and the tectonic style of the Miocene to middle Pleistocene crustal shortening with the articulate paleogeography and thickness of the continental lithosphere involved in the subduction process. In particular, we emphasized two major episodes of crustal backstop that occurred during the orogenic evolution, corresponding to the chain docking with the thick lithosphere underlying the Apennine and Apulian Platforms. In the first case (late Serravallian), the main subduction detachment moved toward the foreland, with the overthrusting of Apennine carbonates onto the pelagic Lagonegro-Molise Basin successions, which, in the late Miocene, were offscraped and variously piled up through dominantly thin-skinned thrusting. The second backstop occurred in the early–middle Pliocene, when thick-skinned tectonics involved the buried Apulian Platform succession, triggering breaching thrusting at depth and diffuse out-of-sequence deformation in the allochthonous wedge. The surficial thrust faults caused the doubling of the thrust sheets with the interposition of younger and younger wedge-top basin deposits moving toward the foreland.

This study highlighted another crucial step in the thrust-front migration of the orogenic wedge during the passage between Langhian and Serravallian times. In fact, before the Serravallian, the tectonic vergences for the Ligurian and Apennine Platform units were mainly directed to the south; after that time, from the Serravallian to the Pleistocene, they were directed to the east. This change was probably related to the articulated paleogeography of the continental part of the Adria plate.

Finally, the provided paleogeographic maps were derived by combining different geologic data, including pre- and synorogenic stratigraphy and thrusting events. Compared to previous works, we emphasize the role of the forebulge stage, starting from the Oligocene, in every paleogeographic map. Crustal flexure is a common feature of the two opposite orogenic thrust-front migration episodes of the Apennines and Dinarides, and it shows an axis that is oblique to the orogenic fronts up to the early Messinian and then subsequently parallel.

ACKNOWLEDGMENTS

We are very grateful to the associate editor, E. Tavarnelli, and the two anonymous reviewers for their useful suggestions, which greatly improved this work.

REFERENCES CITED

Accordi, B., 1964, Lineamenti strutturali del Lazio e dell'Abruzzo meridionale: Memorie della Società Geologica Italiana, v. 4, p. 595–633.

Accordi, B., Devoto, G., La Monica, G.B., Praturlon, A., Sirna, G., and Zalaffi, M., 1967, Il Neogene nell'Appennino laziale-abruzzese: Giornale di Geologia, v. 35, p. 235–265.

Agosta, F., Manniello, C., Cavalcante, F., Belviso, C., and Prosser, G., 2021, Late Cretaceous transtensional faulting of the Apulian Platform, Italy: Marine and Petroleum Geology, v. 127, https://doi.org/10.1016/j.marpetgeo.2020.104889.

Alberti, A.U., Bergomi, C., Catenacci, V., Centamore, E., Cestari, G., Chiocchini, M., Chiocchini, U., Manganelli, V., Molinari-Paganelli, V., Panseri-Crescenzi, C., Salvati, L., and Tilia-Zuccari, A., 1975, Note Illustrative del Foglio 389 Anagni: Carta Geologica d'Italia: Rome, Italy, Servizio Geologico d'Italia, Istituto Poligrafico e Zecca dello Stato, scale 1:50,000.

Aldega, L., Cello, G., Corrado, S., Cuadros, J., Di Leo, P., Giampaolo, C., Invernizzi, C., Martino, C., Mazzoli, S., Schiattarella, M., Zattin, M., and Zuffa, G., 2003, Tectono-sedimentary evolution of the southern Apennines (Italy): Thermal constraints and modelling: Atti Ticinensi di Scienze della Terra, v. 9, p. 135–140.

Alvarez, W., 1976, A former continuation of the Alps: Geological Society of America Bulletin, v. 87, p. 891–896, https://doi.org/10.1130/0016-7606(1976)87<891:AFCOTA>2.0.CO;2.

Alvarez, W., 1991, Tectonic evolution of the Corsica-Apennines-Alps region studied by the method of successive approximations: Tectonics, v. 10, p. 936–947, https://doi.org/10.1029/91TC00232.

Alvarez, W., and Shimabukuro, D.H., 2009, The geological relationships between Sardinia and Calabria during Alpine and Hercynian times: Italian Journal of Geosciences, v. 128, p. 257–268, https://doi.org/10.3301/IJG.2009.128.2.257.

Amodio-Morelli, L., Bonardi, G., Colonna, V., Dietrich, D., Giunta, G., Ippolito, F., Liguori, V., Lorenzoni, S., Paglionico, A., Perrone, V., Piccarreta, G., Russo, M., Scandone, P., Zanetti-Lorenzoni, E., and Zuppetta, A., 1976, L'Arco Calabro-Peloritano nell'orogene appenninico-maghrebide: Memorie della Societa Geologica Italiana, v. 17, p. 1–60.

Amore, O., Bonardi, G., Ciampo, G., de Capoa, P., Perrone, V., and Sgrosso, I., 1988, Relazioni tra "flysch interni" e domini appenninici: Reinterpretazione delle formazioni di Pollica, San Mauro e Albidona e il problema dell'evoluzione inframiocenica delle zone esterne appenniniche: Memorie della Societa Geologica Italiana, v. 41, p. 285–299.

Amore, O., Basso, C., Ciarcia, S., Di Nocera, S., Matano, F., Torre, M., Ciampo, G., Di Donato, V., Esposito, P., and Staiti, D., 1998, Nuovi dati stratigrafici sul Pliocene affiorante tra il fiume Ufita e il torrente Cervaro (Irpinia, Appennino meridionale): Bollettino della Società Geologica Italiana, v. 117, p. 455–466.

Ascione, A., Ciarcia, S., Di Donato, V., Mazzoli, S., and Vitale, S., 2012, The Pliocene–Quaternary wedge-top basins of southern Italy: An expression of propagating lateral slab tear beneath the Apennines: Basin Research, v. 24, p. 456–474, https://doi.org/10.1111/j.1365-2117.2011.00534.x.

Bally, A.W., Gordy, P.L., and Stewart, G.A., 1966, Structure, seismic data and orogenic evolution of Southern Canada Rocky Mountains: Bulletin of Canadian Petroleum Geology, v. 14, p. 337–381.

Barchi, M.R., and Tavarnelli, E., 2022, Thin vs. thick-skinned tectonics in the Umbria-Marche fold-and-thrust belt: Contrast or coexistence?, *in* Koeberl, C., Claeys, P., and Montanari, A., eds., From the Guajira Desert to the Apennines, and from Mediterranean Microplates to the Mexican Killer Asteroid: Honoring the Career of Walter Alvarez: Geological Society of America Special Paper 557, p. 71–84, https://doi.org/10.1130/2022.2557(05).

Barone, M., Dominici, R., Muto, F., and Critelli, S., 2008, Detrital modes in a late Miocene wedge-top basin, northeastern Calabria, Italy: Compositional record of wedge-top partitioning: Journal of Sedimentary Research, v. 78, p. 693–711, https://doi.org/10.2110/jsr.2008.071.

Bartiromo, A., Graziano, R., Raspini, A., and Bravi, S., 2019, A new terrestrial plant-rich fossil-lagerstätte from the middle Cenomanian (Late Cretaceous) of the Apennine carbonate platform (Magliano Vetere, southern Italy): Depositional and palaeoenvironmental settings: Sedimentary Geology, v. 388, p. 37–65, https://doi.org/10.1016/j.sedgeo.2019.04.010.

Basso, C., Ciampo, G., Ciarcia, S., Di Nocera, S., Matano, F., and Torre, M., 2002, Geologia del settore irpino-dauno dell'Appennino meridionale: Implicazioni sui domini paleogeografici delle unità bacinali meso-cenozoiche e nuovi vincoli stratigrafici nell'evoluzione tettonica mio-pliocenica del settore esterno della catena: Studi Geologici Camerti, v. 2, p. 7–27.

Beaumont, C., Ellis, S., Hamilton, J., and Fullsack, P., 1996, Mechanical model for subduction-collision tectonics of Alpine-type compressional orogens: Geology, v. 24, p. 675–678, https://doi.org/10.1130/0091-7613(1996)024<0675:MMFSCT>2.3.CO;2.

Bernoulli, D., 2001, Mesozoic–Tertiary carbonate platforms, slopes and basins of the external Apennines and Sicily, *in* Vai, G.B., and Martini, P., eds., Anatomy of a Orogen: The Apennines and Adjacent Mediterranean Basins: Dordrecht, Netherlands, Kluwer Academic Publishers, p. 307–325, https://doi.org/10.1007/978-94-015-9829-3_18.

Bertotti, G., Picotti, V., Chilovi, C., Fantoni, R., Merlini, S., and Mosconi, A., 2001, Neogene to Quaternary sedimentary basin in the south Adriatic (Central Mediterranean): Foredeeps and lithospheric buckling: Tectonics, v. 20, p. 771–787, https://doi.org/10.1029/2001TC900012.

Bessière, E., Scaillet, S., Augier, R., Jolivet, L., Azañón, J.M., Booth-Rea, G., Romagny, A., and Duval, F., 2022, ^{40}Ar/^{39}Ar age constraints on HP/LT metamorphism in extensively overprinted units: The example of the Alpujárride subduction complex (Betic Cordillera, Spain): Tectonics, v. 41, no. 2, https://doi.org/10.1029/2021TC006889.

Bigi, G., Cosentino, D., Parotto, M., Sartori, R., and Scandone, P., eds., 1992, Structural Model of Italy and Gravity Map, Scale 1:500,000, Progetto Finalizzato Geodinamica Consiglio Nazionale delle Ricerche: Quaderni de la Ricerca Scientifica, v. 3, p. 114.

Bigi, S., and Di Bucci, D., 1987, Rilevamento geologico delle strutture di Monte Picca e di Monte La Queglia, Appennino abruzzese: Geologica Romana, v. 26, p. 413–418.

Bonardi, G., Amore, O., Ciampo, G., de Capoa, P., Miconnet, P., and Perrone, V., 1988a, Il Complesso Liguride Auct.: Stato delle conoscenze e problemi aperti sulla sua evoluzione pre-appenninca ed i suoi rapporti con l'arco calabro: Memorie della Società Geologica Italiana, v. 41, p. 17–35.

Bonardi, G., D'Argenio, B., and Perrone, V., 1988b, Carta Geologica dell'Appennino Meridionale: Memorie della Società Geologica Italiana, v. 41, scale 1:250,000, 1 sheet.

Bonardi, G., De Capoa, P., Fioretti, B., and Perrone, V., 1993, L'age des métacalcaires de l'Unité du Frido (région calabro-lucanienne, Italie) et ses implications géodynamiques: Comptes Rendus de l'Académie des Sciences, v. 317, no. II, p. 955–962.

Bonardi, G., Cavazza, W., Perrone, V., and Rossi, S., 2001, Calabria-Peloritani terrane and northern Ionian Sea, *in* Vai, G.B., and Martini, I.P., eds., Anatomy of an Orogen: The Apennines and Adjacent Mediterranean Basins: Dordrecht, Netherlands, Kluwer Academic Publishers, p. 287–306.

Bonardi, G., de Capoa, P., Di Staso, A., Perrone, V., Sonnino, M., and Tramontana, M., 2005, The age of the Paludi Formation: A major constraint to the beginning of the Apulia-verging orogenic transport in the northern sector of the Calabria-Peloritani arc: Terra Nova, v. 17, p. 331–337, https://doi.org/10.1111/j.1365-3121.2005.00618.x.

Bonardi, G., Ciarcia, S., Di Nocera, S., Matano, F., Sgrosso, I., and Torre, M., 2009, Carta delle principali unità Cinematiche dell'Appennino meridionale: Nota illustrativa: Italian Journal of Geosciences, v. 128, p. 47–60, scale 1:250,000, 1 sheet.

Boni, M., 1974, Le argille rosse continentali del passaggio Paleocene–Miocene nella piattaforma carbonatica campano-lucana: Bollettino della Società Geologica Italiana, v. 93, p. 1059–1094.

Boni, M., Reddy, S.M., Mondillo, N., Balassone, G., and Taylor, R., 2012, A distant magmatic source for Cretaceous karst bauxites of Southern Apennines (Italy), revealed through SHRIMP zircon age dating: Terra Nova, v. 24, p. 326–332, https://doi.org/10.1111/j.1365-3121.2012.01068.x.

Bosellini, A., and Hsü, K., 1973, Mediterranean plate tectonics and Triassic palaeogeography: Nature, v. 244, p. 144–146, https://doi.org/10.1038/244144a0.

Boullin, J.P., 1984, Nouvelle interprétation de la liason Apennin-Maghrebides en Calabre: Consequences sur la palaéogéographie téthysienne entre Gibraltar et les Alpes: Revue de Géologie Dynamique et de Géographie Physique, v. 25, p. 321–338.

Brandt, S., and Schenk, V., 2020, Metamorphic response to Alpine thrusting of a crustal-scale basement nappe in southern Calabria (Italy): Journal of Petrology, v. 61, https://doi.org/10.1093/petrology/egaa063.

Bucci, F., Novellino, R., Tavarnelli, E., Prosser, G., Guzzetti, F., Cardinali, M., Gueguen, E., Guglielmi, P., and Adurno, I., 2014, Frontal collapse during thrust propagation in mountain belts: A case study in the Lucania Apennines, southern Italy: Journal of the Geological Society, v. 171, no. 4, p. 571–581, https://doi.org/10.1144/jgs2013-103.

Bucci, F., Tavarnelli, E., Prosser, G., Novellino, R., Palladino, G., Bentivenga, M., Guglielmi, P., and Laurita, S., 2019, The history of the Southern Apennines of Italy preserved in the geosites along a geological itinerary in the High Agri Valley: Geoheritage, v. 11, p. 1489–1508, https://doi.org/10.1007/s12371-019-00385-y.

Bucci, F., Novellino, R., Guglielmi, P., and Tavarnelli, E., 2020, Growth and dissection of a fold and thrust belt: The geological record of the High Agri Valley, Italy: Journal of Maps, v. 16, p. 245–256, https://doi.org/10.1080/17445647.2020.1737254.

Burton, A.N., compiler, 1971, Carta Geologica della Calabria, Sheets 228–229: Rome, Italy, Cassa per il Mezzogiorno, scale 1:25,000.

Butler, R.W.H., 1987, Thrust sequences: Journal of the Geological Society, v. 144, p. 619–634, https://doi.org/10.1144/gsjgs.144.4.0619.

Butler, R.W.H., Mazzoli, S., Corrado, S., De Donatis, M., Di Bucci, D., Gambini, R., Naso, G., Nicolai, C., Scrocca, D., Shiner, P., and Zucconi, V., 2004, Applying thick-skinned tectonic models to the Apennine thrust belt of Italy and implications, *in* McClay, K.R., ed., Thrust Tectonics and Hydrocarbon Systems: America Association of Petroleum Geologists Memoir 82, p. 647–667, https://doi.org/10.1306/M82813C34.

Calamita, F., Esestime, P., Paltrinieri, W., Scisciani, V., and Tavarnelli, E., 2009, Structural inheritance of pre- and syn-orogenic normal faults on the arcuate geometry of Pliocene–Quaternary thrusts: Examples from the Central and Southern Apennine chain: Italian Journal of Geosciences, v. 128, p. 381–394, https://doi.org/10.3301/IJG.2009.128.2.381.

Calamita, F., Satolli, S., and Turtù, A., 2012, Analysis of thrust shear zones in curve-shaped belts: Deformation mode and timing of the Olevano-Antrodoco-Sibillini thrust (Central/Northern Apennines of Italy): Journal of Structural Geology, v. 44, p. 179–187, https://doi.org/10.1016/j.jsg.2012.07.007.

Cardello, G.L., Vico, G., Consorti, L., Sabbatino, M., Carminati, E., and Doglioni, C., 2021, Constraining the passive to active margin tectonics of the internal Central Apennines: Insights from biostratigraphy, structural, and seismic analysis: Geosciences, v. 11, https://doi.org/10.3390/geosciences11040160.

Carminati, E., and Doglioni, C., 2012, Alps vs Apennines: The paradigm of a tectonically asymmetric Earth: Earth-Science Reviews, v. 112, p. 67–96, https://doi.org/10.1016/j.earscirev.2012.02.004.

Carminati, E., Corda, L., Mariotti, G., and Brandano, M., 2007, Tectonic control on the architecture of a Miocene carbonate ramp in the Central Apennines (Italy): Insights from facies and backstripping analyses: Sedimentary Geology, v. 198, p. 233–253, https://doi.org/10.1016/j.sedgeo.2006.12.005.

Carminati, E., Lustrino, M., and Doglioni, C., 2012, Geodynamic evolution of the central and western Mediterranean: Tectonics vs. igneous petrology constraints: Tectonophysics, v. 579, p. 173–192, https://doi.org/10.1016/j.tecto.2012.01.026.

Carrara, A., and Zuffa, G.G., 1976, Alpine structures in northwestern Calabria; Italy: Geological Society of America Bulletin, v. 87, p. 1229–1246, https://doi.org/10.1130/0016-7606(1976)87<1229:ASINCI>2.0.CO;2.

Casero, P., Roure, F., Endignoux, L., Moretti, I., Muller, C., Sage, L., and Vially, R., 1988, Neogene geodynamic evolution of the southern Apennines: Memorie della Società Geologica Italiana, v. 41, p. 109–120.

Castellano, M.C., and Sgrosso, I., 1996, Età e significato dei depositi miocenici della formazione di M. Sierio e possibile evoluzione cinematica dell'unità Monti della Maddalena nell'Appennino campano-lucano: Memorie della Società Geologica Italiana, v. 51, p. 239–249.

Catalano, S., Monaco, C., Tortorici, L., Paltrinieri, W., and Steel, N., 2004, Neogene–Quaternary tectonic evolution of the Southern Apennines: Tectonics, v. 23, TC2003, https://doi.org/10.1029/2003TC001512.

Centamore, E., Bigi, S., Berti, D., Micarelli, A., and Morelli, C., 1992, Nuovi dati sui depositi neogenici di avanfossa del Pescarese: Bollettino della Società Geologica Italiana, v. 111, p. 437–447.

Centamore, E., Di Manna, P., and Rossi, D., 2007, Kinematic evolution of the Volsci Range: A new overview: Italian Journal of Geosciences, v. 126, p. 159–172.

Cerisola, R., and Montone, P., 1992, Analisi strutturale di un settore della catena dei Monti Ausoni–Aurunci (Lazio, Italia centrale): Bollettino della Società Geologica Italiana, v. 111, p. 449–457.

Chalouan, A., and Michard, A., 1990, The Ghomarides nappes, Rif coastal range, Morocco: A Variscan chip in the Alpine belt: Tectonics, v. 9, no. 6, p. 1565–1583, https://doi.org/10.1029/TC009i006p01565.

Channell, J.E.T., 1996, Palaeomagnetism and palaeogeography of Adria, *in* Morris, A., and Tarling, D.H., eds., Palaeomagnetism and Tectonics of the Mediterranean Region: Geological Society, London, Special Publication 105, p. 119–132, https://doi.org/10.1144/GSL.SP.1996.105.01.11.

Ciaranfi, N., Pieri, P., and Ricchetti, G., 1988, Note alla carta geologica delle Murge e del Salento (Puglia centro-meridionale): Memorie della Società Geologica Italiana, v. 41, p. 449–460, scale 1:250,000, 1 sheet.

Ciarapica, G., and Passeri, L., 1998, Evoluzione paleogeografica degli Appennini: Atti Ticinensi di Scienze della Terra, v. 40, p. 233–290.

Ciarcia, S., and Vitale, S., 2013, Sedimentology, stratigraphy and tectonics of evolving wedge-top depozone: Ariano Basin, Southern Apennines, Italy: Sedimentary Geology, v. 290, p. 27–46, https://doi.org/10.1016/j.sedgeo.2013.02.015.

Ciarcia, S., Di Nocera, S., Matano, F., and Torre, M., 2003, Evoluzione tettono-sedimentaria e paleogeografica dei depocentri "wedge-top" nell'ambito del "foreland basin system" pliocenico dell'Appennino meridionale (settore Irpino-Dauno): Bollettino della Società Geologica Italiana, v. 122, p. 117–137.

Ciarcia, S., Vitale, S., Di Staso, A., Iannace, A., Mazzoli, S., and Torre, M., 2009a, Stratigraphy and tectonics of an Internal unit of the Southern Apennines: Implications for the geodynamic evolution of the peri-Tyrrhenian mountain belt: Terra Nova, v. 21, p. 88–96, https://doi.org/10.1111/j.1365-3121.2008.00859.x.

Ciarcia, S., Torre, M., and Mitrano, T., 2009b, Stratigrafia della Formazione del Ponticello (Miocene Superiore, Appennino campano): Bollettino della Società Geologica Italiana, v. 128, p. 715–721.

Ciarcia, S., Mazzoli, S., Vitale, S., and Zattin, M., 2012, On the tectonic evolution of the Ligurian accretionary complex in southern Italy: Geological Society of America Bulletin, v. 124, p. 463–483, https://doi.org/10.1130/B30437.1.

Cinque, A., Patacca, E., Scandone, P., and Tozzi, M., 1993, Quaternary kinematic evolution of the southern Apennines: Relationships between surface geological features and deep lithospheric structures: Annali di Geofisica, v. 36, p. 249–260.

Cipollari, P., and Cosentino, D., 1995, Miocene unconformities in the Central Apennines: Geodynamic significance and sedimentary basin evolution: Tectonophysics, v. 252, p. 375–389, https://doi.org/10.1016/0040-1951(95)00088-7.

Cipollari, P., Cosentino, D., Esu, D., Girotti, O., Gliozzi, E., and Praturlon, A., 1999, Thrust-top lacustrine-lagoonal basin development in accretionary wedges: Late Messinian (Lago-Mare) episode in the Central Apennines (Italy): Palaeogeography, Palaeoclimatology, Palaeoecology, v. 151, p. 149–166, https://doi.org/10.1016/S0031-0182(99)00026-7.

Cippitelli, G., 2007, The CROP-04 seismic profile: Interpretation and structural setting of the Agropoli-Barletta Geotraverse: Bollettino della Società Geologica Italiana, Special Issue 7, p. 267–281.

Civitelli, G., and Brandano, M., 2005, Atlante delle litofacies e modello deposizionale dei Calcari a Briozoi e Litotamni nella Piattaforma carbonatica laziale-abruzzese: Bollettino della Società Geologica Italiana, v. 124, p. 611–643.

Colacicchi, R., Devoto, G., and Praturlon, A., 1967, Depositi messiniani oligoalini al bordo orientale del Fucino e descrizione di *Tyrrhenocythere ruggierii* Devoto, nuova specie di ostracode: Bollettino della Società Geologica Italiana, v. 86, p. 21–37.

Colella, A., 1995, Sedimentation, deformational events and eustacy in the peri-Tyrrhenian Amantea Basin: Prelimimary synthesis: Giornale di Geologia, v. 3, no. 57, p. 179–193.

Corrado, S., Di Bucci, D., Naso, G., and Damiani, A.V., 1998, Rapporti tra le grandi unità stratigrafico-strutturali delle aree esterne dell'Appennino centrale: Evoluzione geologica dell'Alto Molise: Bollettino della Società Geologica Italiana, v. 117, p. 761–776.

Corrado, S., Aldega, L., Perri, F., Critelli, S., Muto, F., Schito, A., and Tripodi, V., 2019, Detecting syn-orogenic extension and sediment provenance of the Cilento wedge top basin (Southern Apennines, Italy): Mineralogy and geochemistry of fine-grained sediments and petrography of dispersed organic matter: Tectonophysics, v. 750, p. 404–418, https://doi.org/10.1016/j.tecto.2018.10.027.

Cosentino, D., Cipollari, P., Di Donato, V., Sgrosso, I., and Sgrosso, M., 2002, The Volsci Range in the kinematic evolution of the Northern and Southern Apennine orogenetic system: Bollettino della Società Geologica Italiana, Special Issue 1, p. 209–218.

Cosentino, D., Cipollari, P., and Pipponzi, G., 2003, Il sistema orogenico dell'Appennino centrale: Vincoli stratigrafici e cronologia della migrazione, *in* Cipollari, P., and Cosentino, D., eds., Evoluzione Cinematica del Sistema Orogenico dell'Appennino Centro-Meridionale: Caratterizzazione Stratigrafico-Strutturale dei Bacini Sintettonici: Studi Geologici Camerti Numero Speciale 2003, p. 85–99.

Cosentino, D., Cipollari, P., Marsili, P., and Scrocca, D., 2010, Geology of the central Apennines: A regional review, *in* Beltrando, M., Peccerillo, A., Mattei, M., Conticelli, S., and Doglioni, C., eds., The Geology of Italy: Tectonics and Life along Plate Margins: Journal of the Virtual Explorer, v. 36, paper 12, https://doi.org/10.3809/jvirtex.2010.00223.

Cristi Sansone, M.T., Prosser, G., Rizzo, G., and Tartarotti, P., 2012, Spinel-peridotite of the Frido Unit ophiolites (Southern Apennine-Italy): Evidence for oceanic evolution: Periodico di Mineralogia, v. 81, p. 35–59.

Critelli, S., 1999, The interplay of lithospheric flexure and thrust accomodation in forming stratigraphic sequences in the southern Apennines foreland basin system Italy: Rendiconti Lincei, v. 10, no. 4, p. 257–326, https://doi.org/10.1007/BF02904390.

Critelli, S., 2018, Provenance of Mesozoic to Cenozoic circum-Mediterranean sandstones in relation to tectonic setting: Earth-Science Reviews, v. 185, p. 624–648, https://doi.org/10.1016/j.earscirev.2018.07.001.

Critelli, S., and Le Pera, E., 1995, La Formazione di Castelvetere nell'evoluzione petrostratigrafica dell'avanfossa del Tortoniano-Messiniano dell'Appennino meridionale: Bollettino della Società Geologica Italiana, v. 114, p. 615–634.

Critelli, S., de Capoa, P., Le Pera, E., and Perrone, V., 1994, Stratigrafia e petrografia delle Arenarie di Albanella (valle del Calore, Appennino campano): Bollettino della Società Geologica Italiana, v. 113, p. 451–463.

Crostella, A., and Vezzani, L., 1964, La geologia dell'Appennino foggiano: Bollettino della Società Geologica Italiana, v. 83, p. 121–142.

D'Agostino, N., Speranza, F., and Funiciello, R., 1997, Le Brecce Mortadella dell'Appennino Centrale: Primi risultati di stratigrafia magnetica: Il Quaternario, v. 10, p. 385–388.

Damiani, A.V., Chiocchini, M., Colacicchi, R., Mariotti, G., Parotto, M., Passeri, L., and Praturlon, A., 1992, Elementi litostratigrafici per una sintesi delle facies carbonatiche Meso-Cenozoiche dell'Appennino centrale: Studi Geologici Camerti, v. 1991, no. 2, p. 187–214 [special volume].

D'Argenio, B., Pescatore, T., and Scandone, P., 1973, Schema geologico dell'Appennino meridionale (Campania e Lucania): Atti Accademia Nazionale Lincei: Quaderni, v. 183, p. 49–72.

Davis, D.M., Suppe, J., and Dahlen, F.A., 1983, Mechanics of fold and thrust belts and accretionary wedges: Journal of Geophysical Research, v. 88, p. 1153–1172, https://doi.org/10.1029/JB088iB02p01153.

Dazzaro, L., Di Nocera, S., Pescatore, T., Rapisardi, L., Romeo, M., Russo, B., Senatore, M., and Torre, M., 1988, Geologia del margine della catena appenninica tra il F. Fortore ed il T. Calaggio (Monti della Daunia - App. Merid.): Memorie della Società Geologica Italiana, v. 41, p. 411–422.

De Alfieri, A., Guzzi, R., Sacchi, M., D'Argenio, B., Perrone, V., and Zamparelli, V., 1986, Monte Foraporta Unit: A minor element of Southern Apennine nappe pile: Stratigraphic and tectonic study: Rendiconti della Società Geologica Italiana, v. 9, p. 171–178.

De Blasio, I., Lima, A., Perrone, V., and Russo, M., 1981, Nuove vedute sui depositi miocenici della Penisola Sorrentina: Bollettino della Società Geologica Italiana, v. 100, p. 57–70.

DeCelles, P.G., 2012, Foreland basin systems revisited: Variations in response to tectonic settings, *in* Busby, C., and Azor, A., eds., Tectonics of Sedimentary Basins: Recent Advances: Oxford, UK, Wiley-Blackwell, p. 405–426, https://doi.org/10.1002/9781444347166.ch20.

DeCelles, P.G., and Giles, K.A., 1996, Foreland basin systems: Basin Research, v. 8, p. 105–123, https://doi.org/10.1046/j.1365-2117.1996.01491.x.

De Corso, S., Scrocca, D., and Tozzi, M., 1998, Geologia dell'anticlinale del Matese e implicazioni per la tettonica dell'Appennino molisano: Bollettino della Società Geologica Italiana, v. 117, p. 419–441.

D'Erasmo, G., 1956, Pietra leccese: Lexique Stratigraphique International [Paris], v. 1, p. 81–82.

Dewey, J.F., Helman, M.L., Turco, E., Hutton, D.H.W., and Knott, S.D., 1989, Kinematics of the western Mediterranean, *in* Coward, M.P., Dietrich, D., and Park, R.G., eds., Alpine Tectonics: Geological Society, London, Special Publication 45, p. 265–283, https://doi.org/10.1144/GSL.SP.1989.045.01.15.

Dickinson, W.R., 1974, Plate tectonics and sedimentation, *in* Dickinson, W.R., ed., Tectonics and Sedimentation: Society for Sedimentary Geology (SEPM) Special Publication 22, p. 1–27, https://doi.org/10.2110/pec.74.22.0001.

Dietrich, D., 1976, La geologia della Catena Costiera calabra tra Cetraro e Guardia Piemontese: Memorie della Società Geologica Italiana, v. 17, p. 61–121.

Dietrich, D., 1988, Sense of overthrust shear in the Alpine nappes of Calabria (southern Italy): Journal of Structural Geology, v. 10, p. 373–381, https://doi.org/10.1016/0191-8141(88)90015-6.

Di Girolamo, P., Sgrosso, I., De Gennaro, R., and Giurazzi, S., 2000, Metamorphic rocks in Campania (southern Italy): The 'Mondragone marbles': Petrological and geological study: Bollettino della Società Geologica Italiana, v. 119, p. 761–766.

Di Nocera, S., Ortolani, F., Russo, M., and Torre, M., 1974, Successioni sedimentarie messiniane e limite Miocene-Pliocene nella Calabria settentrionale: Bollettino della Società Geologica Italiana, v. 93, p. 575–607.

Di Nocera, S., Matano, F., Pescatore, T., Pinto, F., and Torre, M., 2011, Caratteri geologici del settore esterno dell'Appennino campano-lucano nei Fogli CARG: Rendiconti online della Società Geologica Italiana, v. 12, p. 39–43.

Di Staso, A., and Giardino, S., 2002, New integrated biostratigraphic data about the Saraceno Formation (North-Calabrian unit; southern Apennines): Bollettino della Società Geologica Italiana, Special Issue 1, no. 2, p. 517–526.

Di Stefano, A., Vinci, G., and Romeo, M., 2002, The Plio-Pleistocene deposits at the southeastern border of the Sant'Arcangelo basin (southern Apennines): Structural setting and biostratigraphical data: Bollettino della Società Geologica Italiana, Special Issue 1, p. 527–537.

Doglioni, C., 1993, Some remarks on the origin of foredeeps: Tectonophysics, v. 228, p. 1–20, https://doi.org/10.1016/0040-1951(93)90211-2.

Doglioni, C., Harabaglia, P., Martinelli, G., Mongelli, F., and Zito, G., 1996, A geodynamic model of the Southern Apennines accretionary prism: Terra Nova, v. 8, p. 540–547, https://doi.org/10.1111/j.1365-3121.1996.tb00783.x.

Donzelli, G., and Crescenti, U., 1962, Lembi di Flysch oligocenico affiorante a SE della Piana del Sele: Memorie della Società Geologica Italiana, v. 3, p. 569–592.

Dubois, R., 1976, La suture calabro-apenninique Cretacé-Eocene et l'ouverture tyrrhenienne Neogene: Etude petrographique et structurale de la Calabre centrale [These]: R Paris, France, Université Paris, Pierre-et-Marie-Curie, 567 p.

Eberli, G.P., Bernoulli, D., Vecsei, A., Sekti, R., Grasmueck, M., Lüdmann, T., Anselmetti, F.S., Mutti, M., and Della Porta, G., 2019, Cretaceous carbonate drift delta in the Montagna della Maiella, Italy: Sedimentology, v. 66, no. 4, p. 1266–1301, https://doi.org/10.1111/sed.12590.

Faccenna, C., Davy, P., Brun, J.P., Funiciello, R., Giardini, D., Mattei, M., and Nalpas, T., 1996, The dynamics of back-arc extension: An experimental approach to the opening of the Tyrrhenian Sea: Geophysical Journal International, v. 126, p. 781–795, https://doi.org/10.1111/j.1365-246X.1996.tb04702.x.

Faccenna, C., Becker, T.W., Lucente, F.P., Jolivet, L., and Rossetti, F., 2001a, History of subduction and back-arc extension in the central Mediterranean: Geophysical Journal International, v. 145, p. 809–820, https://doi.org/10.1046/j.0956-540x.2001.01435.x.

Faccenna, C., Funiciello, F., Giardini, D., and Lucente, P., 2001b, Episodic back-arc extension during restricted mantle convection in the central Mediterranean: Earth and Planetary Science Letters, v. 187, p. 105–116, https://doi.org/10.1016/S0012-821X(01)00280-1.

Faccenna, C., Becker, T.W., Conrad, C.P., and Husson, L., 2013, Mountain building and mantle dynamics: Tectonics, v. 32, no. 1, p. 80–93, https://doi.org/10.1029/2012TC003176.

Faccenna, C., Becker, T.W., Holt, A.F., and Brun, J.P., 2021, Mountain building, mantle convection, and supercontinents: Holmes (1931) revisited: Earth and Planetary Science Letters, v. 564, https://doi.org/10.1016/j.epsl.2021.116905.

Faure, M., 1980, Microtectonique et charriage est-ouest des nappes alpines profondes de Sila (Calabre-Itlalie meridionale): Revue de Géologie Dynamique et de Géographie Physique, v. 22, p. 135–146.

Fedele, L., Tramparulo, F.D.A., Vitale, S., Cappelletti, P., Prinzi, E.P., and Mazzoli, S., 2018, Petrogenesis and deformation history of the lawsonite-bearing blueschist facies metabasalts of the Diamante-Terranova oceanic unit (southern Italy): Journal of Metamorphic Geology, v. 36, p. 691–714, https://doi.org/10.1111/jmg.12303.

Fornelli, A., Micheletti, F., Langone, A., and Perrone, V., 2015, First U-Pb detrital zircon ages from Numidian Sandstones in Southern Apennines (Italy): Evidences of Numidian provenance: Sedimentary Geology, v. 320, p. 19–29, https://doi.org/10.1016/j.sedgeo.2015.02.005.

Fornelli, A., Festa, V., Micheletti, F., Spiess, R., and Tursi, F., 2020, Building an orogen: Review of U-Pb zircon ages from the Calabria-Peloritani terrane to constrain the timing of the southern Variscan belt: Minerals, v. 10, no. 11, https://doi.org/10.3390/min10110944.

Garzanti, E., Doglioni, C., Vezzoli, G., and Ando, S., 2007, Orogenic belts and orogenic sediment provenance: The Journal of Geology, v. 115, no. 3, p. 315–334, https://doi.org/10.1086/512755.

Ghisetti, F., and Vezzani, L., 1988a, Rapporti strutturali tra il fronte del Gran Sasso ed il flysch della Laga (Appennino centrale): Memorie della Società Geologica Italiana, v. 41, p. 1171–1178.

Ghisetti, F., and Vezzani, L., 1988b, Geometric and kinematic complexities in the Marche-Abruzzi external zones (Central Apennines, Italy): Geologische Rundschau, v. 77, p. 63–78, https://doi.org/10.1007/BF01848676.

Giannandrea, P., Marino, M., Romeo, M., and Schiattarella, M., 2014, Pliocene to Quaternary evolution of the Ofanto Basin in southern Italy: An approach based on the unconformity-bounded stratigraphic units: Italian Journal of Geosciences, v. 133, p. 27–44, https://doi.org/10.3301/IJG.2013.11.

Gueguen, E., Doglioni, C., and Fernandez, M., 1998, On the post–25 Ma geodynamic evolution of the western Mediterranean: Tectonophysics, v. 298, p. 259–269, https://doi.org/10.1016/S0040-1951(98)00189-9.

Guerrera, F., Martín-Martín, M., Perrone, V., and Tramontana, M., 2005, Tectono-sedimentary evolution of the southern branch of the western Tethys (Maghrebian Flysch Basin and Lucanian Ocean): Consequences for western Mediterranean geodynamics: Terra Nova, v. 17, p. 358–367, https://doi.org/10.1111/j.1365-3121.2005.00621.x.

Guerrera, F., Martín-Martín, M., and Tramontana, M., 2020, Evolutionary models of the Cenozoic basins of central-western Mediterranean area: A review of methodological approaches: Geosciences, v. 10, https://doi.org/10.3390/geosciences10090366.

Handy, M.R., Schmid, S.M., Bousquet, R., Kissling, E., and Bernoulli, D., 2010, Reconciling plate-tectonic reconstructions of Alpine Tethys with the geological-geophysical record of spreading and subduction in the Alps: Earth-Science Reviews, v. 102, p. 121–158, https://doi.org/10.1016/j.earscirev.2010.06.002.

Hippolyte, J.-C., Angelier, J., and Roure, F., 1994, A major geodynamic change revealed by Quaternary stress patterns in the Southern Apennines (Italy): Tectonophysics, v. 230, p. 199–210, https://doi.org/10.1016/0040-1951(94)90135-X.

Iannace, A., Parente, M., and Zamparelli, V., 2005, The Upper Triassic platform margin facies of southern Apennines and their Jurassic fate: State of the art: Bollettino della Società Geologica Italiana, v. 124, p. 203–214.

Iannace, A., Vitale, S., D'Errico, M., Mazzoli, S., Di Staso, A., Macaione, E., Messina, A., Reddy, S.M., Somma, R., Zamparelli, V., Zattin, M., and Bonardi, G., 2007, The carbonate tectonic units of northern Calabria (Italy): A record of Apulian paleomargin evolution and Miocene convergence, continental crust subduction, and exhumation of HP-LT rocks: Journal of the Geological Society, v. 164, p. 1165–1186, https://doi.org/10.1144/0016-76492007-017.

Ietto, A., Pescatore, T., and Cocco, E., 1965, Il flysch mesozoico-terziario del Cilento occidentale: Bollettino della Società di Naturalisti in Napoli, v. 74, p. 396–402.

Ingersoll, R.V., 1988, Tectonics of sedimentary basins: Geological Society of America Bulletin, v. 100, p. 1704–1719, https://doi.org/10.1130/0016-7606(1988)100<1704:TOSB>2.3.CO;2.

Ingersoll, R.V., 2012, Tectonics of sedimentary basins, with revised nomenclature, *in* Busby, C., and Azor, A., eds., Tectonics of Sedimentary Basins: Recent Advances: New York, Wiley-Blackwell, p. 3–43, https://doi.org/10.1002/9781444347166.ch1.

Innamorati, G., and Santantonio, M., 2018, Evidence for extended Hercynian basement and a preserved Jurassic basin-margin tract in northern Calabria (southern Italy): The Longobucco Basin: Sedimentary Geology, v. 376, p. 147–163, https://doi.org/10.1016/j.sedgeo.2018.08.009.

Ippolito, F., D'Argenio, B., Pescatore, T., and Scandone, P., 1973, Unità stratigrafico-strutturali e schema tettonico dell'Appennino meridionale (translated from The Guide-Book of Italy): Napoli, Italy, Istituto di Geologia e Geofisica, Università di Napoli, Petroleum Exploration Society of Libya Publication 15, p. 134–155.

Istituto Superiore per la Protezione e la Ricerca Ambientale (ISPRA), 1975, Geological Maps of Italy, Sheet 389 Anagni: Rome, Italy, ISPRA, scale 1:50,000, https://www.isprambiente.gov.it/Media/carg/389_ANAGNI/Foglio.html.

Istituto Superiore per la Protezione e la Ricerca Ambientale (ISPRA), 1997, Geological Maps of Italy, Sheet 376 Subiaco: Rome, Italy, ISPRA, scale 1:50,000, https://www.isprambiente.gov.it/Media/carg/376_SUBIACO/Foglio.html.

Istituto Superiore per la Protezione e la Ricerca Ambientale (ISPRA), 2005a, Geological Maps of Italy, Sheet 367 Tagliacozzo: Rome, Italy, ISPRA, scale 1:50,000, https://www.isprambiente.gov.it/Media/carg/367_TAGLIACOZZO/Foglio.html.

Istituto Superiore per la Protezione e la Ricerca Ambientale (ISPRA), 2005b, Geological Maps of Italy, Sheet 369 Sulmona: Rome, Italy, ISPRA, scale 1:50,000, https://www.isprambiente.gov.it/Media/carg/369_SULMONA/Foglio.html.

Istituto Superiore per la Protezione e la Ricerca Ambientale (ISPRA), 2005c, Geological Maps of Italy, Sheet 360 Torre de' Passeri: Rome, Italy, ISPRA, scale 1:50,000, https://www.isprambiente.gov.it/Media/carg/360_TORRE_DE_PASSERI/Foglio.html.

Istituto Superiore per la Protezione e la Ricerca Ambientale (ISPRA), 2005d, Geological Maps of Italy, Sheet 506 Sant'Arcangelo: Rome, Italy, ISPRA, scale 1:50,000, https://www.isprambiente.gov.it/Media/carg/506_SANT_ARCANGELO/Foglio.html.

Istituto Superiore per la Protezione e la Ricerca Ambientale (ISPRA), 2006, Catalogo delle Formazioni Geologiche Italiane: Marne ad Orbulina: Rome, Italy, ISPRA, p. 1–13, https://sgi.isprambiente.it/catalogo-formazioni-italiane/pdf/3168.pdf.

Istituto Superiore per la Protezione e la Ricerca Ambientale (ISPRA), 2007a, Geological Maps of Italy: Catalogo delle Formazioni (VII), Gruppo delle Argille Variegate: Rome, Italy, ISPRA, scale 1:50,000, https://www.ISPRAmbiente.gov.it/files/pubblicazioni/periodicitecnici/quaderni-sgi/quaderno7fasc7/quaderno7-vii-appennino-argillevariegate.pdf.

Istituto Superiore per la Protezione e la Ricerca Ambientale (ISPRA), 2007b, Geological Maps of Italy: Catalogo delle Formazioni (VI), Scaglia Bianca: Rome, Italy, ISPRA, scale 1:50,000, https://www.isprambiente.gov.it/files/pubblicazioni/periodicitecnici/quaderni-sgi/quaderno7fasc6/quad-7-vi-scaglia-bianca.pdf.

Istituto Superiore per la Protezione e la Ricerca Ambientale (ISPRA), 2007c, Geological Maps of Italy: Catalogo delle Formazioni (VI), Scaglia Rossa: Rome, Italy, ISPRA, scale 1:50,000, https://www.isprambiente.gov.it/files/pubblicazioni/periodicitecnici/quaderni-sgi/quaderno7fasc6/quad-7-vi-scaglia-rossa.pdf.

Istituto Superiore per la Protezione e la Ricerca Ambientale (ISPRA), 2007d, Geological Maps of Italy: Catalogo delle Formazioni (VI), Scaglia Cinerea: Rome, Italy, ISPRA, scale 1:50,000, https://www.isprambiente.gov.it/files/pubblicazioni/periodicitecnici/quaderni-sgi/quaderno7fasc6/quad-7-vi-scaglia-cinerea.pdf.

Istituto Superiore per la Protezione e la Ricerca Ambientale (ISPRA), 2007e, Geological Maps of Italy: Catalogo delle Formazioni (VII), Trubi: Rome, Italy, ISPRA, scale 1:50,000, https://www.isprambiente.gov.it/files/pubblicazioni/periodicitecnici/quaderni-sgi/quaderno7fasc7/quaderno7-vii-sicilia-trubi.pdf.

Istituto Superiore per la Protezione e la Ricerca Ambientale (ISPRA), 2010a, Geological Maps of Italy, Sheet 504 Sala Consilina: Rome, Italy, ISPRA, scale 1:50,000, https://www.isprambiente.gov.it/Media/carg/504_SALA_CONSILINA/Foglio.html.

Istituto Superiore per la Protezione e la Ricerca Ambientale (ISPRA), 2010b, Geological Maps of Italy, Sheet 431 Caserta Est: Rome, Italy, ISPRA, scale 1:50,000, https://www.isprambiente.gov.it/Media/carg/431_CASERTA_EST/Foglio.html.

Istituto Superiore per la Protezione e la Ricerca Ambientale (ISPRA), 2010c, Geological Maps of Italy, Sheet 378 Scanno: Rome, Italy, ISPRA, scale 1:50,000, https://www.isprambiente.gov.it/Media/carg/378_SCANNO/Foglio.html.

Istituto Superiore per la Protezione e la Ricerca Ambientale (ISPRA), 2010d, Geological Maps of Italy, Sheet 349 Gran Sasso d'Italia: Rome, Italy, ISPRA, scale 1:50,000, http://www.isprambiente.it/Media/carg/349_GRANSASSO/Foglio.html.

Istituto Superiore per la Protezione e la Ricerca Ambientale (ISPRA), 2010e, Geological Maps of Italy, Sheet 542 Verbicaro: Rome, Italy, ISPRA, scale 1:50,000, https://www.isprambiente.gov.it/Media/carg/542_VERBICARO/Foglio.html.

Istituto Superiore per la Protezione e la Ricerca Ambientale (ISPRA), 2010f, Geological Maps of Italy, Sheet 419 San Giorgio la Molara: Rome, Italy, ISPRA, scale 1:50,000, https://www.isprambiente.gov.it/Media/carg/419_SANGIORGIO_LAMOLARA/Foglio.html.

Istituto Superiore per la Protezione e la Ricerca Ambientale (ISPRA), 2010 g, Geological Maps of Italy, Sheet 361 Chieti: Rome, Italy, ISPRA, scale 1:50,000, https://www.isprambiente.gov.it/Media/carg/361_CHIETI/Foglio.html.

Istituto Superiore per la Protezione e la Ricerca Ambientale (ISPRA), 2010 h, Geological Maps of Italy, Sheet 407 San Bartolomeo in Galdo: Rome, Italy, ISPRA, scale 1:50,000, https://www.isprambiente.gov.it/Media/carg/407_SANBARTOLOMEO/Foglio.html.

Istituto Superiore per la Protezione e la Ricerca Ambientale (ISPRA), 2011a, Geological Maps of Italy, Sheet 484 Isola di Capri: Rome, Italy, ISPRA, scale 1:50,000, https://www.isprambiente.gov.it/Media/carg/484_ISOLADICAPRI/Foglio.html.

Istituto Superiore per la Protezione e la Ricerca Ambientale (ISPRA), 2011b, Geological Maps of Italy, Sheet 433 Ariano Irpino: Rome, Italy, ISPRA, scale 1:50,000, https://www.isprambiente.gov.it/Media/carg/433_ARIANO_IRPINO/Foglio.html.

Istituto Superiore per la Protezione e la Ricerca Ambientale (ISPRA), 2011c, Geological Maps of Italy, Sheet 393 Trivento: Rome, Italy, ISPRA, scale 1:50,000, https://www.isprambiente.gov.it/Media/carg/393_TRIVENTO/Foglio.html.

Istituto Superiore per la Protezione e la Ricerca Ambientale (ISPRA), 2011d, Geological Maps of Italy, Sheet 402 Ceccano: Rome, Italy, ISPRA, scale 1:50,000, http://www.isprambiente.it/Media/carg/402_CECCANO/Foglio.html.

Istituto Superiore per la Protezione e la Ricerca Ambientale (ISPRA), 2012, Geological Maps of Italy, Sheet 470 Potenza: Rome, Italy, ISPRA, scale 1:50,000, http://www.isprambiente.it/Media/carg/470_POTENZA/Foglio.html.

Istituto Superiore per la Protezione e la Ricerca Ambientale (ISPRA), 2013, Geological Maps of Italy, Sheet 537 Capo di Santa Maria di Leuca: Rome, Italy, ISPRA, scale 1:50,000, https://www.isprambiente.gov.it/Media/carg/537_CAPO_SANTAMARIALEUCA/Foglio.html.

Istituto Superiore per la Protezione e la Ricerca Ambientale (ISPRA), 2014a, Geological Maps of Italy, Sheet 505 Moliterno: Rome, Italy, ISPRA, scale 1:50,000, https://www.isprambiente.gov.it/Media/carg/505_MOLITERNO/Foglio.html.

Istituto Superiore per la Protezione e la Ricerca Ambientale (ISPRA), 2014b, Geological Maps of Italy, Sheet 521 Lauria: Rome, Italy, ISPRA, scale 1:50,000, https://www.isprambiente.gov.it/Media/carg/521_LAURIA/Foglio.html.

Istituto Superiore per la Protezione e la Ricerca Ambientale (ISPRA), 2014c, Geological Maps of Italy, Sheet 485 Termini: Rome, Italy, ISPRA, scale 1:50,000, https://www.isprambiente.gov.it/Media/carg/466_485_SORRENTO_TERMINI/Foglio.html.

Istituto Superiore per la Protezione e la Ricerca Ambientale (ISPRA), 2015, Geological Maps of Italy, Sheet 405 Campobasso: Rome, Italy, ISPRA, scale 1:50,000, https://www.isprambiente.gov.it/Media/carg/405_CAMPOBASSO/Foglio.html.

Istituto Superiore per la Protezione e la Ricerca Ambientale (ISPRA), 2016a, Geological Maps of Italy, Sheet 519

Capo Palinuro: Rome, Italy, ISPRA, scale 1:50,000, https://www.isprambiente.gov.it/Media/carg/519_CAPO_PALINURO/Foglio.html.
Istituto Superiore per la Protezione e la Ricerca Ambientale (ISPRA), 2016b, Geological Maps of Italy, Sheet 520 Sapri: Rome, Italy, ISPRA, scale 1:50,000, https://www.isprambiente.gov.it/Media/carg/520_SAPRI/Foglio.html.
Istituto Superiore per la Protezione e la Ricerca Ambientale (ISPRA), 2016c, Geological Maps of Italy, Sheet 468 Eboli: Rome, Italy, ISPRA, scale 1:50,000, https://www.isprambiente.gov.it/Media/carg/468_EBOLI/Foglio.html.
Istituto Superiore per la Protezione e la Ricerca Ambientale (ISPRA), 2017a, Geological Maps of Italy, Sheet 471 Irsina: Rome, Italy, ISPRA, scale 1:50,000, https://www.isprambiente.gov.it/Media/carg/471_IRSINA/Foglio.html.
Istituto Superiore per la Protezione e la Ricerca Ambientale (ISPRA), 2017b, Geological Maps of Italy, Sheet 384 Vico del Gargano: Rome, Italy, ISPRA, scale 1:50,000, https://www.isprambiente.gov.it/Media/carg/384_VICO_DELGARGANO/Foglio.html.
Istituto Superiore per la Protezione e la Ricerca Ambientale (ISPRA), 2021, Geological Maps of Italy, Sheet 388 Velletri: Rome, Italy, ISPRA, scale 1:50,000, https://www.isprambiente.gov.it/Media/carg/388_VELLETRI/Foglio.html.
Knott, S.D., 1987, The Liguride Complex of southern Italy—A Cretaceous to Paleogene accretionary wedge: Tectonophysics, v. 142, p. 217–226, https://doi.org/10.1016/0040-1951(87)90124-7.
La Bruna, V., Agosta, F., Lamarche, J., Viseur, S., and Prosser, G., 2018, Fault growth mechanisms and scaling properties in foreland basin system: The case study of Monte Alpi, Southern Apennines, Italy: Journal of Structural Geology, v. 116, p. 94–113, https://doi.org/10.1016/j.jsg.2018.08.009.
La Monica, G.B., 1966, Caratteristiche granulometriche e sedimentologiche delle arenarie di Torrice (Frosinone-Lazio meridionale): Atti Accademia Gioenia Scienze Naturali, v. 18, p. 285–312.
Langone, A., Gueguen, E., Prosser, G., Caggianelli, A., and Rottura, A., 2006, The Curinga-Girifalco fault zone (Northern Serre, Calabria) and its significance within the Alpine tectonic evolution of the western Mediterranean: Journal of Geodynamics, v. 42, p. 140–158, https://doi.org/10.1016/j.jog.2006.06.004.
Langone, A., Godard, G., Prosser, G., Caggianelli, A., Rottura, A., and Tiepolo, M., 2010, *P-T-t* path of the Hercynian low-pressure rocks from the Mandatoriccio complex (Sila Massif, Calabria, Italy): New insights for crustal evolution: Journal of Metamorphic Geology, v. 28, no. 2, p. 137–162, https://doi.org/10.1111/j.1525-1314.2009.00858.x.
Lentini, F., 1979, Le unità Sicilidi della Val d'Agri (Appennino Lucano): Geologica Romana, v. 18, p. 215–224.
Liberi, F., and Piluso, E., 2009, Tectonometamorphic evolution of the ophiolitic sequences from northern Calabria-Peloritani terrane: Italian Journal of Geosciences, v. 128, p. 483–493.
Liberi, F., Morten, L., and Piluso, E., 2006, Geodynamic significance of ophiolites within the Calabria-Peloritani terrane: The Island Arc, v. 15, p. 26–43, https://doi.org/10.1111/j.1440-1738.2006.00520.x.
Lombardi, L., 1968, Il pozzo Fogliano nei pressi di Latina e la paleogeografia dell'area: Bollettino della Società Geologica Italiana, v. 87, p. 13–18.
Lustrino, M., Morra, V., Fedele, L., and Franciosi, L., 2009, The beginning of the Apennine subduction system in central-western Mediterranean: Constraints from Cenozoic 'orogenic' magmatic activity of Sardinia (Italy): Tectonics, v. 28, https://doi.org/10.1029/2008TC002419.
Macchiavelli, C., Mazzoli, S., Megna, A., Saggese, F., Santini, S., and Vitale, S., 2012, Applying the multiple inverse method to the analysis of earthquake focal mechanism data: New insights into the active stress field of Italy and surrounding regions: Tectonophysics, v. 580, p. 124–149, https://doi.org/10.1016/j.tecto.2012.09.007.
Malinverno, A., and Ryan, W.B.F., 1986, Extension in the Tyrrhenian Sea and shortening in the Apennines as a result of arc migration driven by sinking of the lithosphere: Tectonics, v. 5, p. 227–245, https://doi.org/10.1029/TC005i002p00227.
Marrone, S., Monié, P., Rossetti, F., Lucci, F., Theye, T., Bouybaouene, M.L., and Zaghloul, M.N., 2021, The pressure-temperature-time-deformation history of the Beni Mzala unit (Upper Sebtides, Rif belt, Morocco): Refining the Alpine tectono-metamorphic evolution of the Alboran domain of the western Mediterranean: Journal of Metamorphic Geology, v. 39, no. 5, p. 591–615, https://doi.org/10.1111/jmg.12587.
Martin, A.K., 2006, Oppositely directed pairs of propagating rifts in back-arc basins: Double saloon door seafloor spreading during subduction rollback: Tectonics, v. 25, TC3008, https://doi.org/10.1029/2005TC001885.
Martinis, B., 1967, Note geologiche sui dintorni di Casarano e Castro (Lecce): Rivista Italiana di Paleontologia e Stratigrafia, v. 73, no. 4, p. 1297–1380.
Massari, F., and Prosser, G., 2013, Late Cenozoic tectono-stratigraphic sequences of the Crotone Basin: Insights on the geodynamic history of the Calabrian arc and Tyrrhenian Sea: Basin Research, v. 25, no. 1, p. 26–51, https://doi.org/10.1111/j.1365-2117.2012.00549.x.
Mattei, M., Cipollari, P., Cosentino, D., Argentieri, A., Rossetti, F., Speranza, F., and Di Bella, L., 2002, The Miocene tectonosedimentary evolution of the southern Tyrrhenian Sea: Stratigraphy, structural and paleomagnetic data from the onshore Amantea Basin (Calabrian arc, Italy): Basin Research, v. 14, p. 147–168, https://doi.org/10.1046/j.1365-2117.2002.00173.x.
Mattei, M., Cifelli, F., and D'Agostino, N., 2007, The evolution of the Calabrian arc: Evidence from paleomagnetic and GPS observations: Earth and Planetary Science Letters, v. 263, p. 259–274, https://doi.org/10.1016/j.epsl.2007.08.034.
Mattioni, L., Shiner, P., Tondi, E., Vitale, S., and Cello, G., 2006, The Argille Varicolori unit of Lucania (Italy): A record of tectonic offscraping and gravity sliding in the Mesozoic–Tertiary Lagonegro Basin, Southern Apennines, *in* Moratti, G., and Chalouan, A., eds., Geology and Active Tectonics of the Western Mediterranean Region and North Africa: Geological Society, London, Special Publication 262, p. 277–288, https://doi.org/10.1144/GSL.SP.2006.262.01.17.
Mazzei, R., Margiotta, S., Foresi, L.M., Riforgiato, F., and Salvatorini, G., 2009, Biostratigraphy and chronostratigraphy of the Miocene Pietra Leccese in the type area of Lecce (Apulia, southern Italy): Bollettino della Società Paleontologica Italiana, v. 48, p. 129–145.
Mazzoli, S., Aldega, L., Corrado, S., Invernizzi, C., and Zattin, M., 2006, Pliocene–Quaternary thrusting, syn-orogenic extension and tectonic exhumation in the Southern Apennines (Italy): Insights from the Monte Alpi area, *in* Mazzoli, S., and Butler, R.W.H., eds., Styles of Continental Contraction: Geological Society of America Special Paper 414, p. 55–77, https://doi.org/10.1130/2006.2414(04).
Mazzoli, S., D'Errico, M., Aldega, L., Corrado, S., Invernizzi, C., Shiner, P., and Zattin, M., 2008, Tectonic burial and 'young' (<10 Ma) exhumation in the Southern Apennines fold and thrust belt (Italy): Geology, v. 36, p. 243–246, https://doi.org/10.1130/G24344A.1.
Mazzoli, S., Ascione, A., Candela, S., Iannace, A., Megna, A., Santini, S., and Vitale, S., 2013, Subduction and continental collision events in the southern Apennines: Constraints from two crustal cross-sections: Rendiconti online della Società Geologica Italiana, v. 25, p. 78–84, https://doi.org/10.3301/ROL.2013.07.
Mehmood, M., Ciarcia, S., Lo Schiavo, L., Natale, J., and Vitale, S., 2023, Paleogeographic and tectonic evolution of the earliest wedge-top basin in the Southern Apennines: New insights from the paleocurrent analysis of the Cilento Group deposits (southern Italy): Geosciences, v. 13, no. 8, p. 238, https://doi.org/10.3390/geosciences13080238.
Menardi Noguera, A., and Rea, G., 2000, Deep structure of the Campanian-Lucanian arc (Southern Apennines): Tectonophysics, v. 324, p. 239–265, https://doi.org/10.1016/S0040-1951(00)00137-2.
Michard, A., Chalouan, A., Feinberg, H., Goffé, B., and Montigny, R., 2002, How does the Alpine belt end between Spain and Morocco?: Bulletin de la Société Géologique de France, v. 173, p. 3–15, https://doi.org/10.2113/173.1.3.
Michard, A., Negro, F., Saddiqi, O., Bouybaouene, M.L., Chalouan, A., Montigny, R., and Goffé, B., 2006, Pressure-temperature-time constraints on the Maghrebide mountain building: Evidence from the Rif-Betic transect (Morocco, Spain), Algerian correlations, and geodynamic implications: Comptes Rendus Geoscience, v. 338, p. 92–114, https://doi.org/10.1016/j.crte.2005.11.011.
Milli, S., Critelli, S., Amicone, E., Campilongo, G., Muto, F., Tripodi, V., Tentori, D., and Perri, F., 2021, Facies, composition and provenance of the Agnone Flysch in the context of the early Messinian evolution of the Southern Apennine foredeep (Molise, Italy): Italian Journal of Geosciences, v. 140, no. 2, p. 275–312, https://doi.org/10.3301/IJG.2021.01.
Morley, C.K., 1988, Out-of-sequence thrusts: Tectonics, v. 7, p. 539–561, https://doi.org/10.1029/TC007i003p00539.
Morsilli, M., Hairabian, A., Borgomano, J., Nardon, S., Adams, E., and Bracco Gartner, G., 2017, The Apulia carbonate platform—Gargano Promontory, Italy (Upper Jurassic–Eocene): American Association of Petroleum Geologists Bulletin, v. 101, no. 4, p. 523–531, https://doi.org/10.1306/011817DIG17031.
Mostardini, F., and Merlini, S., 1986, Appennino centro-meridionale: Sezioni geologiche e proposta di modello strutturale: Memorie della Società Geologica Italiana, v. 35, p. 177–202.
Naso, G., and Tallini, M., 1993, Tettonica compressiva e distensiva nei Monti Aurunci occidentali (Appennino centrale): Prime considerazioni: Geologica Romana, v. 29, p. 455–462, 1 sheet, scale 1:10,000.
Naso, G., Tallini, M., and Tozzi, M., 1995, Caratteristiche geologico-strutturali dell'area di Miranda (Isernia): Un contributo alla comprensione dei rapporti tra falde molisane e avanfossa del Messiniano-Pliocene inferiore: Bollettino della Società Geologica Italiana, v. 114, p. 423–441.
Ogniben, L., 1957, Flysch miocenico autoctono e parautoctono e Argille Scagliose alloctone nella zona di Caiazzo (Caserta): Bollettino della Società Geologica Italiana, v. 75, p. 169–179.
Ogniben, L., 1960, Nota illustrativa dello schema geologico della Sicilia Nord-orientale: Rivista Mineraria Siciliana, v. 64/65, p. 183–212.
Ogniben, L., 1962, Le Argille Scagliose e i sedimenti messiniani a sinistra del Trionto (Rossano, Cosenza): Geologica Romana, v. 1, p. 255–282.
Ogniben, L., 1969, Schema introduttivo alla geologia del confine Calabro-Lucano: Memorie della Società Geologica Italiana, v. 8, p. 453–763.
Ortolani, F., Torre, M., and Di Nocera, S., 1979, I depositi alto miocenici del bacino di Amantea (Catena Costiera Calabra): Bollettino della Società Geologica Italiana, v. 98, p. 559–587.
Ortolano, G., Visalli, R., Fazio, E., Fiannacca, P., Godard, G., Pezzino, A., Punturo, R., Sacco, V., and Cirrincione, R., 2020, Tectono-metamorphic evolution of the Calabria continental lower crust: The case of the Sila Piccola Massif: International Journal of Earth Sciences, v. 109, p. 1295–1319, https://doi.org/10.1007/s00531-020-01873-1.
Pantosti, D., and Velonà, M., 1986, Tettonica recente nell'isola di Zannone e nella piattaforma circostante (Arcipelago Pontino, Italia centrale): Memorie della Società Geologica Italiana, v. 35, no. 2, p. 623–629.
Pantosti, D., Salvini, F., and Velonà, M., 1986, Assetto geologico strutturale del promontorio del Circeo (Italia centrale): Memorie della Società Geologica Italiana, v. 35, p. 611–621.
Parotto, M., and Praturlon, A., 1975, Geological summary of the Central Appennines: Quaderni della Ricerca Scientifica, v. 90, p. 257–306.
Parotto, M., and Praturlon, A., 1981, Structural Sketch of the Middle-Eastern Mediterranean Area: Rome, Italy, G.E.O., Consiglio Nazionale della Ricerche (CNR), Italian Geodynamic Publication 269, scale 1:1.500,000.
Passeri, L., Ciarapica, G., Reggiani, L., and Rutledge, D.C., 2014, The significance of Longobucco unit (Calabria-Peloritani arc) in the evolution of the Ionian and Alpine

oceans: Italian Journal of Geosciences, v. 133, no. 2, p. 249–270, https://doi.org/10.3301/IJG.2014.07.
Patacca, E., and Scandone, P., 1989, Post-Tortonian mountain building in the Apennines: The role of the passive sinking of a relict lithospheric slab, *in* Boriani, A., Bonafede, M., Piccardo, G.B., and Vai, G.B., eds., The Lithosphere in Italy: Advances in Earth Science Research: Atti Convegni dell'Accademia Nazionale dei Lincei, v. 80, p. 157–176.
Patacca, E., and Scandone, P., 2001, Late thrust propagation and sedimentary response in the thrust-belt–foredeep system of the Southern Apennines (Pliocene–Pleistocene), *in* Vai, G.B., and Martini, I.P., eds., Anatomy of an Orogen: The Apennines and Adjacent Mediterranean Basins: Dordrecht, Netherlands, Kluwer Academic Publishers, p. 401–440, https://doi.org/10.1007/978-94-015-9829-3_23.
Patacca, E., and Scandone, P., 2007, Geology of southern Apennines, *in* Mazzotti, A., Patacca, E., and Scandone, P., eds., Results of the CROP Project, Sub-Project CROP-04: Bollettino della Società Geologica Italiana, Special Issue 7, p. 75–119.
Patacca, E., and Scandone, P., 2011, Calabria and Peloritani: Where did they stay before the Corsica-Sardinia rotation?: Boundary conditions, internal geological constraints and first-order open problems: Rendiconti Online Società Geologica Italiana, v. 15, p. 97–101.
Patacca, E., and Scandone, P., 2014, Il contributo degli studi stratigrafici di superficie e sottosuolo alla conoscenza dell'Appennino Campano-Lucano, *in* Atti del 1° Congresso dell'Ordine dei Geologi di Basilicata, Ordine Geologi Basilicata, ed., Potenza, Ordine Geologi Basilicata, p. 97–153, https://www.geologibasilicata.it/Comunicazione/Atti-Congresso-2012/11-Sessione/Etta-Patacca-e-Paolo-Scandone.
Patacca, E., and Scandone, P., 2021, Geological Map of the Majella Mountain: Rome, Italy, Istituto Superiore per la Protezione e la Ricerca Ambientale (ISPRA), Servizio Geologico d'Italia, Dimensione Ricerca Ecologia Ambiente (D.R.E.A.M.) Italia, scale 1:25,000.
Patacca, E., Sartori, R., and Scandone, P., 1990, Tyrrhenian basin and Apenninic arcs: Kinematic relations since Late Tortonian times: Memorie della Società Geologica Italiana, v. 45, p. 425–451.
Patacca, E., Scandone, P., Bellatalla, M., Perilli, N., and Santini, U., 1992a, La zona di giunzione tra l'arco appenninico settentrionale e l'arco appenninico meridionale nell'Abruzzo e nel Molise, *in* Tozzi, M., Cavinato, G.P., and Parotto, M., eds., Studi Preliminari all'Acquisizione Dati del Profilo CROP 11 Civitavecchia-Vasto: Studi Geologici Camerti, Volume Speciale 1991–2, p. 417–441.
Patacca, E., Scandone, P., Bellatalla, M., Perilli, N., and Santini, U., 1992b, The Numidian-sand event in the southern Apennines: Memorie di Scienze Geologiche, v. 18, p. 297–337.
Perri, E., 1996, Tettonica post-tortoniana del settore nord-occidentale dell'Arco Calabro: Studi Geologici Camerti, v. 14, p. 155–175.
Perri, F., Muto, F., and Belviso, C., 2011, Links between composition and provenance of Mesozoic siliciclastic sediments from western Calabria (southern Italy): Italian Journal of Geosciences, v. 130, p. 318–329, https://doi.org/10.3301/IJG.2011.04.
Perrone, V., Torre, M., and Zuppetta, A., 1973, Il Miocene della Catena Costiera calabra: 1° contributo: Zona Diamante-Bonifati-Sant'Agata d'Esaro (Cosenza): Rivista Italiana di Paleontologia e Stratigrafia, v. 79, p. 157–205.
Pescatore, T., 1965, Ricerche geologiche sulla depressione molisano-sannitica: Atti Accademia Scienze Fisiche Matematiche Napoli, v. 3, no. 5, p. 101–145.
Pescatore, T., and Sgrosso, I., 1973, I rapporti tra la piattaforma campano-lucana e la piattaforma abruzzese-campana nel Casertano: Bollettino della Società Geologica Italiana, v. 92, p. 925–938.
Pescatore, T., Renda, P., and Tramutoli, M., 1988, Rapporti tra le unità lagonegresi e le unità sicilidi nella media Valle del Basento, Lucania (Appennino meridionale): Memorie della Società Geologica Italiana, v. 41, p. 353–361.
Pescatore, T., Renda, P., Schiattarella, M., and Tramutoli, M., 1999, Stratigraphic and structural relationships between Meso-Cenozoic Lagonegro basin and coeval carbonate platforms in Southern Apennines, Italy: Tectonophysics, v. 315, p. 269–286, https://doi.org/10.1016/S0040-1951(99)00278-4.
Pescatore, T., Di Nocera, S., Matano, F., Pinto, F., Quarantiello, R., Amore, O., Boiano, U., Civile, D., Fiorillo, L., and Martino, C., 2008, Geologia del settore centrale dei Monti del Sannio: Nuovi dati stratigrafi ci e strutturali: Memorie Descrittive Carta Geologica d'Italia, v. 77, p. 77–95.
Pescatore, T.S., Sgrosso, I., and Torre, M., 1970, Lineamenti di tettonica e sedimentazione nel Miocene dell'Appennino Campano-Lucano: Memorie della Società Naturalisti in Napoli, v. 78, p. 337–408.
Pescatore, T.S., Di Nocera, S., Matano, F., and Pinto, F., 2000, L'unità del Fortore nel quadro della geologia del settore orientale dei Monti del Sannio (Appennino meridionale): Bollettino della Società Geologica Italiana, v. 119, p. 587–601.
Pieri, P., Sabato, L., Loiacono, F., and Marino, M., 1994, Il bacino piggyback di Sant'Arcangelo: Evoluzione tettonico-sedimentaria: Bollettino della Società Geologica Italiana, v. 113, p. 465–481.
Quitzow, H.W., 1935, Diabas–porphirite und Glaukophangesteine in der Trias von Nordkalabrien: Nachrichten von der Gesellschaft der Wissenschaften zu Göttingen, Mathematisch-Physikalische Klasse IV, Special Issue 9, p. 83–118.
Randazzo, V., Di Stefano, P., Schlagintweit, F., Todaro, S., Cacciatore, M.S., and Zarcone, G., 2021, The migration path of Gondwanan dinosaurs toward Adria: New insights from the Cretaceous of NW Sicily (Italy): Cretaceous Research, v. 126, https://doi.org/10.1016/j.cretres.2021.104919.
Roda, C., 1964, Distribuzione e facies dei sedimenti Neogenici nel Bacino Crotonese: Geologica Romana, v. 3, p. 319–366.
Rossetti, F., Faccenna, C., Goffé, B., Monié, P., Argentieri, A., Funiciello, R., and Mattei, M., 2001, Alpine structural and metamorphic signature of the Sila Piccola Massif nappe stack (Calabria, Italy): Insights for the tectonic evolution of the Calabria-Peloritani terrane: Tectonics, v. 20, p. 112–133, https://doi.org/10.1029/2000TC900027.
Rossetti, F., Goffé, B., Monié, P., Faccenna, C., and Vignaroli, G., 2004, Alpine orogenic *P-T-t*-deformation history of the Catena Costiera area and surrounding regions (Calabria arc, southern Italy): The nappe edifice of north Calabria revised with insights on the Tyrrhenian-Apennine system formation: Tectonics, v. 23, TC6011, https://doi.org/10.1029/2003TC001560.
Rossetti, F., Lucci, F., Theye, T., Bouybaouene, M.L., Gerdes, A., Opitz, J., Dini, A., and Lipp, C., 2020, Hercynian anatexis in the envelope of the Beni Bousera peridotites (Alboran Domain, Morocco): Implications for the tectono-metamorphic evolution of the deep crustal roots of the Mediterranean region: Gondwana Research, v. 83, p. 157–182, https://doi.org/10.1016/j.gr.2020.01.020.
Roure, F., Casero, P., and Addoum, B., 2012, Alpine inversion of the North African margin and delamination of its continental lithosphere: Tectonics, v. 31, TC3006, https://doi.org/10.1029/2011TC002989.
Royden, L., 1988, Flexural behavior of the continental lithosphere in Italy: Constraints imposed by gravity and deflection data: Journal of Geophysical Research, v. 93, p. 7747–7766, https://doi.org/10.1029/JB093iB07p07747.
Royden, L., Patacca, E., and Scandone, P., 1987, Segmentation and configuration of subducted lithosphere in Italy: An important control on thrust-belt and foredeep basin evolution: Geology, v. 15, p. 714–717, https://doi.org/10.1130/0091-7613(1987)15<714:SACOSL>2.0.CO;2.
Royden, L.H., 1993, The tectonic expression slab pull at continental convergent boundaries: Tectonics, v. 12, p. 303–325, https://doi.org/10.1029/92TC02248.
Russo, F., and Schiattarella, M., 1992, Osservazioni preliminari sull'evoluzione morfostrutturale del bacino di Castrovillari (Calabria settentrionale): Studi Geologici Camerti, Special Issue 1, p. 271–278.
Russo, M., Zuppetta, A., and Guida, A., 1995, Alcune precisazioni stratigrafiche sul Flysch del Cilento (Appennino meridionale): Bollettino della Società Geologica Italiana, v. 114, p. 353–359.
Sabato, L., Bertini, A., Masini, F., Albianelli, A., Napoleone, G., and Pieri, P., 2005, The lower and middle Pleistocene geological record of the San Lorenzo lacustrine succession in the Sant'Arcangelo Basin (Southern Apennines, Italy): Quaternary International, v. 131, p. 59–69, https://doi.org/10.1016/j.quaint.2004.07.001.
Sabbatino, M., Vitale, S., Tavani, S., Consorti, L., Corradetti, A., Cipriani, A., Arienzo, I., and Parente, M., 2020, Constraining the onset of flexural subsidence and peripheral bulge extension in the Miocene foreland of the Southern Apennines (Italy) by Sr-isotope stratigraphy: Sedimentary Geology, v. 401, https://doi.org/10.1016/j.sedgeo.2020.105634.
Sabbatino, M., Tavani, S., Vitale, S., Ogata, K., Corradetti, A., Consorti, L., Arienzo, I., Cipriani, A., and Parente, M., 2021, Forebulge migration in the foreland basin system of the Central-Southern Apennine fold-thrust belt (Italy): New high-resolution Sr-isotope dating constraints: Basin Research, v. 33, no. 5, p. 2817–2836, https://doi.org/10.1111/bre.12587.
Sani, F., Del Ventisette, C., Montanari, D., Coli, M., Nafissi, P., and Piazzini, A., 2004, Tectonic evolution of the internal sector of the Central Apennines, Italy: Marine and Petroleum Geology, v. 21, p. 1235–1254, https://doi.org/10.1016/j.marpetgeo.2004.09.004.
Santangelo, N., Romano, P., Ascione, A., and Russo Ermolli, E., 2017, Quaternary evolution of the Southern Apennines coastal plains: A review: Geologica Carpathica, v. 68, p. 43–56, https://doi.org/10.1515/geoca-2017-0004.
Santantonio, M., and Fabbi, S., 2020, Anatomy and Jurassic evolution of a Hercynian basement high (Caloveto High-Calabria, southern Italy): Italian Journal of Geosciences, v. 139, no. 1, p. 30–53, https://doi.org/10.3301/IJG.2019.16.
Santantonio, M., and Teale, C., 1987, An example of the use of detrital episodes in elucidating complex basin histories: The Caloveto and Longobucco Groups of NE Calabria, S Italy, *in* Legget, J.K., and Zuffa, G.G., eds., Marine Clastic Sedimentology: Dordrecht, Netherlands, Springer, p. 62–74, https://doi.org/10.1007/978-94-009-3241-8_3.
Santo, A., 1996, Le ruditi dei Monti Alburni nel quadro dell'evoluzione altomiocenica dell'Appennino campano: Bollettino della Società Geologica Italiana, v. 115, p. 519–528.
Santo, A., and Senatore, M.R., 1988, La successione stratigrafica dell'unità dauna a Monte Sidone (Castelluccio Valmaggiore, Foggia): Memorie della Società Geologica Italiana, v. 41, p. 431–438.
Sartori, R., Carrara, G., Torelli, L., and Zitellini, N., 2001, Neogene evolution of the southwestern Tyrrhenian Sea (Sardinia Basin and western bathyal plain): Marine Geology, v. 175, p. 47–66, https://doi.org/10.1016/S0025-3227(01)00116-5.
Savelli, C., 2002, Time-space distribution of magmatic activity in the western Mediterranean and peripheral orogens during the past 30 Ma (a stimulus to geodynamic considerations): Journal of Geodynamics, v. 34, p. 99–126, https://doi.org/10.1016/S0264-3707(02)00026-1.
Scandone, P., 1967, Studi di geologia lucana; la serie calcareo silico marnosa e i suoi rapporti con l'Appennino calcareo: Bollettino della Società di Naturalisti in Napoli, v. 76, p. 301–469.
Scandone, P., 1972, Studi di geologia lucana: Carta dei terreni della serie calcareo-silico-marnosa e note illustrative: Bollettino della Società di Naturalisti in Napoli, v. 81, p. 225–300.
Scandone, P., and Sgrosso, I., 1965, Sulla paleogeografia della Penisola Sorrentina dal Cretacico Superiore al Miocene: Bollettino della Società di Naturalisti in Napoli, v. 74, p. 159–177.
Scandone, P., and Sgrosso, I., 1974, La successione miocenica dell'alta Vallimala nella finestra tettonica di Campagna (Monti Picentini): Bollettino della Società Geologica Italiana, v. 93, p. 1043–1047.
Scandone, P., Sgrosso, I., and Bruno, F., 1964, Appunti di geologia sul M. Bulgheria: Bollettino della Società di Naturalisti in Napoli, v. 72, p. 19–27.

Scarsella, F., 1953, Relazioni preliminari sui rilevamenti geologici fatti durante il 1953 nei fogli 139–1'Aquila e 140–Teramo: Bollettino Servizio Geologico d'Italia, v. 73, p. 309–320.

Schenk, V., 1980, U-Pb and Rb-Sr radiometric dates and their correlation with metamorphic events in the granulite facies basement of the Serre, southern Calabria (Italy): Contributions to Mineralogy and Petrology, v. 73, p. 23–38, https://doi.org/10.1007/BF00376258.

Schettino, A., and Turco, E., 2011, Tectonic history of the western Tethys since the Late Triassic: Geological Society of America Bulletin, v. 123, p. 89–105, https://doi.org/10.1130/B30064.1.

Schiattarella, M., 1998, Quaternary tectonics of the Pollino Ridge, Calabria-Lucania boundary, southern Italy, *in* Holdsworth, R.E., Strachan, R.A., and Dewey, J.F., eds., Continental Transpressional and Transtensional Tectonics: Geological Society, London, Special Publication 135, p. 341–354, https://doi.org/10.1144/GSL.SP.1998.135.01.22.

Schmid, S.M., Pfiffner, O.A., Froitzheim, N., Schönborn, G., and Kissling, E., 1996, Geophysical-geological transect and tectonic evolution of the Swiss-Italian Alps: Tectonics, v. 15, p. 1036–1064, https://doi.org/10.1029/96TC00433.

Sciamanna, S., Sassi, W., Gambini, R., Rudkiewicz, J.L., Mosca, F., and Nicolai, C., 2004, Predicting hydrocarbon generation and expulsion in the Southern Apennines thrust belt by 2-D integrated structural and geochemical modeling: Part I—Structural and thermal evolution, *in* Swennen, R., Roure, F., and Granath, J.W., eds., Deformation, Fluid Flow, and Reservoir Appraisal in Foreland Fold and Thrust Belts: American Association of Petroleum Geologists Hedberg Series 1, p. 51–67.

Scrocca, D., 2010, Southern Apennines: Structural setting and tectonic evolution, *in* Beltrando, M., Peccerillo, A., Mattei, M., Conticelli, S., and Doglioni, C., eds., The Geology of Italy: Tectonics and Life along Plate Margins: Journal of the Virtual Explorer, v. 36, paper 14, https://doi.org/10.3809/jvirtex.2010.00225.

Scrocca, D., and Tozzi, M., 1999, Tettogenesi mio-pliocenica dell'Appennino molisano: Bollettino della Società Geologica Italiana, v. 118, p. 423–441.

Scrocca, D., Tozzi, M., and Parotto, M., 1995, Assetto strutturare del settore compreso tra il Matese, le Mainarde e l'unità di Frosolone: Implicazioni per l'evoluzione neogenica del sistema di sovrascorrimenti nell'Appennino centro-meridionale: Studi Geologici Camerti, Volume Speciale 2, p. 407–418.

Segre, A.G., 1953, Biogeografia dell'isola di Zannone: Morfologia e geologia: Rendiconti Accademia Nazionale Lincei, v. 4–5, serie 4, p. 135–150.

Selli, R., 1957, Sulla trasgressione del Miocene nell'Italia meridionale: Giornale di Geologia, v. 26, p. 1–54.

Selli, R., 1960, Il Messiniano Mayer-Eymar 1867: Proposta di un neostratotipo: Giornale di Geologia, v. 28, p. 1–33.

Selli, R., 1962, Il Paleogene nel quadro della geologia dell'Italia centro meridionale: Memorie della Società Geologica Italiana, v. 3, p. 737–789.

Servizio Geologico d'Italia, 1968a, Foglio 171 Gaeta: Rome, Italy, Servizio Geologico d'Italia, scale 1:100,000, http://sgi.ISPRAmbiente.it/geologia100k/mostra_foglio.aspx?numero_foglio=171.

Servizio Geologico d'Italia, 1968b, Foglio 189 Altamura: Rome, Italy, Servizio Geologico d'Italia, scale 1:100,000, http://sgi.ISPRAmbiente.it/geologia100k/mostra_foglio.aspx?numero_foglio=189.

Servizio Geologico d'Italia, 1969, Foglio 214 Gallipoli: Rome, Italy, Servizio Geologico d'Italia, scale 1:100,000, http://sgi.ISPRAmbiente.it/geologia100k/mostra_foglio.aspx?numero_foglio=214.

Servizio Geologico d'Italia, 1970a, Foglio 210 Lauria: Rome, Italy, Servizio Geologico d'Italia, scale 1:100,000, http://sgi.ISPRAmbiente.it/geologia100k/mostra_foglio.aspx?numero_foglio=210.

Servizio Geologico d'Italia, 1970b, Foglio 162 Campobasso: Rome, Italy, Servizio Geologico d'Italia, scale 1:100,000, http://sgi.ISPRAmbiente.it/geologia100k/mostra_foglio.aspx?numero_foglio=162.

Servizio Geologico d'Italia, 1971, Foglio 201 Matera: Rome, Italy, Servizio Geologico d'Italia, scale 1:100,000, http://sgi.ISPRAmbiente.it/geologia100k/mostra_foglio.aspx?numero_foglio=201.

Sgrosso, I., 1998, Possibile evoluzione cinematica miocenica nell'orogene centro-sud appenninico: Bollettino della Società Geologica Italiana, v. 117, p. 679–724.

Shimabukuro, D.H., Wakabayashi, J., Alvarez, W., and Chang, S.-C., 2012, Cold and old: The rock record of subduction initiation beneath a continental margin, Calabria, southern Italy: Lithosphere, v. 4, p. 524–532, https://doi.org/10.1130/L222.1.

Shiner, P., Beccacini, A., and Mazzoli, S., 2004, Thin-skinned versus thick-skinned structural models for Apulian carbonate reservoirs: Constraints from the Val D'Agri Fields: Marine and Petroleum Geology, v. 21, p. 805–827, https://doi.org/10.1016/j.marpetgeo.2003.11.020.

Siravo, G., Speranza, F., and Macrì, P., 2022, First pre-Miocene paleomagnetic data from the Calabrian block document a 160° post–Late Jurassic CCW rotation as a consequence of left-lateral shear along Alpine Tethys: Tectonics, v. 41, no. 7, https://doi.org/10.1029/2021TC007156.

Sobolev, S.V., and Brown, M., 2019, Surface erosion events controlled the evolution of plate tectonics on Earth: Nature, v. 570, p. 52–57, https://doi.org/10.1038/s41586-019-1258-4.

Spadea, P., 1976, I carbonati nelle rocce metacalcaree della Formazione del Frido della Lucania: Ofioliti, v. 1, p. 431–456.

Tavarnelli, E., and Prosser, G., 2003, The complete Apennines orogenic cycle preserved in a transient single outcrop near San Fele, Lucania, southern Italy: Journal of the Geological Society, v. 160, p. 429–434, https://doi.org/10.1144/001602-130.

Tavarnelli, E., Scisciani, V., Patruno, S., Calamita, F., Pace, P., and Iacopini, D., 2019, The role of structural inheritance in the evolution of fold-and-thrust belts: Insights from the Umbria-Marche Apennines, Italy, *in* Koeberl, C., and Bice, D.M., eds., 250 Million Years of Earth History in Central Italy: Celebrating 25 Years of the Geological Observatory of Coldigioco: Geological Society of America Special Paper 542, p. 191–212, https://doi.org/10.1130/2019.2542(10).

Thomas, M.F.H., Bodin, S., Redfern, J., and Irving, D.H.B., 2010, A constrained African craton source for the Cenozoic Numidian Flysch: Implications for the palaeogeography of the western Mediterranean basin: Earth-Science Reviews, v. 101, p. 1–23, https://doi.org/10.1016/j.earscirev.2010.03.003.

Thomson, S.N., 1998, Assessing the nature of tectonic contacts using fission-track thermochronology: An example from the Calabria-Peloritani terrane, southern Italy: Terra Nova, v. 10, p. 32–36, https://doi.org/10.1046/j.1365-3121.1998.00165.x.

Tozer, R.S.J., Butler, R.W.H., Corrado, S., Geologiche, S., Tre, R., San, L., and Murialdo, L., 2002, Comparing thin- and thick-skinned thrust tectonic models of the Central Apennines, Italy, *in* Bertotti, G., Schulmann, K., and Cloetingh, S.A.P.L., eds., Continental Collision and the Tectono-Sedimentary Evolution of Forelands: European Geosciences Union (EGU) Stephan Mueller Special Publication Series 1, p. 181–194, https://doi.org/10.5194/smsps-1-181-2002.

Tropeano, M., Sabato, L., and Pieri, P., 2002, Filling and cannibalization of a foredeep: The Bradanic Trough, southern Italy, *in* Jones, S.J., and Frostick, L.E., eds., Sediment Flux to Basins: Causes, Controls and Consequences: Geological Society, London, Special Publication 191, p. 55–79, https://doi.org/10.1144/GSL.SP.2002.191.01.05.

Tsujimori, T., and Ernst, W.G., 2014, Lawsonite blueschists and lawsonite eclogites as proxies for palaeo-subduction zone processes: A review: Journal of Metamorphic Geology, v. 32, p. 437–454, https://doi.org/10.1111/jmg.12057.

Tursi, F., Bianco, C., Brogi, A., Caggianelli, A., Prosser, G., Ruggieri, G., and Braschi, E., 2020, Cold subduction zone in northern Calabria (Italy) revealed by lawsonite-clinopyroxene blueschists: Journal of Metamorphic Geology, v. 38, p. 451–469, https://doi.org/10.1111/jmg.12528.

van Hinsbergen, D.J.J., Vissers, R.L.M., and Spakman, W., 2014, Origin and consequences of western Mediterranean subduction, rollback, and slab segmentation: Tectonics, v. 33, p. 393–419, https://doi.org/10.1002/2013TC003349.

Vannucchi, P., Sage, F., Phipps, M.J., Remitti, F., and Collot, J.Y., 2012, Toward a dynamic concept of the subduction channel at erosive convergent margins with implications for interplate material transfer: Geochemistry, Geophysics, Geosystems, v. 13, Q02003, https://doi.org/10.1029/2011GC003846.

Vecchio, E., Barattolo, F., and Hottinger, L., 2006, *Alveolina* horizons in the Trentinara formation (southern Apennines, Italy): Stratigraphic and paleogeographic implications: Rivista Italiana di Paleontologia e Stratigrafia, v. 13, p. 21–42.

Vezzani, L., 1966, La sezione tortoniana di Perosa sul Fiume Sinni presso Episcopia (Potenza): Geologica Romana, v. 5, p. 263–290.

Vezzani, L., 1970, Il Flysch di Albidona nell'area al confine tra Calabria e Lucania: Geologica Romana, v. 9, p. 101–126.

Vezzani, L., and Ghisetti, F.C., 1998, Carta Geologica dell'Abruzzo: Regione Abruzzo: Firenze, Italy, Settore Urbanistica-Beni Ambientali e Cultura (SELCA), scale 1:100,000.

Vezzani, L., Festa, A., and Ghisetti, F.C., 2010, Geology and Tectonic Evolution of the Central-Southern Apennines, Italy: Geological Society of America Special Paper 469, 58 p., https://doi.org/10.1130/2010.2469.

Vignaroli, G., Minelli, L., Rossetti, F., Balestrieri, M.L., and Faccenna, C., 2012, Miocene thrusting in the eastern Sila Massif: Implication for the evolution of the Calabria-Peloritani orogenic wedge (southern Italy): Tectonophysics, v. 538–540, p. 105–119, https://doi.org/10.1016/j.tecto.2012.03.011.

Visibility of Petroleum Exploration Data in Italy (ViDEPI) Project, 1955, Casoli 001 Well Log: https://www.videpi.com/videpi/pozzi/dettaglio.asp?cod=1297 (accessed August 2024).

Visibility of Petroleum Exploration Data in Italy (ViDEPI) Project, 1956a, Fogliano 001 Well Log: https://www.videpi.com/videpi/pozzi/dettaglio.asp?cod=2614 (accessed August 2024).

Visibility of Petroleum Exploration Data in Italy (ViDEPI) Project, 1956b, Casaborselli 001 Well Log: https://www.videpi.com/videpi/pozzi/dettaglio.asp?cod=1247 (accessed August 2024).

Visibility of Petroleum Exploration Data in Italy (ViDEPI) Project, 1958, Villalfonsina 001 Well Log: https://www.videpi.com/videpi/pozzi/dettaglio.asp?cod=6907 (accessed August 2024).

Visibility of Petroleum Exploration Data in Italy (ViDEPI) Project, 1960a, Castelfrentano 005 Well Log: https://www.videpi.com/videpi/pozzi/dettaglio.asp?cod=1345 (accessed August 2024).

Visibility of Petroleum Exploration Data in Italy (ViDEPI) Project, 1960b, Marcone 001 Well Log: https://www.videpi.com/videpi/pozzi/dettaglio.asp?cod=3494 (accessed August 2024).

Visibility of Petroleum Exploration Data in Italy (ViDEPI) Project, 1961a, Frosolone 001 Well Log: https://www.videpi.com/videpi/pozzi/dettaglio.asp?cod=2710 (accessed August 2024).

Visibility of Petroleum Exploration Data in Italy (ViDEPI) Project, 1961b, Castelfrentano 006 Well Log: https://www.videpi.com/videpi/pozzi/dettaglio.asp?cod=1346 (accessed August 2024).

Visibility of Petroleum Exploration Data in Italy (ViDEPI) Project, 1962, Torrente Bilioso 001 Well Log: https://www.videpi.com/videpi/pozzi/dettaglio.asp?cod=6410 (accessed August 2024).

Visibility of Petroleum Exploration Data in Italy (ViDEPI) Project, 1981, Orsogna 001 Well Log: https://www.videpi.com/videpi/pozzi/dettaglio.asp?cod=4194 (accessed August 2024).

Visibility of Petroleum Exploration Data in Italy (ViDEPI) Project, 1982, Gargano 001 Well Log: https://www.videpi.com/videpi/pozzi/dettaglio.asp?cod=2811. (accessed August 2024).

Visibility of Petroleum Exploration Data in Italy (ViDEPI) I Project, 1983, Fontemaggiore 002 DIR Well Log: https://www.videpi.com/videpi/pozzi/dettaglio.asp?cod=2624 (accessed August 2024).

Visibility of Petroleum Exploration Data in Italy (ViDEPI) Project, 1986, Puglia 001 Well Log: https://www.videpi.com/videpi/pozzi/dettaglio.asp?cod=4874 (accessed August 2024).

Visibility of Petroleum Exploration Data in Italy (ViDEPI) Project, 2009–2015, Visibility of Petroleum Exploration Data in Italy: http://unmig.sviluppoeconomico.gov.it/videpi/pozzi/pozzi.asp (accessed August 2024).

Vitale, S., and Ciarcia, S., 2013, Tectono-stratigraphic and kinematic evolution of the Southern Apennines/Calabria-Peloritani terrane system (Italy): Tectonophysics, v. 583, p. 164–182, https://doi.org/10.1016/j.tecto.2012.11.004.

Vitale, S., and Ciarcia, S., 2018, Tectono-stratigraphic setting of the Campania region (southern Italy): Journal of Maps, v. 14, no. 2, p. 9–21, https://doi.org/10.1080/17445647.2018.1424655.

Vitale, S., and Ciarcia, S., 2022, The dismembering of the Adria platforms following the Late Cretaceous–Eocene abortive rift: A review of the tectono-stratigraphic record in the southern Apennines: Journal of Geology Review, v. 64, no. 20, p. 2866–2889, https://doi.org/10.1080/00206814.2021.2004559.

Vitale, S., and Mazzoli, S., 2009, Finite strain analysis of a natural ductile shear zone in limestones: Insights into 3-D coaxial vs. non-coaxial deformation partitioning: Journal of Structural Geology, v. 31, p. 104–113, https://doi.org/10.1016/j.jsg.2008.10.011.

Vitale, S., Ciarcia, S., Mazzoli, S., Iannace, A., and Torre, M., 2010, Structural analysis of the 'Internal' units of Cilento, Italy: New constraints on the Miocene tectonic evolution of the Southern Apennine accretionary wedge: Comptes Rendus Geoscience, v. 342, p. 475–482, https://doi.org/10.1016/j.crte.2010.03.005.

Vitale, S., Ciarcia, S., and Tramparulo, F.D.A., 2013a, Deformation and stratigraphic evolution of the Ligurian accretionary complex in the Southern Apennines (Italy): Journal of Geodynamics, v. 66, p. 120–133, https://doi.org/10.1016/j.jog.2013.02.008.

Vitale, S., Fedele, L., Tramparulo, F.D.A., Ciarcia, S., Mazzoli, S., and Novellino, A., 2013b, Structural and petrological analyses of the Frido Unit (southern Italy): New insights into the early tectonic evolution of the Southern Apennines–Calabrian arc system: Lithos, v. 168–169, p. 219–235, https://doi.org/10.1016/j.lithos.2013.02.006.

Vitale, S., Zaghloul, M.N., El Ouaragli, B., Tramparulo, F.D., and Ciarcia, S., 2015, Polyphase deformation of the Dorsale Calcaire complex and the Maghrebian Flysch Basin units in the Jebha area (Central Rif, Morocco): New insights into the Miocene tectonic evolution of the Central Rif belt: Journal of Geodynamics, v. 90, p. 14–31, https://doi.org/10.1016/j.jog.2015.07.002.

Vitale, S., Tramparulo, F.D.A., Ciarcia, S., Amore, F.O., Prinzi, E.P., and Laiena, F., 2017, The northward tectonic transport in the Southern Apennines: Examples from the Capri Island and western Sorrento Peninsula (Italy): International Journal of Earth Sciences, v. 106, p. 97–113, https://doi.org/10.1007/s00531-016-1300-9.

Vitale, S., Amore, O.F., Ciarcia, S., Fedele, L., Grifa, C., Prinzi, E.P., Tavani, S., and Tramparulo, F.D.A., 2018, Structural, stratigraphic and petrological clues for a Cretaceous–Paleogene abortive rift in the southern Adria domain (Southern Apennines, Italy): Geological Journal, v. 53, no. 2, p. 660–681, https://doi.org/10.1002/gj.2919.

Vitale, S., Ciarcia, S., Fedele, L., and Tramparulo, F.D., 2019a, The Ligurian oceanic successions in southern Italy: The key to decrypting the first orogenic stages of the Southern Apennines–Calabria chain system: Tectonophysics, v. 750, p. 243–261, https://doi.org/10.1016/j.tecto.2018.11.010.

Vitale, S., Prinzi, E.P., Ciarcia, S., Sabbatino, M., Tramparulo, F.D.A., and Verazzo, G., 2019b, Polyphase out-of-sequence thrusting and occurrence of marble detritus within the wedge-top basin deposits in Mt. Massico (Southern Apennines): Insights into the late Miocene tectonic evolution of the central Mediterranean: International Journal of Earth Sciences, v. 108, no. 2, p. 501–519, https://doi.org/10.1007/s00531-018-1664-0.

Vitale, S., Prinzi, E.P., Tramparulo, F.D.A., De Paola, C., Di Maio, R., Piegari, E., Sabbatino, M., Natale, J., Notaro, P., and Ciarcia, S., 2020a, Late Miocene–early Pliocene out-of-sequence thrusting in the Southern Apennines (Italy): Geosciences, v. 10, https://doi.org/10.3390/geosciences10080301.

Vitale, S., Prinzi, E.P., Monda, M., Tramparulo, F.D.A., and Ciarcia, S., 2020b, Structural and stratigraphic setting of Campagna and Giffoni tectonic windows: New insights on the orogenic evolution of the Southern Apennines (Italy): Geosciences, v. 10, https://doi.org/10.3390/geosciences10100405.

Vitale, S., Tramparulo, F.D., Cappuccio, F., and Ciarcia, S., 2020c, Brittle vs. ductile strain during the synorogenic exhumation of HP-LT rocks: An example from the Lungro-Verbicaro unit mylonites (northern Calabria, Italy): Journal of Geodynamics, v. 135, https://doi.org/10.1016/j.jog.2020.101719.

Willett, S., Beaumont, C., and Fullsack, P., 1993, Mechanical model for the tectonics of doubly vergent compressional orogens: Geology, v. 21, p. 371–374, https://doi.org/10.1130/0091-7613(1993)021<0371:MMFTTO>2.3.CO;2.

Willett, S.D., 1999, Orogeny and orography: The effects of erosion on the structure of mountain belts: Journal of Geophysical Research, v. 104, no. B12, 28957, https://doi.org/10.1029/1999JB900248.

Young, J.R., Teale, C.T., and Bown, P.R., 1986, Revision of the stratigraphy of the Longobucco Group (Liassic, southern Italy) based on new data from nannofossils and ammonites: Eclogae Geologicae Helvetiae, v. 79, no. 1, p. 117–135.

Zarcone, G., Petti, F.M., Cillari, A., Di Stefano, P., Guzzetta, D., and Nicosia, U., 2010, A possible bridge between Adria and Africa: New palaeobiogeographic and stratigraphic constraints on the Mesozoic palaeogeography of the central Mediterranean area: Earth-Science Reviews, v. 103, p. 154–162, https://doi.org/10.1016/j.earscirev.2010.09.005.

Zuppetta, A., Russo, M., and Turco, E., 1984, Alcune osservazioni sulle Tufiti di Tusa nell'area compresa tra la Valsinni e Rocca Imperiale (confine calabro-lucano): Bollettino della Società Geologica Italiana, v. 103, p. 623–627.

Science Editor: Mihai Ducea
Associate Editor: Enrico Tavarnelli

Manuscript Received 28 November 2023
Revised Manuscript Received 8 August 2024
Manuscript Accepted 3 September 2024